AN ANALYTICAL AND EXPERIMENTAL STUDY OF SINGLE

SPAN RIGID FRAMES ON YIELDING

PIER FOUNDATIONS

by

THOMAS RUPERT COLLINSON ROKEBY

Bachelor of Science in Agriculture
University of Toronto
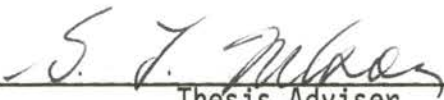Toronto, Canada
1948

Master of Science in Agriculture
University of Toronto
Toronto, Canada
1950

Submitted to the faculty of the Graduate College
of the Oklahoma State University
in partial fulfillment of the requirements
for the degree of
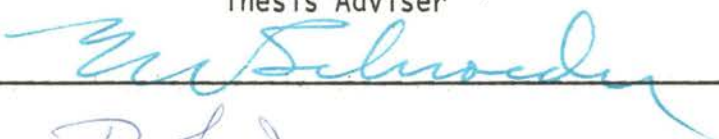DOCTOR OF PHILOSOPHY
May, 1968

AN ANALYTICAL AND EXPERIMENTAL STUDY OF SINGLE

SPAN RIGID FRAMES ON YIELDING

PIER FOUNDATIONS

Thesis Approved:

_____
Thesis Adviser
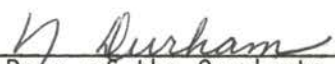
_____

_____

_____

_____
Dean of the Graduate College

ii

ACKNOWLEDGMENTS

LIST OF TABLES

LIST OF FIGURES

viii

CHAPTER I

INTRODUCTION

Background

Rigid single-span gable frames have proved highly adaptable to the construction of farm and light industrial buildings. These frames are usually of the two-hinged or three-hinged configurations. The usual methods of design assume that the frame is attached by means of a frictionless hinge to an unyielding foundation, thus transmitting only horizontal and vertical thrust loads to the foundation. If, however, the frame is rigidly attached to the foundation, resisting moments develop at the supports which reduce the moment occuring at the other critical areas (the haunches and peak). The reduction of maximum moments at haunches and peak permits the section in these areas to be reduced from that required for a two-hinged frame. However, the large moment at the base (which is approximately equal to the haunch moment for a symmetrical vertical load) requires an increased section at the base and moment-resisting connection to the foundation.

In many cases, small-span (on the order of 40 feet or less) frames are built of constant section stock material (steel or wood). The strength provided in the lower part of a constant leg section, which is not utilized efficiently in a two-hinged design, may be used advantageously in the hingeless design.

1

Considerations of economy and convenience in construction suggest the use of vertical cylindrical pier foundations for short-span rigid frames. Such foundations may be cast in place in drilled holes without forming in many soils. By extending the frame legs into the holes, the reinforced concrete foundation pier may be cast around the frame leg, forming a moment-resisting connection. Figure 1 shows a hingeless frame with cylindrical pier foundations.

The moment and thrust transmitted to a foundation pier by such a frame connection tend to cause the pier to rotate and translate horizontally in the plane of the frame. If such movement occurs, the moment and thrust at the base of the frame legs are decreased and the load capacity of the frame is also (usually) decreased. In order to design an adequate frame of this type, the expected foundation movement should be known.

Objectives

1. To evaluate analytically the effect of various degrees of support fixity on shears and moments in single-span hingeless rigid frames.

2. To evaluate the stability of cylindrical piers used as foundations for rigid frames.

3. To determine criteria for the design of cylindrical pier foundations to limit base movement of single-span hingeless and two-hinged rigid frames of configurations and stiffnesses typically used in farm building construction.
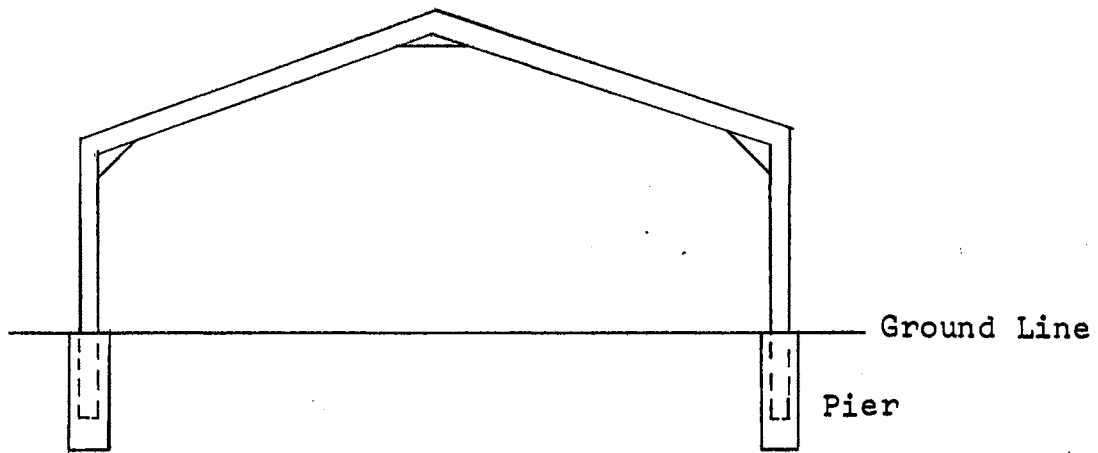
Figure 1.   Hingeless Frame with Cylindrical Pier Foundations.

Limitations of the Study

Assumptions used in the analytical procedure were:

1. The frame deforms elastically due to internal
   moments. Deformation due to shear and axial
   stresses were disregarded.

2. Deformation does not change the frame geometry.

3. The foundation piers rotate and translate as
   rigid bodies in a yielding soil medium, and
   this yielding can be expressed as a function
   of pier geometry, soil characteristics, forces
   and moments applied to the top of the pier,
   duration of loading, and number of load cycles.

A limited experimental program was conducted in the laboratory in order to obtain a relationship between applied moments and thrusts and the yielding of a cylindrical pier, and to check the analytical procedure on a complete frame model. These tests were conducted using small scale models with the piers embedded in dry sand. Dimensional analysis was used in planning and conducting the experimental program in order to assure that the results of the model tests might be applicable to full-scale structures. The prediction equations for pier displacement are valid for piers embedded in dry sand.

CHAPTER II

REVIEW OF PREVIOUS WORK

The subject of rigid frames on yielding foundations can be naturally
divided into two topics--the behavior of the soil-foundation system, and
the stress distribution in the frame resulting from foundation
displacement.

The response of piers--including poles and piles--to applied forces
and moments tending to cause overturning has been studied for many years
by many investigators. Varied approaches to the problem have been used.
Rankine's theory of active and passive pressures, and calculation of
shear resistance of the soil by the Coulomb method have been used to
predict the maximum forces a pier or pole can withstand, but these
methods cannot give any useful information about the amount of rotation
or deflection. Other methods have included applications of the theory
of beams on elastic foundations, the use of a constant horizontal sub-
grade modulus, a non-linear subgrade reaction function, and various
experimental methods involving the testing of full-sized piers in real
soils, and also using the techniques of dimensional analysis to predict
pier performance from observations on models.

The behavior of rigid frames when supports are displaced can be
determined by standard methods of analysis. Foundation movement may
occur as a result of the actions transmitted from the frame. It may

also be caused by expansion or contraction of the soil mass as a result of wetting, drying, or freezing.

This chapter reviews the classical theories of soil pressures and some of the analytical and experimental investigations of pier over-turning, the development of the concept of hingeless rigid frames, and briefly considers foundation movement caused by soil movement.

Soil-Foundation Relations

The behavior of a vertical cylindrical pier foundation in soil, subjected to applied loads and moments, depends upon the geometry of the foundation, the applied forces and moments, and the resistance developed by the soil. In general, the area of concern may be either (a) the ultimate resistance to applied loading developed by the soil-foundation system; for example, the maximum applied moment which the foundation will withstand without overturning, regardless of the amount of deflection or rotation which may occur in the process; or, (b) the relationship between the resistance to applied loads and the movement of the foundation. The former (ultimate load analysis) is of interest only for flexible buildings, such as three-hinged arches, in which foundation movement (unless great enough to alter the geometry of the system) has little significance. In the case of rigid hingeless or one-hinged or two-hinged frames, foundation movement is as important as foundation loads. Theories of earth resistance which apply to both cases will be discussed.

Earth Pressure Theories

Rankine, as reported by Terzaghi and Peck (1), postulated the existence of two characteristic states of stress in cohesionless soil,

the <u>active</u> state, developed as a result of lateral expansion of the soil mass, occurring when a smooth retaining wall moves away from the soil; and the <u>passive</u> state, resulting from compression of the soil, caused by a smooth retaining wall moving toward the soil. The lateral pressures developed were considered to be the minimum and maximum pressures possible, respectively, on a retaining wall, and were given by:

$$P_a = P_v \tan^2 (45 - \phi/2)$$

$$P_p = P_v \tan^2 (45 + \phi/2)$$

where

P_a is active pressure, lb/ft^2

P_p is passive pressure, lb/ft^2

P_v is vertical pressure ($= \gamma Z$ for dry sand at depth Z with no surcharge)

ϕ = angle of internal friction of the soil

γ = effective specific weight of the soil in place, lb/ft^3.

The Rankine theory was extended, by combining it with Coulomb's theory for shear strength of a cohesive soil:

$$S = C + P \tan \phi$$

where

C = cohesion, lb/ft^2 (shear strength when applied normal stress = 0)

S = ultimate shear strength, lb/ft^2

ϕ = apparent angle of friction

to develop a theory for lateral pressure of cohesive soils:

$$P_p = P_v \tan^2 (45 - \phi/2) - 2C \tan (45 - \phi/2)$$

and

$$P_p = P_v \tan^2 (45 + \phi/2) + 2C \tan (45 + \phi/2)$$

According to Rankine's theory, if a smooth vertical wall be embedded in soil and at rest under no external forces, it will be acted upon by equal pressures on each side, the pressures being equal to or greater than the active pressure and less than the passive pressure. If this wall be translated horizontally a distance through the soil mass suffi- cient to mobilize full passive pressure, it will be acted on by full passive pressure, P_p, on the forward surface, and by the active pressure, P_a, on the rearward surface, thus developing a net resistance to further translation of $P_p - P_a$. Further horizontal translation will not alter the net resistance developed (except as a result of changes in the geometry of the system).

According to Terzaghi (2), Rankine's lateral pressure theory considers "only a very small lateral displacement" of the wall is necessary to mobilize active and passive pressures. However, Terzaghi reported that in order to mobilize the Rankine active state in sand to a distance, d, measured perpendicular to the wall, the wall must be moved away a distance, cd, where c is approximately equal to 0.015 for dense sand and considerably larger for loose sand; to mobilize the Rankine passive state to a similar distance requires approximately the same amount of movement of the wall toward the sand deposit.

Tschebotarioff (3) reported, however, that in large scale laboratory tests with movable bulkheads, the outward movement of the bulkhead required to fully mobilize internal shear was much less than the 1.5 to 5 percent of the bulkhead height predicted by Terzaghi.

Terzaghi has pointed out (4) that in the case of vertical piles translated by horizontal loads, the active pressure will not develop fully on the rearward face of the pile, due to an arching action behind the pile.

Several analyses of the action of piles or piers under lateral loading have been based on Rankine's theory. These will be discussed in more detail later.

Coulomb's theory of pressure on a retaining wall, as reported by Terzaghi and Peck (1), considered a wedge of soil tending to slide on a plane surface, and considered the forces, including shear at the sliding surface, necessary for equilibrium of the wedge. Collin (5) early (1840) recognized that the sliding surface, at least in clay, was not a plane, and proposed a cycloidal surface. Several early investigators of the problem of overturning of poles have considered the problem as that of displacing a conical or pyramidal "wedge" of soil, in general analogy with Coulomb's theory.

Various investigators have analyzed laterally loaded piles using the concept of a coefficient of horizontal subgrade reaction, defined as the pressure required to cause unit displacement, lbs/ft^3. The simplest approach makes use of the Winkler hypothesis which assumes the beam to be supported on closely spaced perfectly elastic springs, so that:

$$\frac{P}{y} = k$$

where

P = pressure, lb/ft^2

y = deflection, ft

k = coefficient of subgrade reaction, lb/ft^3 = constant

Vesic (6) found, in tests of horizontal beams on imperfectly elastic material such as compacted silt, that observed bending moments agreed reasonably well with those predicted by application of Winkler's hypothesis, provided that the beams were long or moderately long.

Determination of valid coefficients of horizontal subgrade reaction is complicated by the rheological characteristics of soils. In general, the coefficient may vary with depth, and be influenced by soil type, soil moisture content, and possibly temperature, as well as by the geometry of the pier.

Terzaghi (4) suggested that the coefficient of horizontal subgrade reaction increases approximately linearly with depth in the case of cohesionless soils, and is "more or less" independent of depth in the case of stiff clays. Furthermore, the coefficient is influenced by the width, B, measured perpendicular to the direction of movement of the beam, so that, for clays:

$$k_h = \frac{1}{B} k_{h1}$$

where

k_h = coefficient of horizontal subgrade reaction for a beam of width, B, lb/ft^3

k_{h1} = coefficient of horizontal subgrade reaction for a beam of width one foot, lb/ft^3

B = width of beam, ft

and, for sands

$$k_h = n_h \frac{Z}{B}$$

where

Z = depth below ground surface, ft

n_h = constant of horizontal subgrade reaction on a narrow strip

of width B_1 $(Z/B_1 = 1)$ lb/ft^3.

Terzaghi pointed out that, due to the simplifying assumptions involved, (particularly that of a linear load-deflection relation for soil), the method should not be used for computing deflections. Other investigators, including Matlock and Reese (7) and Davisson and Gill (8), have proposed methods of solution for deflections of laterally loaded piles in which the load-deflection response of the soil need not be linear.

As is well known, the stress-strain relationship for soils is in general non-linear. Kondner (9) proposed, on the basis of laboratory triaxial tests on cohesive soils, a parabolic relationship:

$$\sigma_1 - \sigma_3 = \frac{\varepsilon}{a + b\varepsilon}$$

where

σ_1 = major principle stress, lb/in^2

σ_3 = minor principle stress, lb/in^2

ε = strain, dimensionless

a, b are functions of the axial strain rate, preconsolidation pressure, rebound stress, and the characteristics of the soil, with dimensions of in^2/lb. Expressions for a and b are presented in the paper.

In a later paper, Kondner and Krizek (10) deduced further evidence of a parabolic load deflection relation from field bearing tests, expressing the relation as:

$$\frac{F}{A} = \frac{\frac{X}{C}}{a + b \frac{X}{C}}$$

where

F = load, lb

A = area of bearing plate, ft^2

X = sinkage, ft

C = perimeter of bearing plate, ft

a, b are the soil parameters above, ft^2/lb

In laboratory testing of clays at high rates of strain, Wilson and Dietrich (11) found that the ratio of applied stress to strain was essentially constant. Similar results were obtained by Denisov and Reltov (12). Wilson and Dietrich reported values of the apparent Poisson's ratio, μ, from 0.46 to 0.62. Murayama and Shibata (13) reported an apparent constant modulus of elasticity for clays at applied stresses less than the consolidation stress.

From long-term tests on various soils, Buisman (14) deduced a strain-time relationship of the form:

$$Z_t = \alpha_p + \alpha_s \log t$$

where

Z_t = settlement per unit thickness of supporting layer (dimensionless)

α_p = immediate settlement

α_s = long-time effect

t = time, days

Buisman's strain-time law was corroborated for dense clays by Vialov and Skibitsky (15,16).

Mitchell, Seed, and Paduana (17) studied the creep-deformation and strength of clays under sustained stress. In a review of previous work they observed that the strength of some clays increases as strain continues, in others it decreases. They concluded from their investigation of clay-sand mixtures that the presence of sand interfers with normal consolidation of the clay, and that the sand contributes to the overall strength of the soil. They suggest also that the steady state creep rate may be related to the clay content and plasticity index of the soil.

From triaxial tests of sands, Chen (18) reported that the initial part of the stress-strain curve plotted as a straight line on logarithmic coordinates. He noted that lateral strain of dense sands increased at a faster rate than axial strain, giving an apparent Poisson's ratio (ratio of measured lateral to axial strain) ranging from 0.1 for small strains to 1.6 for large strains. Whitman (19) reported that, in rapid triaxial tests of sands, the compressive strength increased 10 to 15 percent when the time of loading was reduced from a few seconds to 0.05 seconds. Lenoe (20) observed the stress-strain response of sand in a specially designed triaxial machine in which the intermediate principle stress could be varied independently of the minor stress ($\sigma_2 > \sigma_3$) and observed that, for constant minor stress the strain in the σ_1 direction was considerably reduced by increasing the intermediate stress. He concluded that the Coulomb yield criterion will not accurately predict the failure response of sand in a state of three dimensional stress.

Tests and Analyses of Laterally Loaded Piers and Piles

Various investigators have proposed methods of design of laterally-loaded foundations based on the ultimate resistance of the foundation to applied moment or thrust. Abbett (21) and Lee (22) proposed a design formula for sheet piling subject to lateral line thrusts:

$$X^4 - \frac{8HX}{P_p - P_a} - \frac{12\ HhX}{P_p - P_a} - \frac{4H}{P_p - P_a} = 0$$

where

X = depth of penetration, feet, measured from surface of resisting soil.

H = thrust, lb

h = height from soil surface to line of thrust, ft

P_p = passive pressure coefficient, lb/ft^2/ft depth

P_a = active pressure coefficient, lb/ft^2/ft depth.

This formula as derived by Lee is based on development of full active and passive pressures of a cohesionless soil acting at the tip of the pile, decreasing linearly through zero at the axis of rotation to a maximum at some point above the rotation axis, with the maximum possible pressures being maintained from that point to the surface. (It is noted that the maximum active and passive pressure at the surface are both considered to be equal to zero.)

Other investigators have applied modifications of this approach to the analysis of isolated piers and piles. (It should be noted that, according to Terzaghi (4), the assumption of full active pressure on the rearward face of an isolated deflected pile is of doubtful validity, due to arching in the soil.)

Seiler (23) assumed a parabolic distribution of earth pressure over the pile, which agrees fairly well with the distribution used by Lee (22), in deriving a formula to compute the depth of setting required to develop overturning resistance approximately equal to the breaking strength of wooden poles. His formulas for ultimate resistance in three classes of soil were:

$$P = 1250 \ d^2 \text{ for good soils}$$
$$P = 625 \ d^2 \text{ for average soils}$$
$$P = 300 \ d^2 \text{ for poor soils}$$

where

P = ground line thrust, lb

d = depth of setting, ft.

The constants (1250, etc.) are in units of lb/ft^2. He proposed as a safe design value the equation:

$$P = 250 \ d^{2.75} \text{ for good soils.}$$

Feagin (24) from lateral load tests of piles and pile groups at Alton, Illinois, chiefly in sand, reported that sustained loads caused progressive deflection of the pile head, but that repetition of loads of the same magnitude caused more rapid progressive deflection. He proposed an allowable lateral load per pile of four tons if loads were repetitious, or 4 1/2 tons if sustained, for deflection not in excess of 1/4 inch. Raes (25) analyzed pile foundations as rigid bodies rotating about a known point, with full active and passive pressure mobilized throughout the embedded length but reversing in direction at the point of rotation. His general solution was applied to tests of piles in

Belgium and to one pile reported in Feagin's (24) tests, and he concluded that if one-third the calculated load were used permanent deflections would not occur.

Wilkins (26) measured moment and ground line deflections in model hollow steel piles. His results indicate that a triangular pressure distribution, in general agreement with that of Lee (22), gives a reasonable approximation of the true pressure distribution.

Shilts, Graves, and Driscoll (27) investigated pier foundations for sign boards, testing full-size prototypes in the field with various foundation configurations, and one-third size model footings embedded in sand in the laboratory. Using a rectangular pressure distribution as an approximation to the parabolic distribution which they assumed to be correct, they proposed the formula:

$$Q_1/A_1 = P_p \log (1 + 2\Delta^{\tan\phi})$$

where

Q_1/A_1 = "average soil pressure", lb/in^2

P_p = Rankine's passive pressure, lb/in^2

Δ = deflection of post at ground line, inches

ϕ = angle (or apparent angle) of internal friction.

They further concluded that the axis of rotation is at the depth below which there is 0.324 of the total vertical area of the embedded portion of the post. Their report includes considerable detail, including load-displacement curves.

Nelson et al., (28) investigated the displacement six inches above ground line of embedded poles subjected to combined thrust and moment at the ground line with various methods of backfilling. Granular or

concrete backfill greatly decreased the deflection at given loads compared to earth backfill. Repetition of loading caused increased deflection but at a reduced rate, suggesting the possibility of preloading. The axis of rotation was found to be between D/2 and 2D/3 below the ground line (D = depth of embedment). Nelson (29) analyzed the results of the pole tests assuming a parabolic pressure distribution with the axis of rotation at 0.6D and concluded that the rotation at the ground line, ϕ, was predicted by the expression

$$\phi = \frac{\delta}{0.6D} - 0.30 \frac{PD^2}{EI} (0.243 + \frac{H}{D})$$

where

δ = ground line deflection, in

D = depth of setting, in

P = horizontal thrust load, lb

E = modulus of elasticity of pole material, lb/in^2

I = moment of inertia of pole below ground, in^4

H = vertical distance of thrust line above ground line, in.

The observed rotations were further separated into components due to elastic deformation of the soil, plastic deformation of the soil, and elastic deformation of the pole.

Beckett (30) investigated the deflection of model poles embedded in loose and dense sand and saturated sandy clay, subjected to horizontal thrusts at a distance above the ground line. Restrictions introduced in the test limited the dimensionless parameters to three in the case of loose and dense sands:

$$\pi_5 = f(\pi_4, \pi_1)$$

where

$\Pi_5 = Y/D$

$\Pi_4 = P/D^3\gamma$

$\Pi_1 = H/D$

Y = lateral movement, L

D = diameter of pole, L

P = horizontal thrust, F

H = depth of embedment, L

γ = weight of soil per unit volume, FL^{-3}.

Empirical equations were developed for the three soils investigated. For dense sand the prediction equation was:

$$\Pi_5 = 1.68 \, e^{5.5 \, \Pi_4/\Pi_1^{2.13}} \times 10^{-3}.$$

Equations for loose sand and saturated sandy clay are also given in the paper.

Lazard (31) reported the results of tests of some 200 full-size pier foundations of cylindrical and rectangular cross-section for railway catenary supports, and proposed an ultimate overturning moment formula:

$$M_u = TH = K \times 27.45 \, M_b^{2/3}$$

where

M_u = ultimate overturning moment, tons (metric) - meters

T = horizontal thrust, tons

H = height of horizontal thrust line above ground line, meters

K = coefficient for uneven terrain = 1 for level ground

$$M_b = (1 - \varepsilon) M_r$$

$$M_r = K_1 e N_r + K_2 \Delta b D^3$$

ε = ratio of depth of top soil to total depth of setting

K_1, K_2 = functions of the geometry of the foundation and the vertical load

$K_1 = 0.4$ and K_2 ranges from 2.6 for foundations 55 cm diameter to 2.05 for one meter diameter

e = dimension parallel to the direction of overturning, meters

b = dimension perpendicular to direction of overturning, meters

(For cylindrical piers, $e = b = 0.8 \times 2R$)

N_r = vertical load on the foundation

Δ = specific weight of the earth, tons/meter^3

D = depth of setting, meters

R = radius, meters

Lazard observed in the tests that, with foundations subjected to one-third the ultimate moment predicted by the above formula, the mean rotation was eight minutes of arc, with 18 per cent rotating more than 17 minutes, 3 per cent more than 34 minutes. In loading tests continued over several months, the maximum moments ranged from 75 to 100 per cent of those for short-term tests.

Kondner and Green (32) investigated model poles embedded in dense dry sand subject to ground-line thrust and proposed prediction equations for ultimate load and deflection using dimensionless parameters. The basic assumption was that:

$$\frac{y}{L} = f(\frac{c}{L}, \frac{c^2}{A}, \frac{F}{\gamma c^3}, \frac{\gamma t c}{n}, \phi)$$

where

      y = ground line deflection, L

      L = depth of embedment, L

      c = perimeter of pole, L

      A = cross-section area of pole, L^2

      F = thrust at ground line, F

      γ = dry specific weight of sand, FL^{-3}

      ϕ = angle of internal friction, dimensionless

      n = viscosity of sand, $FL^{-2}T$

      t = time of loading, T.

Restrictions and simplifying assumptions used in the test reduce the significant parameters to three, leaving:

$$y/c = f(c/L, F/\gamma c^3).$$

Test data were fitted to the empirical equation:

$$y/c = (0.7 - 0.5 \; c/L)(e^{3.28(c/L)^{2.24} \; F/\gamma c^3} -1) \times 10^{-3}.$$

Solutions to the equation were presented in the paper in the form of nomographs.

Anderson (33, 34) based his analysis on the difference between passive and active pressures, and, assuming a linear stress-strain response of the soil, derived an equation for the allowable moment on a cylindrical footing:

$$M = 1/6 \; a \; D^2 + 1/24 \; b \; D^3$$

where

      M = allowable moment, lb-ft

D = depth of setting, ft

a = 2C $(\tan (45 + \phi/2) + \cot (45 + \phi/2))$

b = G $(\tan^2 (45 + \phi/2) - \cot^2 (45 + \phi/2))$

where

c = coefficient of cohesion, lb/ft^2

G = specific weight of soil, lb/ft^3

ϕ = apparent angle of internal friction, deg.

This formula was simplified to:

$$M = AD^2 + BD^3$$

with values of the parameters A and B given in a table for various soils and footing conformations.

Anderson concluded that the most efficient footing is relatively slim and deep, but, as active and passive pressures increase with depth, wings on the top one-third of the footing, extending perpendicular to the direction of loading, are advisable for maximum efficiency.

Behn (35) conducted tests of full-size cylindrical footings 8 and 12 feet deep for highway sign supports in a plastic, a granular, and an organic soil. Results of both short-term (loading completed within three hours) and long-term (more than 200 days) tests were presented in tables and graphs of load versus deflection and rotation, and rotation versus time, respectively.

Walker and Cox (36) considered that the maximum possible effective pressure was the difference between Rankine's passive and active pressures. Considering only rigid rotation of the footing and limiting ground line deflection to that just necessary to mobilize full passive

pressure, they derived an equation for maximum horizontal thrust, H, independent of any assumption of the position of the axis of rotation:

$$H = \frac{6 \, w \, a^2 \, D^2 + 6 \, w \, a \, b \, D^3 + w \, b^2 \, D^4}{24 \, a \, D + 18 \, b \, D^2 + 36 \, h \, a + 24 \, h \, b \, D}$$

where

H = horizontal thrust, lb

w = width of foundation, ft

D = depth of setting, ft

h = height of thrust line above ground surface, ft

a, b are the soil parameters used by Anderson (33).

The authors pointed out that this equation gives values of H in general agreement with those predicted by Anderson for values of h between 0 and 10 feet.

From short-term tests of 21 piers in clay soil, Walker and Cox concluded that the design thrust load predicted by the equation was in reasonable agreement with a design load based on one-third the ultimate load. (Ultimate load was defined as the horizontal thrust causing 0.5 inch deflection nine inches above the ground line.) Deflections at the design load in all cases were less than 0.1 inch. It was pointed out, however, that creep effects ("slip" in the authors' terminology) were occurring, and that the deflection would be expected to increase with longer duration of loading.

Kent (37) investigated the response of model poles embedded in sand to horizontal thrusts at various heights, and reported a non-linear soil response of the form:

$$p = h^{0.5} \, mz$$

where

p is soil pressure, lb/in^2 on the pole at depth z, FL^{-2}

h is horizontal displacement of the pole, L

z is depth below the surface, L

m is a soil coefficient, $FL^{-3.5}$.

(Values of m ranged from 5.8 to 16.5.) He noted that m appeared to vary inversely with the square root of the width of pole, W, and that the depth to the point of rotation was about 0.7 times the depth of embedment, D, ranging from 0.76 for thrust at the ground line to 0.695 for thrust at a height of 5D.

Broms (38) presented solutions for the ultimate load and deflection of laterally loaded piles. Deflections were computed using the horizontal subgrade reaction coefficients proposed by Terzaghi (4). He observed that "lateral earth pressures are greatly affected by arching", and indicated that the ultimate pressure at failure was more than three times the computed Rankine passive pressure. The linear relation between deflection and pressure implied by the coefficient of subgrade reaction, k_h, was reported to satisfactorily predict pier deflection at working loads less than one-third of the ultimate loads.

The analyses discussed above, with the exception of those of Nelson (28), Kent (37), and Broms (38), assumed that the foundation acted as a rigid body. Behn (35) noted discrepancies in the apparent location of the axis of rotation and attributed them to bending of the foundation. Broms and other authors, considering piles, have proposed methods of solution involving elastic bending of the pile, generally based on the theory of beams on elastic foundations and the differential equation of bending:

$$EI \frac{d^4 y}{dx^4} = -p$$

where

    E = modulus of elasticity of the pile, FL^{-2}

    I = moment of inertia of the pile, L^4

    y = deflection, L

    x = distance along pile axis, L

    p = soil resistance acting on pile, FL^{-1}.

In general, in the solution of piles subjected to lateral thrusts, p is assumed to be some function of Z, the depth below the ground surface, and of y, as well as of the soil parameters ϕ and C. Thus p may take the form:

$$p = yf(z,\phi,C)$$

for a linear stress-strain relationship, or:

$$p = f(z,\phi,C,y)$$

for the general (and more typical) case, in soils in which the stress-strain relationship is not linear.

The coefficient, $f(z,\phi,C)$ may be defined as the "coefficient of horizontal subgrade reaction", k_h. Terzaghi (4) proposed that the width of the beam should be considered so that:

$$k_h = f(z,\phi,C,b)$$

where

    b = width of the beam or pile.

Cummings (39) proposed that laterally-loaded piles be analyzed by equilibrium methods assuming that the soil behaved in agreement with Hooke's law, with the soil modulus a linear function of depth:

$$p = kZy.$$

Palmer and Thompson (40) developed a method of approximate solution, using difference equations, of the equation:

$$EI \frac{d^4y}{dx^4} = - k(x/L)^n y$$

where

k = soil modulus at the pile tip, lb/in^3

x = depth from ground surface, in

L = embedded length, in

n = exponent reflecting the relation between k_h and depth.

Hopkins (41) proposed a soil modulus, k, for laterally deflected piles, ranging from 10 to 50 pounds per $inch^3$ for soft or silty clays, up to more than 500 pounds per $inch^3$ for stiff clay.

Terzaghi (4) discussed factors affecting coefficients of subgrade reaction, k_h, assuming a linear stress-strain relation, and suggested values of k_h for various conditions.

McClelland and Focht (42), as a result of tests of an instrumented pile in submarine clay, reported that the soil modulus was eleven times the secant modulus from laboratory Q_c tests run at the in-place confining pressure:

$$E_s = 11 \frac{\sigma_1 - \sigma_3}{\epsilon}$$

where

E_s = soil modulus, lb/in^2

σ_1 = axial stress, triaxial test, lb/in^2

σ_3 = lateral stress, triaxial test = γZ, lb/in^2

    (γ = specific weight of the soil, Z = depth)

ε = axial strain in laboratory test, dimensionless.

Radosavljevic (43) reasoning from the theory of semi-infinite beams on elastic foundations, proposed the relations:

$$\xi_0 = \frac{2Q_0}{Lbc} + \frac{2M_0}{L^2 bc}$$

$$\Theta_0 = \frac{2Q_0}{L^2 bc} + \frac{4 M_0}{L^3 bc}$$

where

ξ_0 = displacement at ground line, meters

Θ_0 = rotation at ground line, radians

Q_0 = thrust at ground line, tons (metric)

M_0 = moment at ground line, ton-meters

b = width of pile, meters

c = coefficient of soil resistance, $tons/meter^3$

L = characteristic length of pile = $(4EI/bc)^{1/4}$

E = elastic modulus of the pile

I = moment of inertia of the pile section.

He reported good agreement with the performance observed in tests of six full-sized piles.

Bergfelt (44) discussed limitations of the applications of the theory of infinite beams to relatively short piles, concluding that agreement is almost perfect for pile lengths greater than 3L where

$$L = (4EI/kB)^{1/4}$$

where

    k = coefficient of horizontal reaction, lb/ft^3

and that, for lengths less than $1.5 L$ the pile should be considered infinitely stiff. In tests of laterally-loaded piles driven in clay he reported horizontal pressures at a depth of 0.1 meter were greater than the pressure observed at 0.5 meters or greater depths. Pressures of 0.25 to 0.4 kg/cm^2 were observed.

Prakash (45) analyzed the action of rigid poles subjected to generalized thrust, moment, and axial loads, considering a coefficient of horizontal subgrade reaction of the type:

$$k_h = K_h (x/L)^n$$

where

    K_h = value of k_h at the bottom of the pole, lb/in^3

    x = depth coordinate, inches

    L = embedded length of the pole, inches

    n = an empirical constant

        (n approximately equal to 1 for sand, 0.1 for clay),

and derived equations for the location of the axis of rotation, critical buckling load, soil reaction, and moment and shear at any depth. Solutions to these equations were presented in the form of charts. Predicted values of moment and of soil reaction were compared to those observed in tests by Osterberg as quoted by Prakash and show reasonably good agreement.

Matlock and Reese (7, 46) developed methods of solution to the general differential equation:

$$EI \frac{d^4y}{dx^4} = - E_s \, y$$

where E_s is a modulus dependent on depth and deflection, y. The method consists of successive approximations, using successive values of E_s. Methods were given for hand and digital computer calculation.

Davisson and Gill (8) proposed a method of analysis, using an analog computer, of laterally loaded piles in a layered soil system; a method which permits the use of a soil modulus which may be a non-linear function of depth and of strain.

The equations developed by Mindlin (47) for the solution of strains due to forces at the interior of a semi-infinite elastic continuum were used by Milne, Dale, and Suddarth (48) to predict the response of model poles embedded in dry sand. Soil parameters for the Mindlin solution were determined by tests of models. The correlation between predicted and observed deflections in subsequent tests was reported to be satisfactory.

Rigid Frames Subjected to Support Displacements

Methods of analysis for fixed (i.e. hingeless) arches with support yielding are presented in standard structural analysis texts. Moments in arches or rigid frames with generalized loading may be computed by standard methods such as those described by Wang (49) or by the equations presented by Kleinlogel (50) for most normal loading conditions.

Bonnicksen (51) proposed basing the design of pole buildings on the fixity developed at the base of the pole thus making bracing of the superstructure unnecessary.

Polshin and Tokar (52) quote the 1955 USSR Building Code as requiring that settlement of foundations for steel and reinforced concrete frame structures be limited to 0.002L. (L is the distance between foundation centers.)

Roscoe (53) investigated piers as foundations for rigid frames, and concluded that tying opposing piers together at the ground line increased the resistance to overturning moment approximately 70 per cent, as compared to free piers, as well as greatly simplifying the plastic analysis of the frames because the supports could be assumed not to translate, but only to rotate.

Rodda and Paul (54) developed a precast reinforced concrete rigid frame designed to be set in precast footings, with some fixity at the support. In a later paper Wagner and Rodda (55) reported that analysis showed that the frame should be designed for 25 per cent fixity.

Friesen (56) theoretically analyzed the bending moment and shear distribution in both two-hinged and hingeless frames. For dead load plus snow load the predicted values of bending moment at the haunch and at the peak were reduced 15 per cent and 36 per cent, respectively, with full fixity at the base, as compared to the two-hinged configuration. It was observed that reduction in bending moment is of particular significance at these points which may involve discontinuity of the material of the structure. In most cases shear was increased by base fixity.

Friesen and Nelson (57) measured strains and deflections at the haunch and the peak of hingeless and two-hinged frames caused by vertical loads and by rotation and horizontal displacement of the supports. Fair agreement with predicted values was observed. Discrepancies in the observed deflections and moments in the hingeless frame were attributed

to possible support movement and torsional deformation of the
nonsymmetrical (channel) sections used for the frame.

Nelson et al., (58) investigated the stiffness of model arches in
three configurations--three-hinged, one-hinged (hinge located at the
peak) with cylindrical pier foundations in earth, and one-hinged with
full fixity at the base, and observed stiffnesses of 1.00, 1.77, and
2.27, respectively, as determined by deflection at the peak resulting
from vertical loads applied at the peak. Subsequent tests on full-sized
three-hinged and one-hinged arches on pier foundations in clayey soil
gave relative stiffnesses for the one-hinged configuration ranging from
1.55 to 1.85 compared to 1.00 for the three-hinged arch. Stabilizing
wings on the top third of the pier, two and three times as wide as the
pier, extending perpendicular to the plane of applied moments, reduced
foundation movements by 20 and 40 per cent respectively. One-hinged
arches were found to have advantages in erection as compared to three-
hinged arches.

A method of analysis for rigid frames subjected to support movements
was developed by Milne, Dale, and Suddarth (48) in which the frame was
solved by the slope-deflection method, then the resulting reactions were
applied to each support in turn to estimate the support movement. An
approximate solution was obtained by iteration.

Seasonal Soil Movement

A factor which should be considered in the design of indeterminate
arches subject to secondary stresses from foundation movements is soil
movements, resulting from seasonal changes in temperature and moisture
content of the soil, which are essentially independent of loading.

Considerations of frame behavior indicate that vertical movements, if the same in both foundations, will have no effect on stress distribution in an isolated single span rigid frame. However, if differential vertical movement exists, "secondary" stresses will develop in the frame (and probably in secondary framing, between bents). Horizontal translation of foundations in the plane of the frame will also develop stresses in the frame.

Baracos and Bozozuk (59) investigated vertical ground surface movements in grass plots in Leda clay in the Ottawa valley of Canada, and reported increases in elevation of 1.25 inches due to freezing and decreases due to dessication of as much as 1.4 inches in the dry summer of 1953. In the same field near a row of elm trees 60 feet tall the elevation decreased 3.5 inches at the surface and 0.5 inch at a depth of 15 feet. It was concluded that the influence of trees was greatest within a radius from the tree of two-tenths of the height of the trees, and decreased to negligible proportions beyond a radius of eight-tenths of the height. Differential settlements of three to four inches, and occasionally as much as twelve inches, were observed in brick buildings in Ottawa, always near trees.

Schriever and Legget (60) observed movements of foundation slabs in the Ottawa area, and reported frost heaving of one and one-half to four inches at the corners of slabs in unheated buildings. Heaving was much less in heated buildings.

Griffin (61) observed the vertical movement of steel rods attached to welded plates set at depths of 12, 24, 36, 48, and 72 inches in heavy clay soils in the delta area of Mississippi. Differences in the elevation measured at the highest and the lowest soil moisture contents of

the year ranged from 0.132 to 1.52 inches for the plates set at the
12-inch depth; 0.012 to 0.240 for the 72 inch depth. Vertical movements
of a specially prepared house footing were 0.1 and 0.01 inch at adjacent
corners in 1958, 0.04 and 0.07 inch in 1960, and 0.30 and 0.18 in 1961.
This was considered to be "very little vertical movement".

Summary

The classical Rankine-Coulomb theory of lateral soil pressure has
been used to predict the pressures on retaining walls. Investigators
have developed equations to predict the maximum overturning moment of
short piers by assuming that the advancing face of the pier is subjected
to passive pressure and the retreating face to active pressure. Load
tests of full-size and of model piers indicated that the overturning
resistance was several times greater than that predicted by the classical
theory.

Several investigators have analyzed the response of poles or piers
to overturning using a coefficient of horizontal subgrade reaction to
relate the pressure exerted by the soil to the displacement of the pier.
Others have proposed subgrade reaction functions in which the relation
between pressure and displacement is not linear.

Results of laboratory tests on various soils have indicated that
many factors may influence the stress-strain relationship. Strain is
affected by load, confinement pressure, and soil characteristics. Dura-
tion of load is particularly important in clays. Rate of loading affects
the response of sands and clays. The presence of an intermediate
principle stress, greater than the minor principle stress, alters the

stress-strain response of sands. Continued strain may increase or decrease the strength of clays.

Analysis of piles or piers using the theory of beams on elastic supports indicates that the pier may be considered infinitely stiff if the "dimensionless length", βL is less than 1.5 (38), where:

$$\beta = (kD/EI)^{1/4}$$

and

k = subgrade reaction coefficient, FL^{-3}

D = pier diameter, L

EI = stiffness of the pier, FL^{2}

L = embedded length of the pier, L.

Analysis and experiment have indicated that fixing the bases of rigid frames and arches to the foundations can reduce deflection and haunch stresses under load. Movement of the foundations of rigid frames or arches may occur as a result of the loads imposed on the foundation by the arch. Changes in the moisture content of the soil, or freezing, may induce soil movements which could significantly affect the action of hingeless frames or arches.

CHAPTER III

EFFECT OF SUPPORT MOVEMENT ON HINGELESS RIGID FRAME ACTION

The Hingeless Frame

A hingeless rigid frame is characterized by inflexible joints and rigid attachment of the frame to immovable supports. Such an ideal, of course, cannot be realized: even the most massive supporting structure will deflect to some degree in response to the moments and thrusts transmitted to it by the frame. Any such movement of the supporting structure alters the frame action to a degree depending on the extent of the movement and the stiffness of the frame. In the discussion following, the effects of support movement are explored analytically using a single design of frame (the prototype frame) as an example.

Sign Convention

External Forces and Moments

Horizontal forces were considered positive if acting to the right, vertical forces positive if downward. External moments were considered positive if acting clockwise on the structure. (Reactions of the foundations on the frame were considered external.)

Internal Forces and Moments

Moments causing compression in the outer fibre were considered positive. In order to be consistent, shear was considered positive if

the moment of the shear force about any point within the free body is clockwise. Tension was considered positive.

Sign conventions are identified in Figure 2.

The Prototype Frame

A hypothetical prototype frame, of the geometrical configuration shown in Figure 3, was selected as typical of the type of frame commonly used in farm buildings. Section properties were chosen, quite arbitrarily, by selecting a standard rolled steel section (8 x 4B15) with moment of inertia, $I = 48$ inches^4. It should be noted that the frame section is assumed to be constant throughout. Figure 4 shows shears, moments, and foundation reactions of this frame when loaded with a vertical downward load of 8,000 pounds at the peak. Fixed end conditions were assumed. Computed moments were 281,000 pound-inches at the base of each leg, -270,000 at the knee, and 264,000 at the peak.

It was known that, in an actual frame under the assumed loading, the supports would translate and rotate outward. The amount of lateral movement and rotation would depend on the loads applied to the supports by the frame and the characteristics of the foundations and supporting soil. Computations were made to determine the actions induced in the prototype frame by (a) horizontal displacement of the base without rotation; (b) rotation of the base without horizontal displacement; and, (c) combined rotation and displacement.

Effect of Lateral Displacement of Foundation

The foundation of one leg was considered to move outward horizontally a distance, Δ_1, with respect to the other leg of the frame.
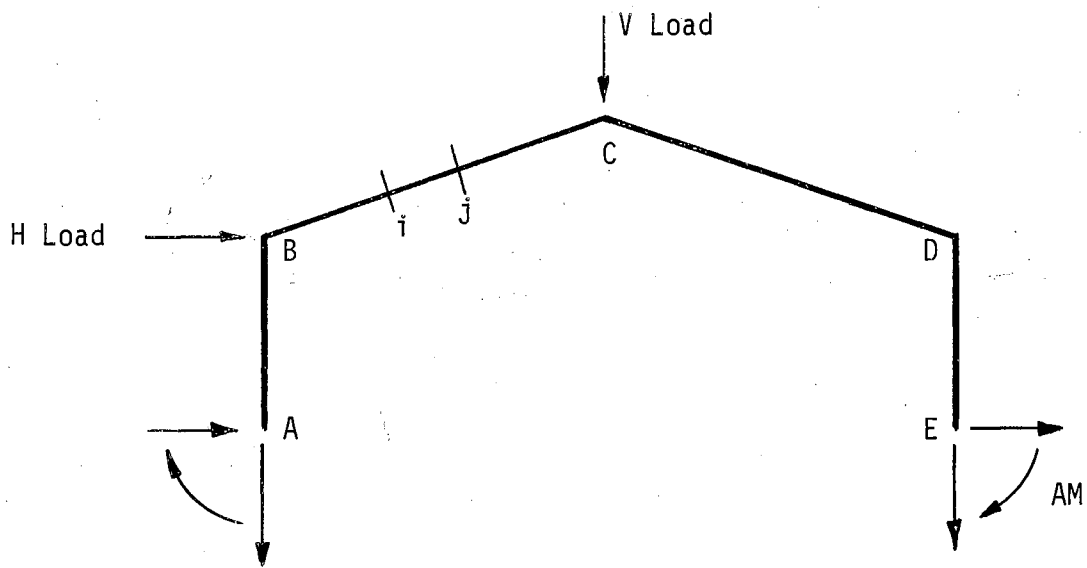
(a) External Forces and Moments, Positive Sense.
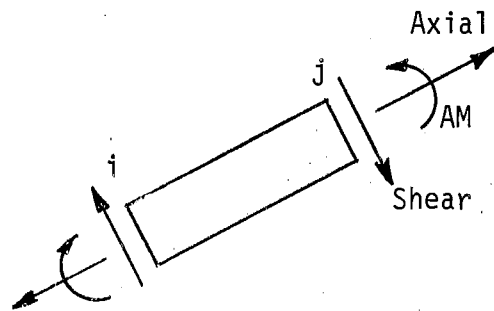
(b) Internal Actions, Positive Sense.

Figure 2. Sign Conventions and Variable Names Used in Computer Program.
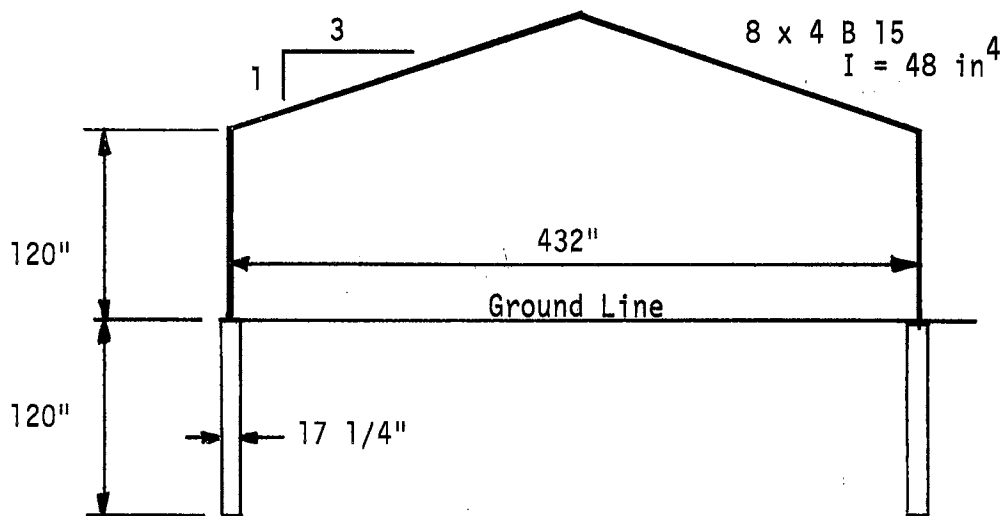
Figure 3. The Prototype Frame.
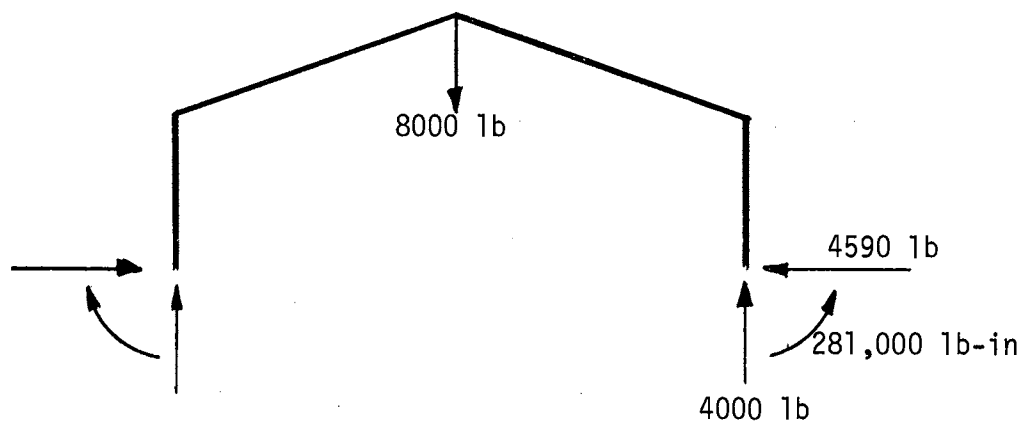
(a) Loads and Reactions, lb
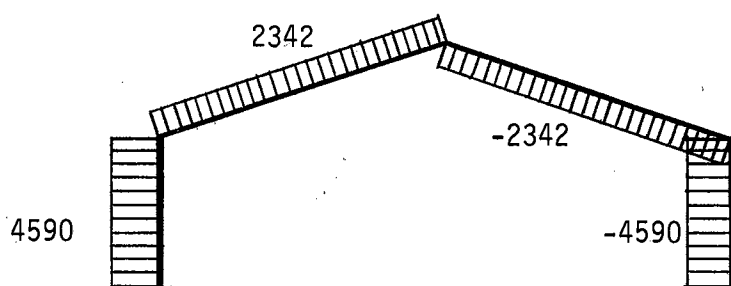
(b) Shear, lb
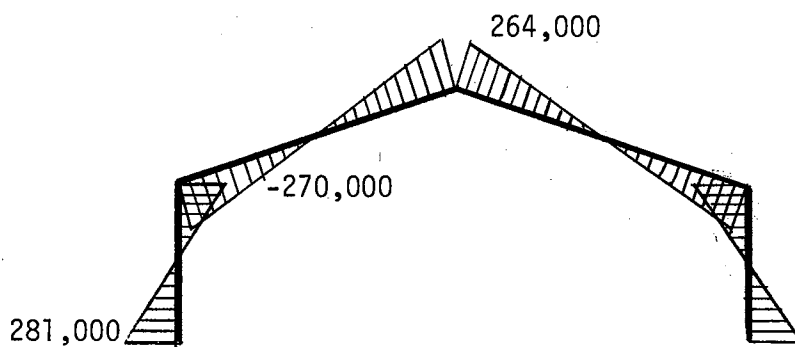
(c) Moment, lb-in

Figure 4. Loads and Actions of Prototype
Frame - Concentrated Load at
Peak.

This displacement was inserted into the deflection equation of the frame (one of three equations obtained by application of the unit load method and the principle of consistent deformations for this particular frame without external loads) and the system of equations solved for the three resulting redundant reactions. The remaining reactions, and the actions (shears and moments within the frame) were computed by application of statics. The reactions, shears and moments in this (prototype) frame as a result of a total foundation displacement of one inch, are shown in Figure 5. It should be noted that, under the usual assumption of linearly elastic material, the reactions and actions are linearly related to the frame stiffness (EI) and to the magnitude of the displacement; that is, for a steel frame of $I = 24$ inches^4 (half that of the prototype) the actions would be one-half of those shown, and if the displacement should be doubled, the actions will also be doubled.

It will be noted from Figure 5 that the outward displacement of the foundation causes a pronounced negative moment (outer fibre in tension) at the base, a small negative moment at the haunch, and a moderate positive moment at the peak.

Effect of Rotation of the Foundation

Symmetrical Rotations

If, as would be expected in a case of symmetrical gravity loading, both foundations rotate outward symmetrically, the induced actions are as shown in Figure 6. Maximum negative moments occur at the bases of the legs, and a positive maximum at the peak. If each support undergoes a rotation of 0.01 radian, the maximum moment induced in the prototype
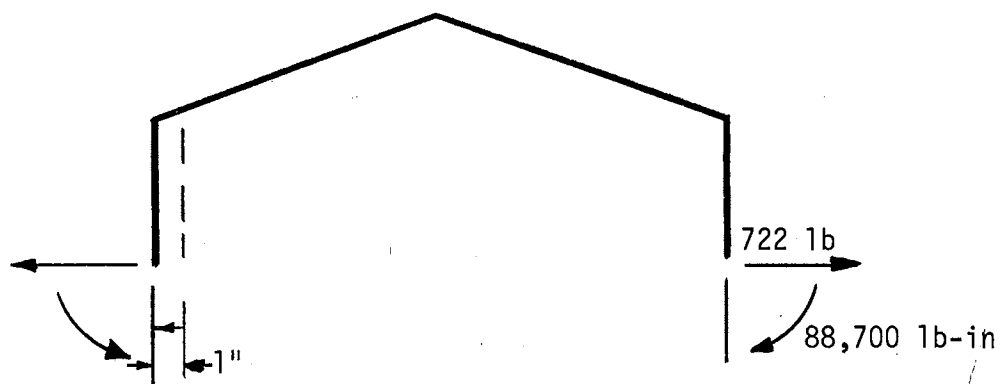
(a)   Reactions
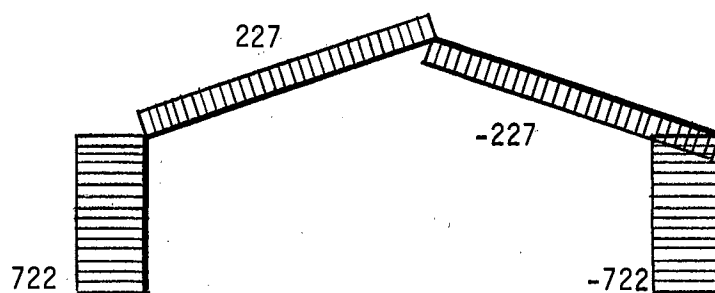
(b)   Shear, lb
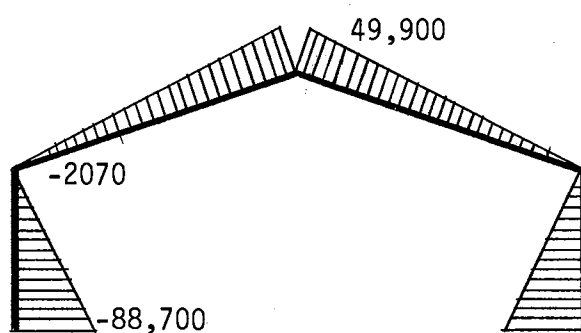
(c)   Moment, lb-in

Figure 5.   Reactions, Shears, and Moments in
Prototype Frame Due to
Foundation Displacement
of 1 Inch.
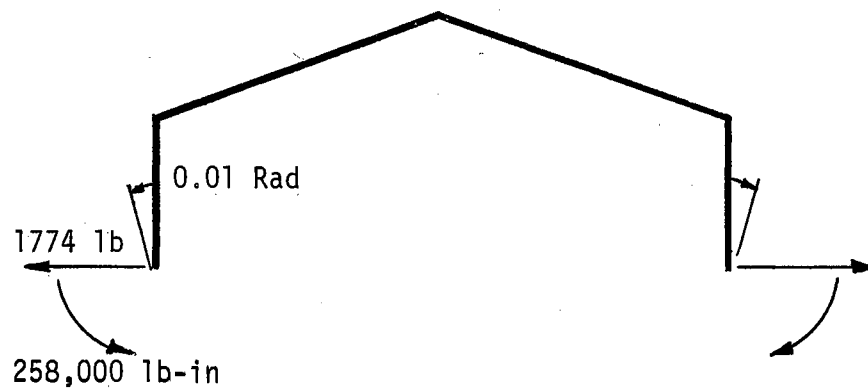
(a) Reactions
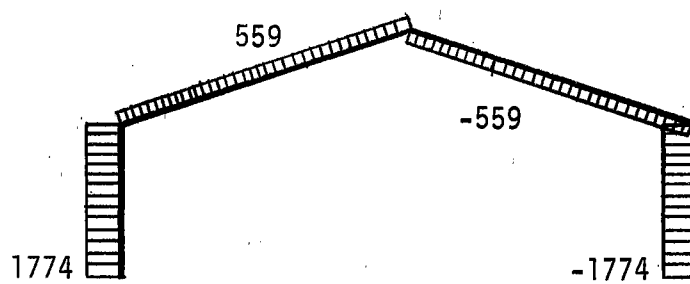
(b) Shear, lb
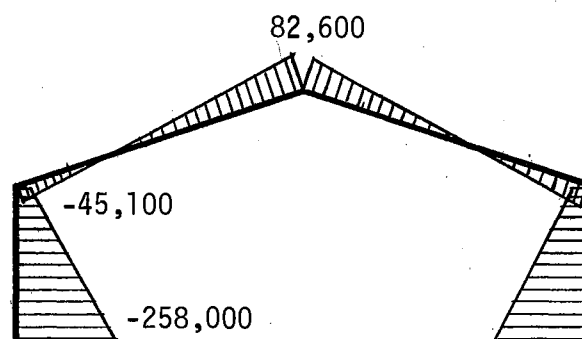
(c) Moment, lb-in

Figure 6.   Reactions, Shears, and Moments in
             Prototype Frame Due to
             Symmetrical Foundation
             Rotations of 0.01
             Radian.

frame at the base of each leg is -258,000 pound-inches and at the peak is 82,600 pound-inches.

Anti-Symmetrical Rotations

If the two foundations rotate anti-symmetrically (e.g., both to the right) without relative displacement, uniform moments are developed in the legs, positive in the left leg, negative in the right. Moments in the rafter members vary linearly from maximum at the haunch to zero at the peak. The shear and moment diagrams, and reactions, computed for foundation rotations of 0.01 radian to the right, are shown in Figure 7. It will be noted that no horizontal thrusts are developed in this case, and no shear exists in the legs.

Rotation of a Single Pier

If one pier rotates without displacement, while the other remains fixed, the actions developed in the frame are as shown in Figure 8. The values shown are for an outward rotation of the right leg of 0.01 radian. The maximum negative moment of -165,000 pound-inches at the base of the leg attached to the rotating foundation changes uniformly to a maximum of 41,300 pound-inches at the peak, then decreases again to a maximum of -93,400 pound-inches at the base of the immovable leg.

Combined Rotation and Deflection

It is most unlikely that the foundations of an actual frame would rotate without relative displacement (except in the special case of anti-symmetric rotation, which is itself not probable). It is even less probable that relative displacement of pier foundations would
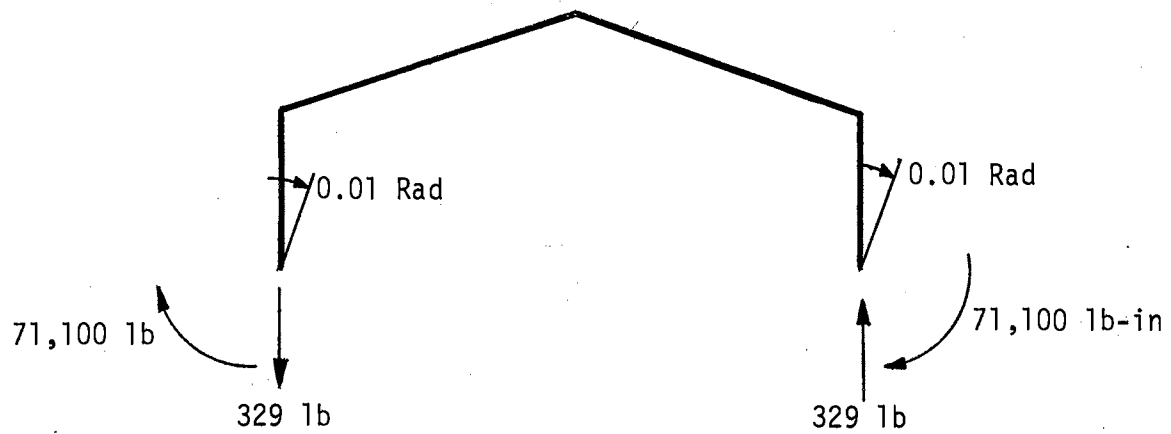
(a) Reactions
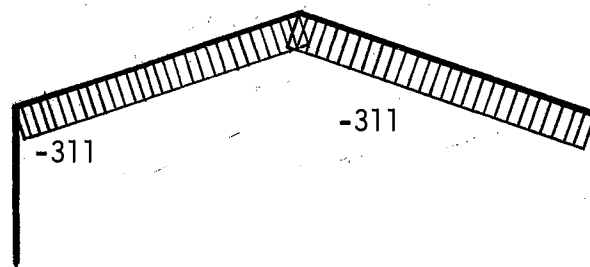
(b) Shear, lb
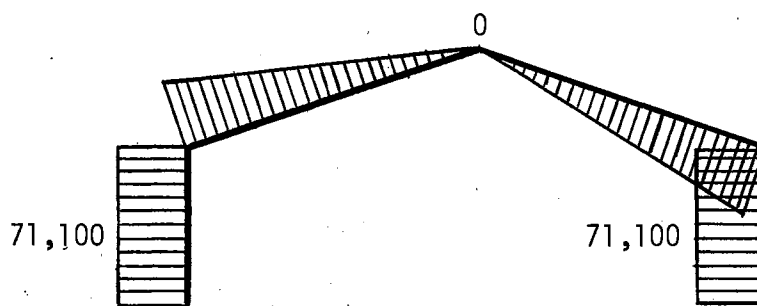
(c) Moment, lb-in

Figure 7. Reactions, Shears, and Moments in Prototype Frame Due to Anti-symmetric Rotations.
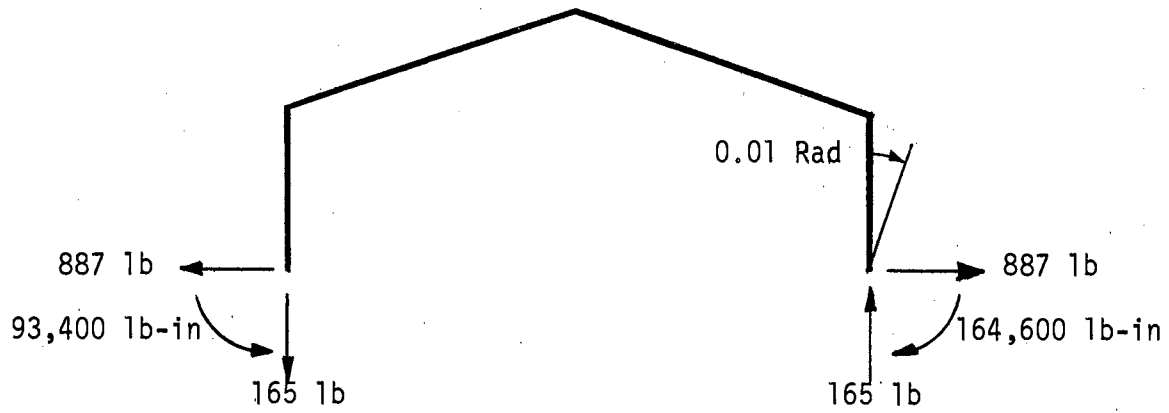
(a) Reactions
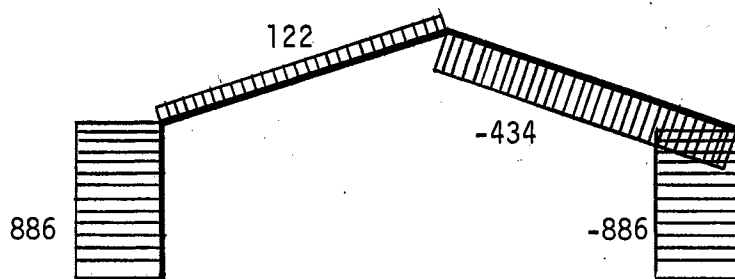
(b) Shear, lb
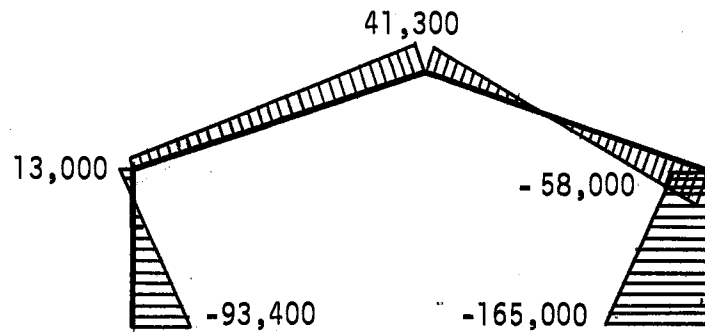
(c) Moment, lb-in

Figure 8. Reactions, Shears, and Moments in
Prototype Frame Due to Rotation
of Right Foundation.

occur without accompanying rotation. In most real structures
combinations of displacement and rotation are to be expected.

The effects of relative displacement and rotation may be combined
(provided the stress-strain response of the structural material is
linear) by superposition. Superposition may, of course, also be used
to determine the combined effects of unequal rotations and accompanying
displacement of the two foundations.

The prototype frame was considered to be supported on two
cylindrical piers, each 120 inches long. If the piers are assumed to
rotate as rigid bodies, the ground line displacement of one pier with
respect to the other may be computed, provided the rotations and the
depth to points of rotation are known. Assuming the point of rotation
at 0.7 times the depth of embedment, which approximates the value re-
ported for sands by Shilts, et al. (27), Kent (37), and Walker and Cox
(36), and considering symmetric rotations of 0.01 radian, the ground
line displacement of one pier relative to the other becomes

$$2 \times 0.7 \times 120 \times 0.01 = 1.68 \text{ inches}$$

Multiplying the values of actions and reactions for a deflection
of one inch, shown in Figure 5, by 1.68 gives:

$$HA = -1230 \text{ lb}$$

$$MA = -149,000 \text{ lb-in}$$

$$MB = -3480 \text{ lb-in}$$

$$MC = 83,830 \text{ lb-in}$$

$$VA = 1230 \text{ lb}$$

$$VB^1 = 382 \text{ lb}$$

where

HA   is horizontal reaction at A

MA   is moment at A

VA   is shear at A

VB^1 is shear in member BC at B

From Figure 6, the actions due to symmetrical rotations of 0.01 radian are:

> HA = -1774 lb
>
> MA = -258,000 lb-in
>
> MB = -45,100 lb-in
>
> MC = 82,600 lb-in
>
> VA = 1774 lb
>
> VB^1 = 559 lb

Summing, the effects of combined symmetrical rotation and displacement are:

> HA = -3004 lb
>
> MA = -407,000 lb-in
>
> MB = -48,600 lb-in
>
> MC = 166,400 lb-in
>
> VA = 3004 lb
>
> VB^1 = 941 lb

Shear and moment diagrams for the combination are shown in Figure 9.

Effect of Differential Settlement of the Foundations

Uniform vertical settlement of the piers will have no effect on the action of the frame. However, differential settlement may occur. This may be caused by unequal vertical loading of the piers, variation
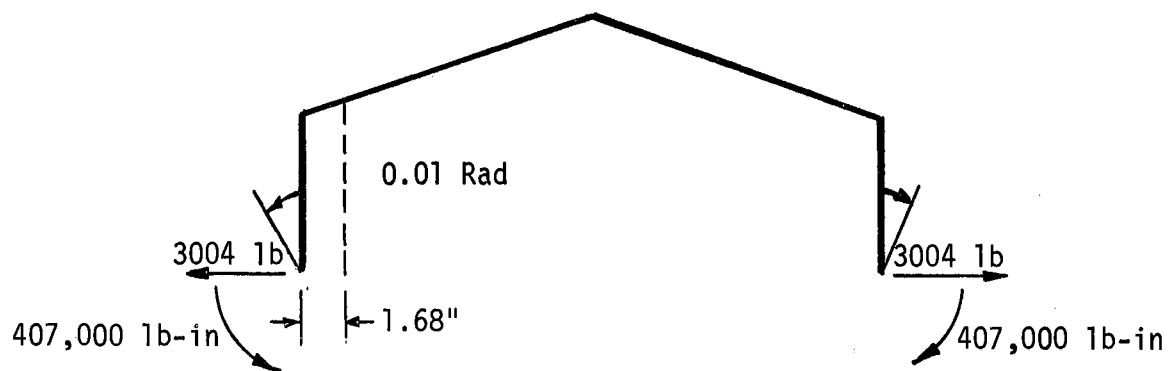
(a) Reactions
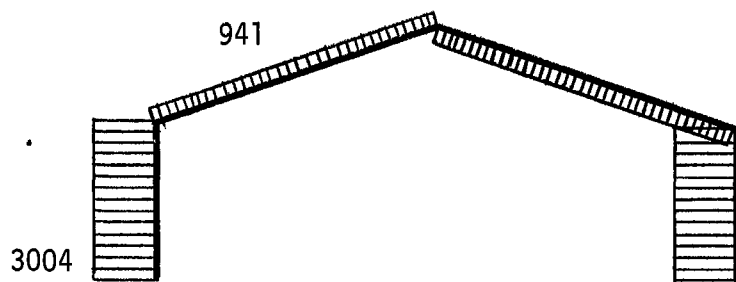
(b) Shear
Scale 1" = 10,000 lb
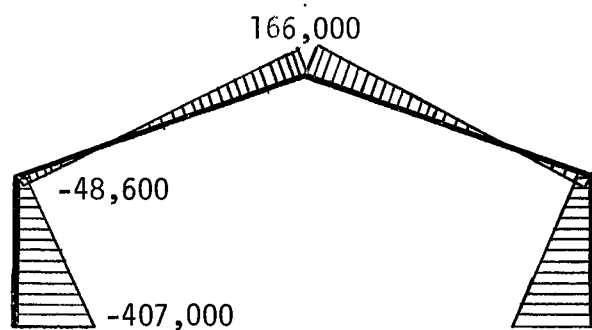
(c) Moment
Scale 1" = 1,000,000 lb-in

Figure 9. Reactions, Shears, and Moments in
Prototype Frame Due to Displace-
ment of 1.68 in and Symmetric
Rotations of 0.01 Rad.

in pier dimensions, variation in soil conditions between the piers, or unequal frost heaving. Such a differential settlement is structurally equivalent to anti-symmetric rotations of the piers, provided the settlement is small. (If settlements are large, the changes in orientation of frame axes will require special consideration of gravity loads.) A differential vertical settlement, δ_v, of one inch with a frame of span ℓ inches, is equivalent to δ_v/ℓ = 1/432 = 0.0023 radian of anti-symmetric rotation for the prototype frame. Large equivalent rotations are unlikely, as the piers may be expected to rotate in a direction to partially relieve the moments developed in the frame.

Effects of Foundation Movements on Loaded Frame

The effects of external loads may be combined with the effects of foundation movements by means of superposition. This has been done for the prototype frame using typical load systems and foundation movements which were considered to be consistent with the particular load system. In each case, the frames are spaced 16 feet between centers, with girts at 2.0 feet spacing and purlins at 1.8 feet spacing. Distributed loads are considered to be applied through the girts or purlins as a series of concentrated loads.

Snow and Dead Load

The prototype frame was considered to be loaded with a total (live and dead load) roof load of 30 pounds per square foot of horizontal projected area. This amounted to a load of 865 pounds at each interior purlin spaced 1.8 feet between centers, and 432 pounds at each eave purlin. Shear and moment in the frame, assuming complete fixity at the supports, is shown in Figure 10.

865 lb

432 lb

6171 lb

6171 lb

351,000
lb-in

351,000
lb-in

8649 lb

8649 lb

(a) Loads and Reactions

5844 lb

-1945 lb

-6171 lb

(b) Shear
Scale 1" = 20,000 lb

101,000

152,000

-389,000

351,000
lb-in
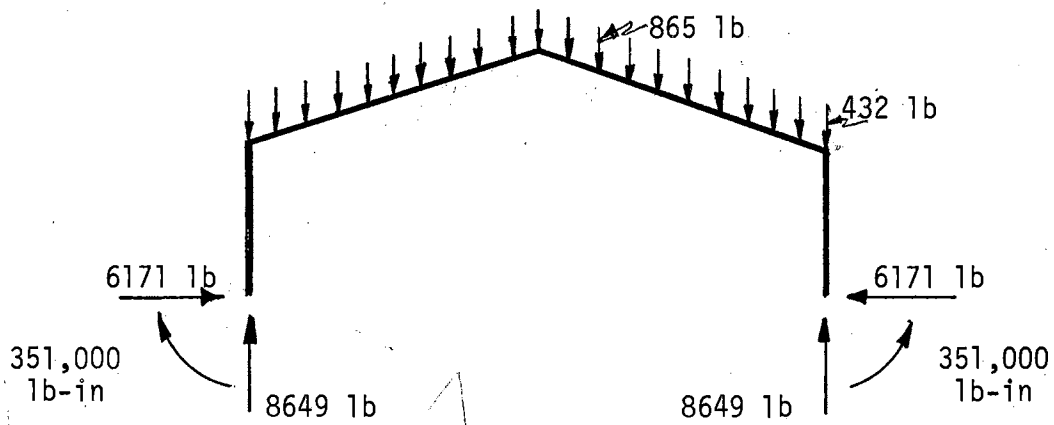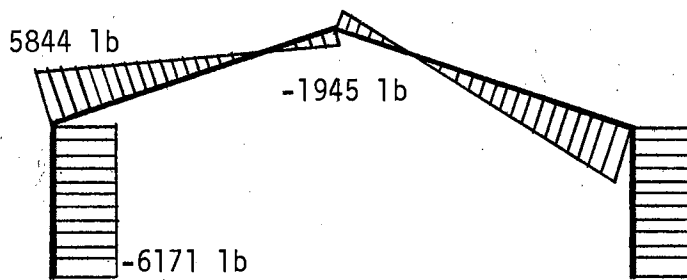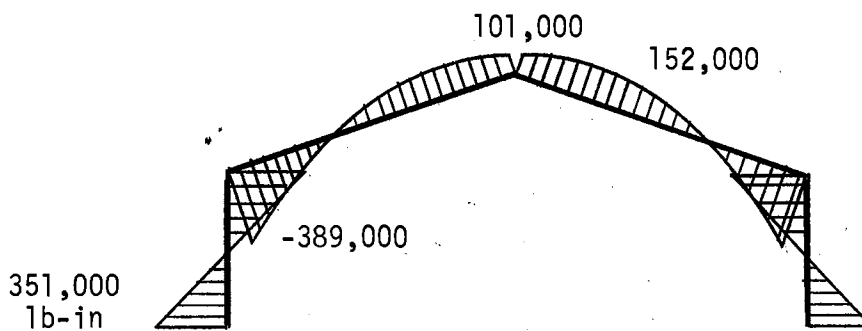
(c) Moment
Scale 1" = 1,000,000 lb-in

Figure 10. Reactions, Shears, and Moments Due to Roof Load,
With Supports Fixed.

Under these conditions of loading, with positive moment at the bases, the thrust and moment applied to the foundation may be expected to cause symmetrical outward rotation and displacement of the piers. For assumed rotations of 0.005 radian and corresponding displacements of 0.84 inch, the shear and moment resulting from the above load with pier displacement are shown in Figure 11. The values shown were computed by superposition of Figures 9 and 10.

The result of pier displacement, in this system of loading, is to greatly decrease the moment at the base, to slightly increase the moment at the knee, and to considerably increase the moment at the peak.

The result of the foundation movement is to reduce the capacity of the frame to withstand the vertical roof loads, due to the increase in moment and corresponding increase in stress at the knee. The increased moment at the peak would not affect the capacity of the frame if the frame were of constant section. However, if the frame section is reduced at the peak, then the change in moment at this point would require consideration.

Wind Load

Actions in the prototype structure were computed for wind load with the wind direction in the plane of the frame. Wind loads were computed for a 50-year recurrence interval using the method described in ASAE Data R288 (62) for Central Oklahoma. Computed loads at each purlin and girt are shown in Figure 12a. Actions and foundation reactions for the frame, with fixed supports assumed, are shown in Figure 12. A maximum moment (negative) of -160,000 pound-inches exists at the base of the windward leg, in conjunction with a horizontal thrust of 2600 pounds. Reactions at the base of the leeward leg are much smaller.

(a) Loads and Reactions

(b) Shear, lb
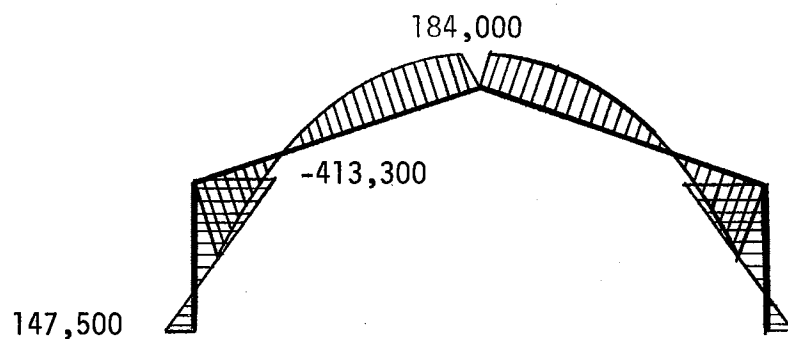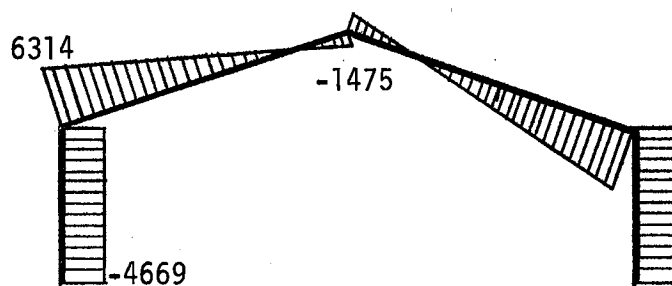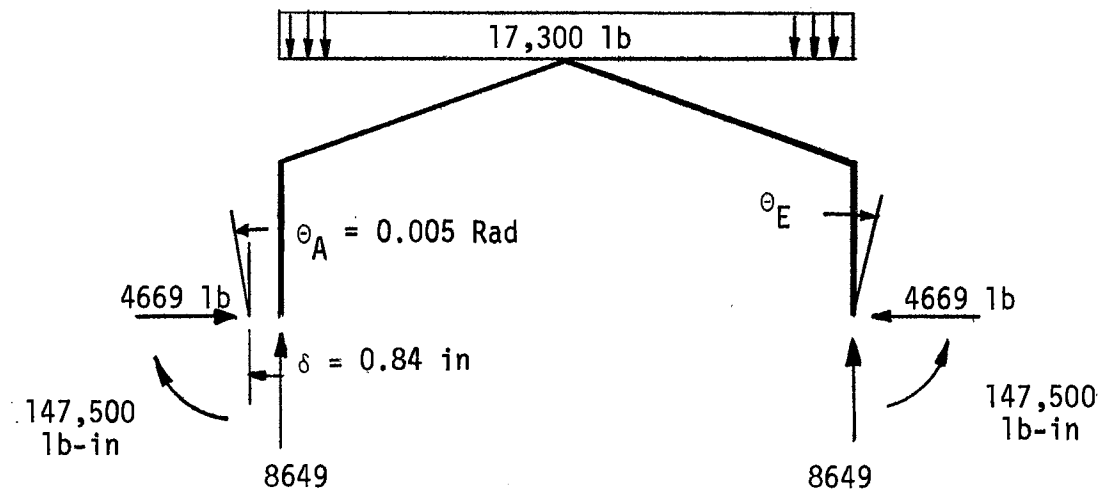
(c) Moments, lb-in

Figure 11. Reactions, Shears and Moments Due To
Roof Load With Support Movement.
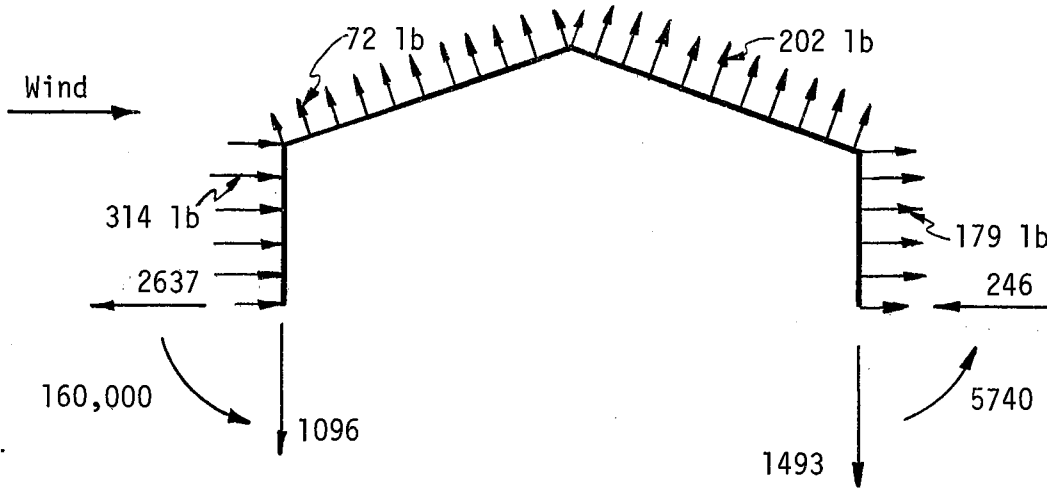
(a) Loads and Reactions
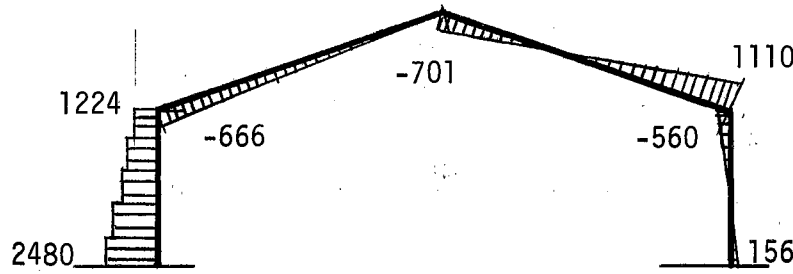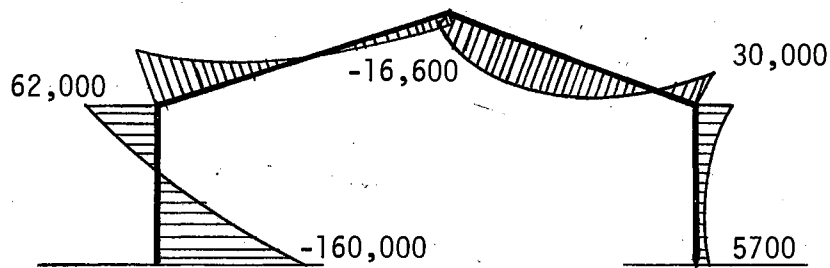
(b) Shear

(c) Moment
Scale 1" = 200,000 lb-in

Figure 12. Reactions, Shears, and Moments Due To
Wind Load, Bases Fixed.

Because of the much greater reactions developed at the windward leg than at the leeward leg, the most probable foundation movement is an inward rotation and accompanying displacement of the windward pier, with the leeward pier remaining relatively stationary.

The results of an inward rotation of the windward pier through an angle of 0.005 radian, with an accompanying displacement of the pier top 0.42 inch inward, on the frame actions are shown in Figure 13. The moment at the critical windward foundation region is substantially reduced, while moments at the knee and peak are increased considerably (but to much lower values than the initial moment at the windward leg). The moment at the leeward knee is reduced slightly, and that at the leeward footing greatly increased, though it is still much less than the maximum moment occurring at the windward support in the fixed leg case.

The result of such a foundation deflection is, for this type of loading, to increase the load-carrying capacity of the frame. In effect, the resisting moments which were critical at the base of the windward leg in the fixed base case are replaced by increased moments in the less critical areas--the windward haunch, the peak, and the leeward support. Shears are also partially equalized throughout the frame.

Grain Bin Loads

Farm buildings are frequently used to store grain. The pressure of grain against the building walls is usually assumed to be horizontal (for shallow bins) and to be equal to the Rankine active pressure:

$$p = wh \tan^2 \left(45° - \frac{\phi}{2}\right)$$
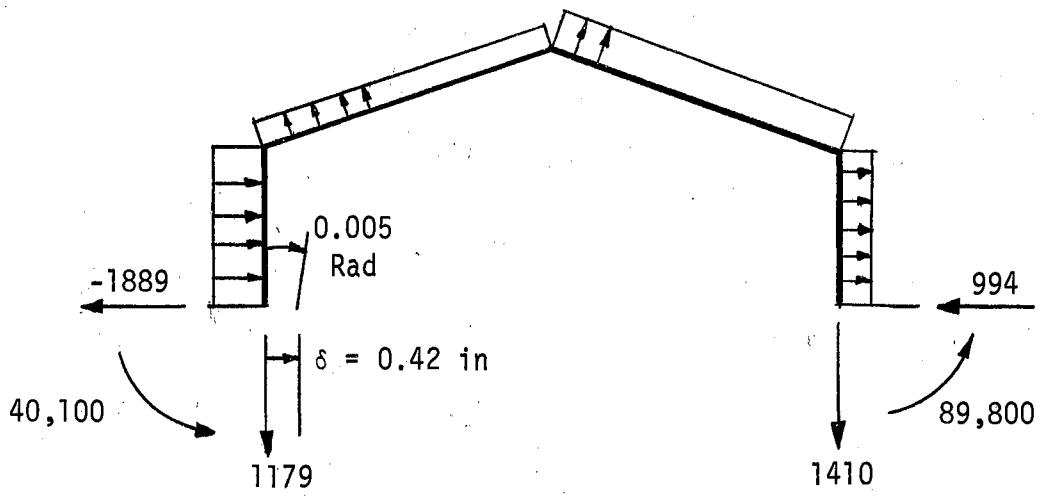
(a) Loads and Reactions
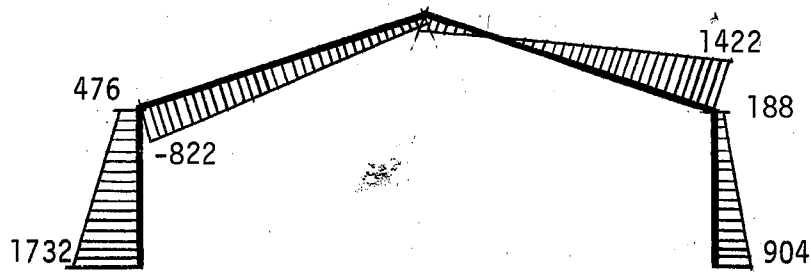
(b) Shear
Scale 1" = 5000 lb
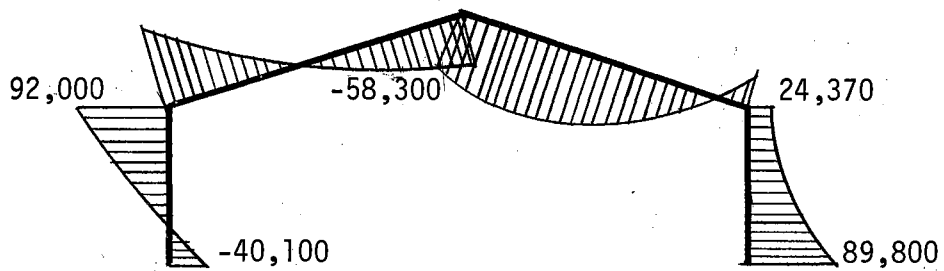
(c) Moment
Scale 1" = 200,000 lb-in

Figure 13. Reactions, Shear and Moment Due To Wind
Load, With Rotation of Left Pier.

where

p = horizontal pressure, lb_f per ft^2

w = specific weight of the grain, lb_f per ft^3

h = depth of grain, ft

Φ = angle of internal friction, degrees.

For the building in question the lateral pressures on the walls were computed assuming the building to be filled with wheat level with the eaves. The wall loads were distributed among the girts, resulting in the loading shown in Figure 14a.

This type of load is characterized, in a hingeless frame, by high moments and shears at the bases of the frame, a moderately high negative moment at about three-fifths of the wall height, and moderate actions throughout the remainder of the frame. Shears, moments, and foundation reactions for this loading, with the supports considered fixed, are shown in Figure 14.

Due to the moment and shear transmitted to the foundation, the piers may be expected to rotate outward, with accompanying relative displacement.

Each pier was considered to have rotated outward by 0.005 radian, with an accompanying relative displacement of 0.84 inch. The resulting reactions, shears and moments in the loaded frame are shown in Figure 15.

The effect of foundation movement is to moderately reduce the critical shear at the base, to greatly reduce the moment at the base, and to increase the moment near the three-fifths points in the legs. Moments and shears at other points in the frame are increased significantly, but in the example, nowhere do they approach the magnitude of the initial (fixed end) base moment.
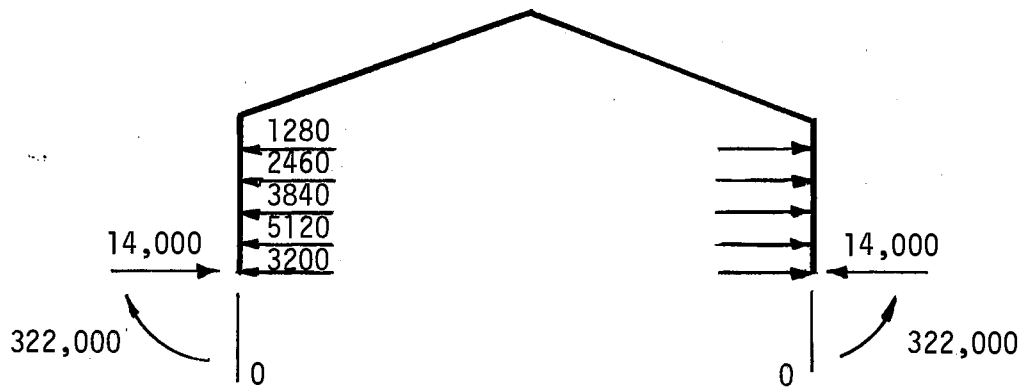
(a) Loads and Reactions
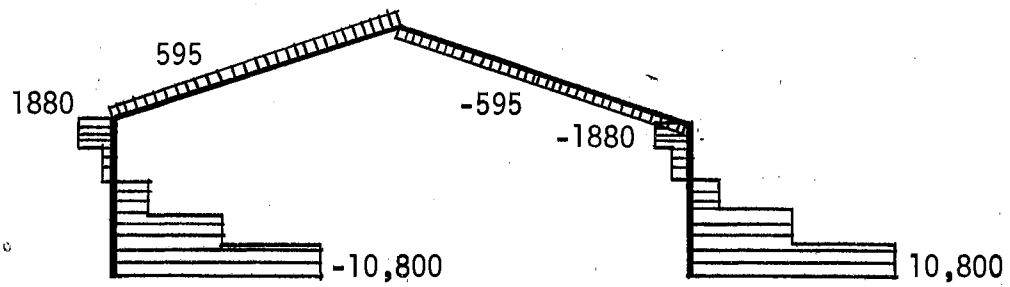
(b) Shear
Scale 1" = 10,000 lb
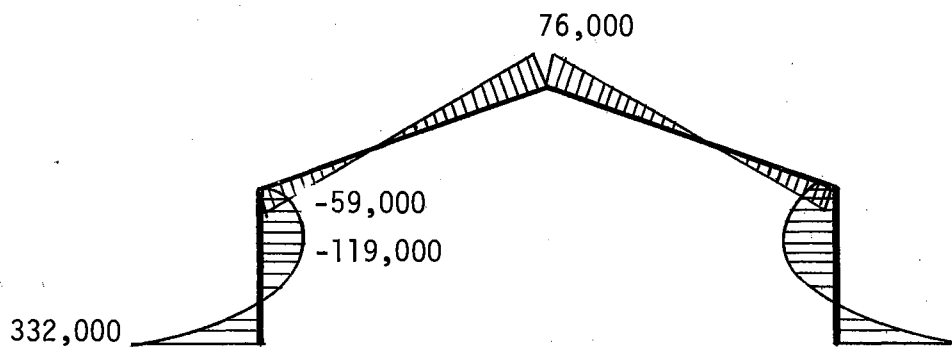
(c) Moment
Scale 1" = 500,000 lb-in

Figure 14. Reactions, Shears and Moments Due To
Grain Bin Loading, Fixed Supports.
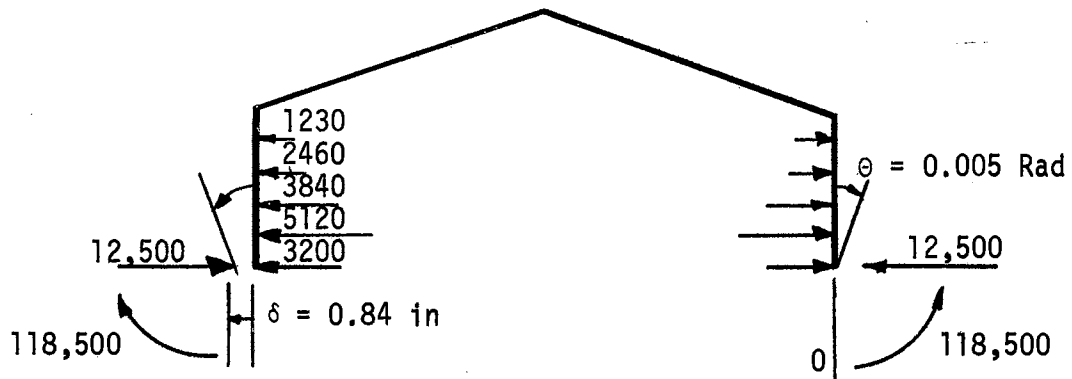
(a) Reactions
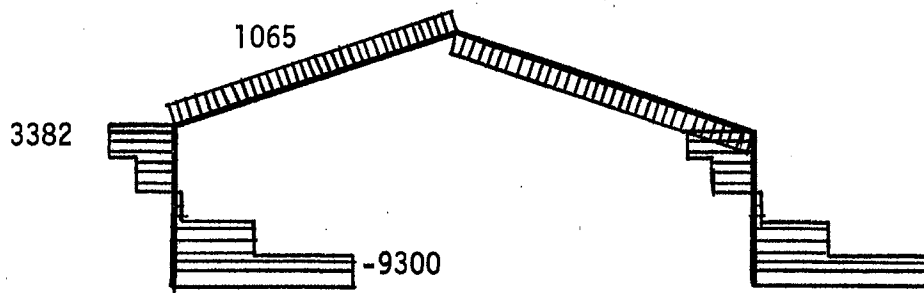
(b) Shear
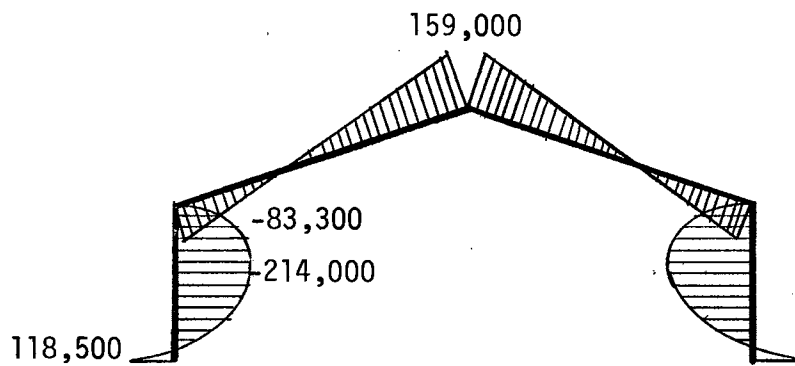
(c) Moment
Scale 1" = 500,000 lb-in

Figure 15. Reactions, Shears and Moments Due To
Grain Bin Loading With Foundation
Movement.

Consequently, for this type of loading, the effect of foundation displacement is to increase the load-carrying capacity of a constant-section frame, by reducing moment and shear at the most critical regions, and increasing them in less critical areas.

Summary

A number of loading conditions, typical of farm buildings, were investigated using an arbitrary design of hingeless rigid frame. Frame actions (shears and moments) and reactions were computed and plotted for each loading system, with full fixity of the supports assumed.

Using these reactions to infer the type of response of yielding foundations, foundation movements of arbitrary magnitude were introduced into the analysis, and actions and reactions computed again.

In the case of a vertical distributed roof loading, the effect of the expected foundation movements was to reduce the load capacity of the frame, mainly through an increase in moment at the knee. However, with wind load and with grain load, which typically involve high moment at one or both supports, the effect of foundation movement was to reduce this critical moment, as well as the maximum shear, and increase the moment at less highly stressed regions of the frame. In consequence, for these two types of loading the load capacity of the frame was increased by the foundation movement.

For general types of loading it appears that for those load systems which are characterized by critical moment at the haunches, the peak, or within the rafters, the capacity of the frame will be decreased by the expected type of foundation movement. On the other hand, where the load induces high moments or shears at the base of the frame, movement

of the foundations in response to the actions applied by the frame are beneficial in redistributing moment and reducing critical stresses.

No attempt has been made in this analysis to evaluate the magnitude of foundation movements. The amounts of foundation movement were selected quite arbitrarily. Computation of foundation movements will be discussed in Chapter VII.

CHAPTER IV

DESIGN OF THE EXPERIMENTS

Earlier investigations had reported only one component of the
motion of piers. Beckett (30) and Rice (63) had investigated the hori-
zontal deflection of poles at some arbitrary distance above ground line.
Kondner and Green (32) had developed prediction equations for the hori-
zontal displacement at the ground line. Welch (64) had investigated the
rotation of piers, but had not studied ground-line deflection. The
action of a hingeless frame supported by yielding piers is influenced
by both rotation and horizontal deflection of the piers. In order to
apply any of the prediction equations developed by the above authors, it
would have been necessary to make some assumption regarding the relation-
ship between deflection and rotation. Assuming some specific point as
the center of rotation would have served this purpose, but it appeared
desirable to avoid arbitrary assumptions which might have been in error.
Consequently, an experiment ("the pier experiment") was designed to
develop prediction equations for both the horizontal ground-line deflec-
tion and the rotation of a cylindrical pier subjected to various
combinations of horizontal thrust and moment.

At the time the pier experiment was being planned, a method of
analyzing rigid frames (Chapter VIII) on yielding pier foundations was
being developed. It appeared desirable to check the behavior of such
frames, predicted by the analysis method, by observation of an actual

frame. In order to do this, a second experiment ("the frame experiment") was planned involving the testing of a model frame and conducted at the same time as the pier experiment.

Dimensional Analysis

The method of dimensional analysis permits simplification of an experimental study, and makes the results of the study more general in application. The method, briefly, consists of selecting the "n" independent variables, defined in "m" fundamental dimensions, which describe the phenomenon to be investigated; grouping these "n" independent pertinent quantities by multiplication into dimensionless parameters (of which there will usually be (m-n)); and then varying the dimensionless parameters, one at a time, through the appropriate ranges of values (65). The resulting set of component equations are then combined, following specified principles described by Murphy (66), to form a prediction equation which adequately describes the phenomenon observed within the ranges investigated.

A particular application of the method of dimensional analysis is in establishing the validity of models. If a model is designed using the principles of dimensional analysis, the results obtained from it should be valid for the prototype. Results obtained from a model which violates these principles cannot safely be extended to other objects.

In the analysis which follows, the frame and the foundation pier were analyzed separately, validity of the proposed models established separately, and then the compatibility and continuity requirements were applied to establish the required relationships between frame and pier in the complete model.

Dimensional Analysis of the Frame

Pertinent Quantities

The geometric variables and actions involved in the frame analysis
are shown in Figure 16, and all pertinent quantities listed in Table I.
In order to simplify the analysis and the experiment as much as possible,
it was decided to limit the experiment to symmetrical frames with sym-
metrically placed loads, with constant modulus of elasticity and moment
of inertia, and to minimize shear and axial deflection by the use of a
rectangular cross-section.

The pertinent quantities in Table I were combined, following the
method of dimensional analysis described by Murphy (66) to form dimen-
sionless parameters (pi terms). By combining E and I into one quantity,
EI, the number of quantities was reduced to ten, and the number of
required pi terms was eight. The pi terms selected are listed in
Table II.

Discussion of Pertinent Quantities and Dimensionless Parameters

In selecting pertinent quantities, only those quantities which
enter into a conventional linearly-elastic frame analysis were
considered. As a result of this, stresses in the frame did not appear
in the analysis, but the assumption of linear elastic action added the
restriction, both in the model and the prototype, that at no point does
the existing stress exceed the yield point of the material.

Furthermore, the effects of axial and shear stresses were
disregarded. In usual frame designs deflections resulting from shear
are small and are ignored. In the proposed model, the section shape
selected was such as to reduce these effects to extremely low values.
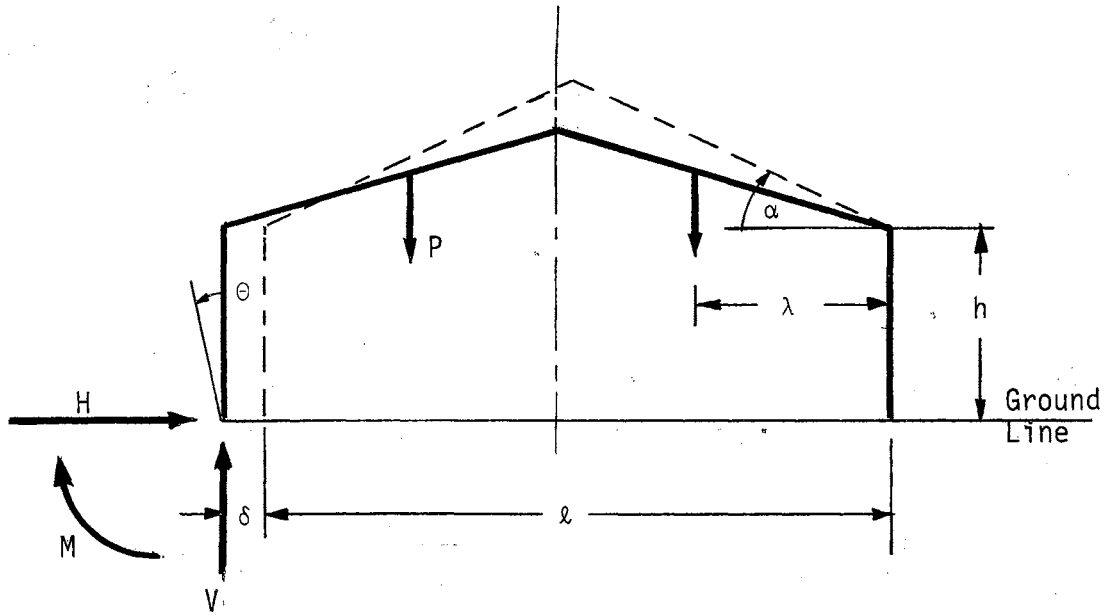
Figure 16.   Pertinent Quantities of the Frame
Geometry.

TABLE I

FRAME PERTINENT QUANTITIES

1	E	Modulus of elasticity	lb_f-in^{-2}	FL^{-2}
2	I	Moment of inertia	in^4	L^4
3	ℓ	Span	in	L
4	h	Leg height	in	L
5	α	Angle of rafter from horizontal	rad	-
6	P	Any load, symmetrical	lb_f	F
7	H	Horizontal thrust at ground	lb_f	F
8	M	Moment at ground	lb_f-in	FL
9	δ	Horizontal movement at ground	in	L
10	Θ	Rotation at ground	rad	-
11	λ	Other pertinent lengths	in	L

TABLE II

DIMENSIONLESS PARAMETERS FOR FRAME

$$\Pi_1 = \alpha$$

$$\Pi_2 = h/\ell$$

$$\Pi_3 = P\ell^2/EI$$

$$\Pi_4 = \delta/\ell$$

$$\Pi_5 = \Theta$$

$$\Pi_6 = H\ell^2/EI$$

$$\Pi_7 = M\ell/EI$$

$$\Pi_8 = \lambda/\ell$$

Application of conventional structural theory showed that, subject to the above restrictions, the variables δ, the horizontal deflection of the frame base, and Θ, the rotation of the frame base, could each be expressed in terms of the other eight variables; alternately, in terms of the dimensionless parameters, π_4 and π_5 could each be expressed in terms of the other six pi terms, leading to two general relations:

$$\pi_4 = f(\pi_1, \pi_2, \pi_3, \pi_6, \pi_7, \pi_8)$$
$$\pi_5 = g(\pi_1, \pi_2, \pi_3, \pi_6, \pi_7, \pi_8)$$

Design and Operating Conditions for the Frame Model

Due to the predominance of geometric factors in the dimensionless parameters of the frame, it was clearly advantageous to try to maintain geometric similarity between model and prototype. However, due to the difficulty of precisely modelling the frame cross-section, both from the standpoint of constructing the model and the possibility of lateral instability during testing of an isolated model, distortion of the cross-section appeared advantageous. It had already been decided to disregard shear and axial stress effects; consequently, distortion of the cross-section did not require compensation, provided that the moment of inertia was properly modelled. A rectangular cross-section, with the minor axis in the plane of loading, was selected because it would be easy to construct, and would minimize possible lateral stability problems. Steel was selected as the material for the model.

Two scales for the model resulted; these were n_1, a length scale, defined by $n_1 = \lambda p/\lambda m$ where

λp = any pertinent length of the prototype

λm = corresponding length of the model,

and n_2 = the moment of inertia scale defined by $n_2 = E_p I_p / E_m I_m$ where

I_p = moment of inertia of prototype

I_m = moment of inertia of model

E_p = elastic modulus of the prototype

E_m = elastic modulus of the model

$n_2 = I_p / I_m$ for the material selected, where $E_p = E_m$

Applying the requirements for a true model, as outlined in Murphy (66), that corresponding pi terms be equal in model and prototype, led to the design and operating conditions following:

1. Geometric similarity (except for cross-section)

2. Material the same (steel) in both model and prototype

3. $P_m = n_1{}^2/n_2 \ P_p$ where P_m is model loading; P_p is prototype load

4. $H_m = n_1{}^2/n_2 \ H_p$

5. $M_m = n_1/n_2 \ M_p$

6. $I_m = 1/n_2 \ I_p$.

Dimensional Analysis of a Rigid Pier Foundation

Pertinent Quantities

Pertinent quantities believed to be applicable to the overturning of a rigid foundation pier embedded in cohesionless soil are shown in Figure 17 and Table III.

It was believed that δ and Θ could each be expressed in terms of the other seven variables. Thus the two equations among eight variables each were expected. Combining these variables into dimensionless parameters resulted in six dimensionless pi terms for both of the two relations. These pi terms are shown in Table IV, and may be combined into the general equations:

Figure 17. Pertinent Quantities of the Pier Geometry.

TABLE III

PERTINENT QUANTITIES, RIGID PIER IN SAND

1	B	Width or diameter of pier	in	L
2	D	Depth of pier below ground	in	L
3	γ	Effective specific weight of soil	lb_f/in^3	FL^{-3}
4	ϕ	Internal friction angle of soil	rad	-
5	δ	Horizontal movement at ground	in	L
6	Θ	Rotation at ground	rad	-
7	H	Horizontal thrust at ground	lb_f	F
8	M	Ground line moment	lb_f-in	FL
9	N	Number of load applications	---	-

TABLE IV

DIMENSIONLESS PARAMETERS FOR PIER

$$\Pi_1 = D/B$$

$$\Pi_2 = H/B^3\gamma*$$

$$\Pi_3 = M/HD = L/D**$$

$$\Pi_4 = \delta/B$$

$$\Pi_5 = \phi$$

$$\Pi_6 = \Theta$$

$$\Pi_7 = N$$

*Π_2 was changed in the analysis to
$\Pi_2/\Pi_1 = H/B^2D\gamma$

**L = Height of thrust line above ground
= M/H

$$\Pi_4 = f(\Pi_1, \Pi_2, \Pi_3, \Pi_5, \Pi_7)$$

$$\Pi_6 = g(\Pi_1, \Pi_2, \Pi_3, \Pi_5, \Pi_7).$$

Discussion of Pertinent Quantities and Dimensionless Parameters

The pertinent quantities selected were believed to adequately define the response of cylindrical piers embedded in cohesionless soil to overturning actions, provided that time-dependent effects, and the effects of previous stress history, could be minimized. It was planned to minimize time-dependent effects by using a loading schedule which would permit equilibrium to be fully established after each load increment, before measuring deflections. The effects of previous loads were controlled by establishing a standard load cycle for the tests involving repeated loads.

The four variables, H, M, Θ and δ appearing in the pier analysis were the same variables appearing in the frame analysis in the case of a hingeless frame. If a two-hinged frame is considered, the M term would disappear and the Θ term would not be the same in the frame and the pier.

Design and Operating Conditions

Setting corresponding pi terms equal in model and prototype led to the design and operating conditions for the model pier. The model length scale was defined as $n_3 = \lambda p/\lambda m$ where λ is any pertinent length, and the sand to be used was considered to be identical in both model and prototype, so that $\phi p = \phi m$. Design and operating conditions thus were:

1. $\phi m = \phi p$

2. Geometric similarity between model and prototype, with
   $$\lambda_m = \lambda_p/n_3$$

3. $H_m = H_p/n_3^3$

4. $M_m = M_p/n_3^4.$

Relating Pier and Frame Conditions

From the analysis of the frame the following conditions were established (in addition to geometric similarity):

$$P_m = \frac{n_1^2}{n_2} P_p$$

$$H_m = \frac{n_1^2}{n_2} H_p$$

$$M_m = \frac{n_1}{n_2} M_p$$

and from the pier analysis

$$H_m = \frac{1}{n_3^3} H_p$$

$$M_m = \frac{1}{n_3^4} M_p .$$

As a result of the continuity of actions and displacements between the frame and pier of a hingeless frame:

H frame = H pier

M frame = M pier

Θ frame = Θ pier

δ frame = δ pier.

Applying the first two of these for the model, and substituting from above, led to:

$$H_m = \frac{n_1^2}{n_2} H_p = \frac{1}{n_3^3} H_p$$

$$\frac{n_1^2}{n_2} = \frac{1}{n_3^3}$$

$$M_m = \frac{n_1}{n_2} M_p = \frac{1}{n_3^4} M_p$$

$$\frac{n_1}{n_2} = \frac{1}{n_3^4}$$

leading to

$$n_1 = n_3$$

$$n_2 = n_1^5.$$

That is, that the length scales in frame and pier should be the same, n_1, and the moment of inertia scale be n_1^5.

Experimental Schedule: The Pier Experiment

The pier experiment was planned to permit the dependent variables Π_4 and Π_6 to be measured while the independent variables Π_1, Π_2, Π_3, and Π_7 were varied one at a time. Originally it was planned to vary Π_5 (ϕ) by saturating the sand with water, but further investigation indicated (Tschebotarioff (67) p. 151) that this would not be effective. (Later results indicated that the behavior of the saturated sand was quite different from the dry sand, and the data were analyzed independently.) The experimental schedule, with values of the independent dimensionless parameters, is shown in Table V.

TABLE V

SCHEDULE OF THE PIER EXPERIMENT

Variable	Values of Dimensionless Parameters				
	Π_4, Π_6	Π_1	Π_2	Π_3	Π_7
	Dry Sand Tests				
Π_1	Measure	3 7	2.0961	2	1
Π_2	Measure	5	0.4192 0.8384 1.2577 1.6769 2.0961	2	1
Π_3	Measure	5	2.0961	0.2 1 3	1
Π_7	Measure	5	2.0961	2	1 2 11
	Saturated Sand Tests				
Π_1	Measure	3 7	2.0961	2	1
Π_2	Measure	5	0.4192 0.8384 1.2577 1.6769 2.0961	2	1
	Wet Sand Tests				
Π_1	Measure	3 7	2.0961	2	1
Π_2	Measure	5	0.4192 0.8384 1.2577 1.6769 2.0961	2	1

A pier diameter of one and one-half inches was chosen. The specific weight of the compacted sand was 108 lb/ft^3 = 0.0625 lb/in^3. With these values as constant throughout the experiment the values of the variable quantities, listed in Table VI, were computed. The dimensions of the piers used are shown in Figure 18.

The Frame Experiment

The frame model was designed to model the prototype frame analyzed in Chapter III, with a basic length scale of 12. This meant that all dimensions (except those of the frame cross-section) of the model frame and its piers were one-twelfth those of the prototype; that is, $\lambda m = \frac{1}{12} \lambda p$. The moment of inertia of the model should have been, according to strict dimensional similarity, $\frac{1}{n^5}$ times that of the prototype:

$$\frac{1}{12^5} \times I_p = 4.03 \times 10^{-6} \times 48 = 1.935 \times 10^{-4} \text{ in}^4.$$

The minor moment of inertia of the 1/8 x 1 1/4 inch bar which was used for the model was computed to be 2.034×10^{-4} inches^4, which was considered acceptably close to the desired value.

The piers used for the model frame were 1 7/16 inch diameter, 10 inches long. The value of π_1, the parameter used in the pier experiment, was 6.96. The value of π_3 was expected to be about 0.5. Both of these values were within the range investigated in the pier experiment for dry sand. As the load was to be varied, π_2 would be variable, but the values were expected to be within the range of those used in the pier experiment.

TABLE VI

PIER EXPERIMENT - VALUES OF VARIABLES

Parameter Varied	B inches	D inches	H lb	L inches	N	γ lb-in^{-3}
			Dry Sand Tests			
π_1	1.5	4.5	1.3228	9.0	1	0.0625
		10.5	3.0864	21.0		
π_2	1.5	7.5	0.4409	15.0	1	0.0625
			0.8818			
			1.3228			
			1.7637			
			2.2046			
π_3	1.5	7.5	2.2046	3.0	1	0.0625
				7.5		
				22.5		
π_7	1.5	7.5	2.2046	15.0	1	0.0625
					2	
					11	
			Saturated Sand Tests			
π_1	1.5	4.5	0.556	9.0	1	0.0264
		10.5	1.2974	21.0		
π_2	1.5	7.5	0.1871	15.0	1	0.0264
			0.3742			
			0.5613			
			0.7484			
			0.9355			
			Wet (Drained) Sand Tests			
π_1	1.5	4.5	1.3228	9.0	1	0.0625
		10.5	3.0864	21.0		
π_3	1.5	7.5	0.4409	15.0	1	0.0625
			0.8818			
			1.3228			
			1.7637			
			2.2046			

Type 32   Type 5—   Type 72

Second type number of Type 5 - depends on hole used.

Figure 18. The Model Piers.

Testing was to be conducted immediately following each set of pier tests, with each test to be replicated three times. Tests were conducted both in dry sand and in saturated sand.

CHAPTER V

PROCEDURE OF THE PIER EXPERIMENT

The Sand Tank

All studies were conducted with models in a bin of Ottawa Flint

Shot sand. The bin was a wooden tank with semicircular ends, 68 inches

long, 31.6 inches wide and 19.7 inches deep inside. Dry sand was

weighed into the bin, with 1642 pounds filling it to a depth of 13.7

inches after compaction. The average specific weight of the compacted

sand was calculated to be 107.7 lb/cu ft, allowing for the displacement

of the piers.

Preliminary testing had shown vibration of the sand mass to be

effective for compaction. A vibrator, consisting of an eccentric weight

driven at about 2000 rpm by an electric motor, was constructed and

attached to the underside of the steel platform which supported the tank.

The compaction procedure consisted of running the vibrator for two

minutes, levelling the sand, vibrating again for two minutes, levelling

again then vibrating for about ten seconds. Between tests the piers

were removed, the sand loosened by pulling a vertical rectangular bar

through the mass at intervals of about three inches in both directions,

then the piers were reset, the sand levelled, and the compaction

procedure repeated.

Scale

The length scale of the model piers was selected to give the longest possible model, thus minimizing measurement errors, while avoiding serious proximity effects between models. It was considered that the zone of soil disturbance ahead of an overturning pier would be in the form of a cone with apex at the axis of rotation and that the limiting surface of the cone would be the Rankine passive failure surface ahead of an overturning wall; that is, at an angle of $(45° - \phi/2)$ from the horizontal. The size of the tank permitted locating nine model piers with center to center spacing of 16 inches in the direction of overturning. With the greatest pier depth, D, of 10.5 inches, and the point of rotation assumed to be at 0.695 D below the surface, the required minimum clear spacing was 14.4 inches which agreed well with the available spacing of 16 inches center to center when 1.5-inch diameter models were used. Consequently, a diameter of 1.5 inches was established for the model piers, with the longest 10.5 inches deep ($\pi_1 = D/B = 10.5/1.5 = 7$). It was considered that soil disturbance below the axis of rotation would be local, and would not influence the behavior of adjacent poles.

Randomization

The experimental schedule for the dry sand tests involved six types of pier. These were randomly numbered 1 through 6, and since nine positions were available, numbers 1, 3, and 5 were duplicated in the first test; numbers 2, 4, and 6 in the second. The nine piers selected were assigned at random to positions in the tank for each test. Positions in the tank are shown in Figure 19.
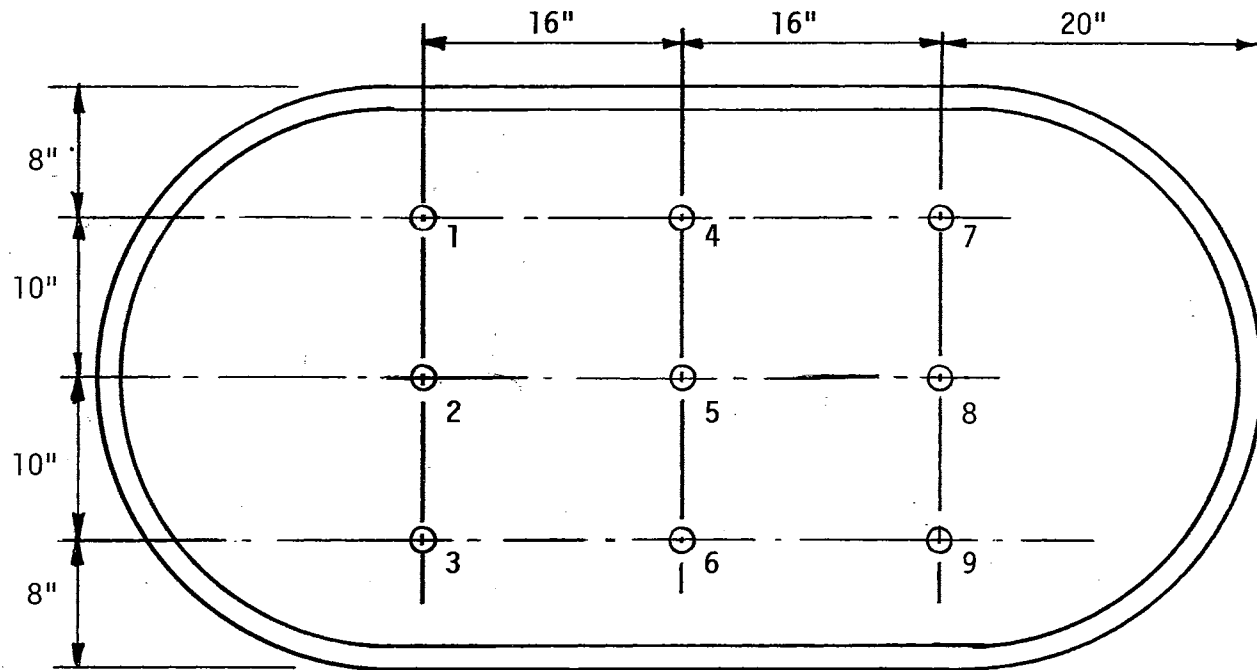
Figure 19. Pier Locations in the Sand Tank.

In the tests using saturated sand and wet sand, only three types of piers were to be used. Thus it was possible to replicate three times in each series. Again the piers were assigned at random to positions within the tank.

Preparation

In the dry sand test the bin had been filled with a known weight of dry sand. The sand was loosened by dragging a vertical steel bar through it from end to end and from side to side. Supporting bars were clamped to the frame over the tank, and the piers clamped to these supporting bars at the predetermined locations. As each pier was placed, sand was removed from its location to permit it to be set to proper depth without forcing it into the sand. As an added precaution against local compaction a tool was passed under the base of each pier after the pier was clamped in place. After all the piers were in place the sand was compacted by vibration, with the sand carefully levelled between vibration cycles. The appearance of the tank with all the piers clamped in place is shown in Figure 20. After compaction the depth of sand was measured and the sand density computed.

Testing

Upon completion of the compaction a row of piers was unclamped from its supporting bar and the bar moved into position to support a fixture carrying two dial gauges, with springs removed, which were graduated in thousandths of an inch. The gauges were located eight inches apart vertically, and the fixture adjusted in height to place the lower dial about 2.25 inches above the sand surface. The gauges were aligned with
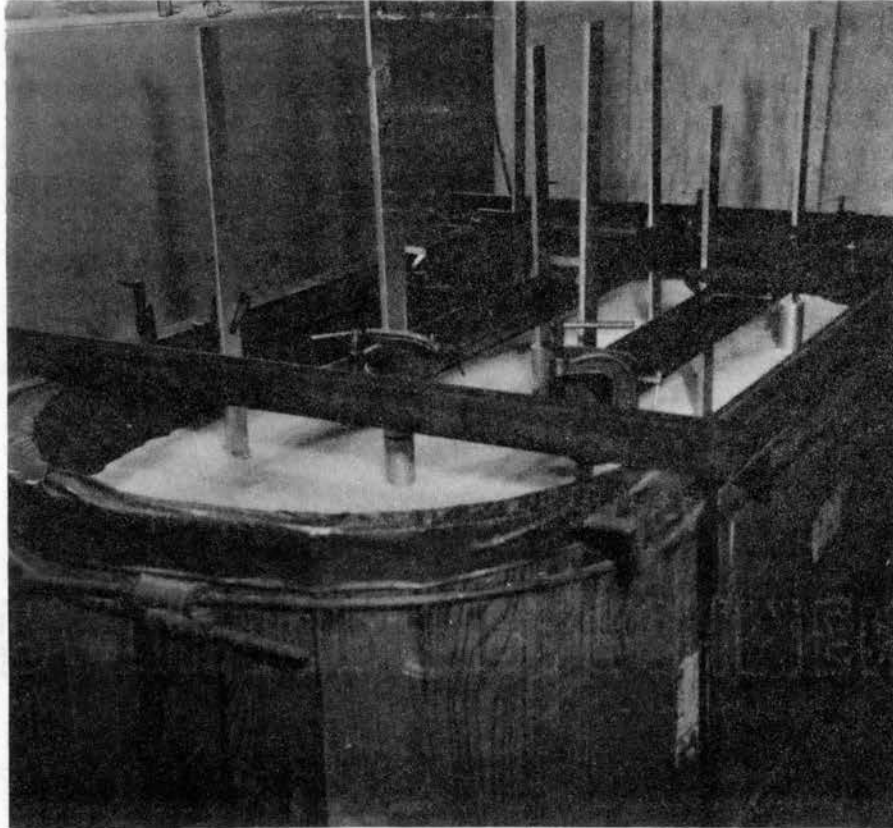
Figure 20.   The Model Piers Clamped in
             Place Before Compacting
             the Sand.

the pier to be tested, and attached to it with small plastic magnets (pieces of magnets removed from magnetic cabinet latches). Initial dial readings were recorded, estimating to one ten-thousandth inch, and the height of the lower dial above the sand surface measured and recorded.

A loading fixture was clamped to the crosspiece of the main frame with the height adjusted so that the top of the ball-bearing pulley was level with the hole in the pier at which load was to be applied. A cord was passed over the pulley, with a wire hook on one end passing through the hole in the pier (Figures 21 and 22). The load was applied to the cord below the pulley by means of 100 gram weights. Initially the load was applied in 200 gram increments but this proved to be too large an increment for the 4.5-inch deep piers and these piers were subsequently loaded by 100 gram increments.

After each increment of loading the load was recorded and the dial indicators watched for evidence of creep. If creep was not apparent, the dial reading was recorded, and loading continued. When creep became apparent with the heavier loads, the dials were watched and the reading recorded after apparent movement had stopped. On the very high loads a limit of two minutes was put on this waiting period. (Observations over longer intervals showed that movement was still continuing slowly). Loading was continued until deflection became excessive or failure occurred, except in the case of pier type 52 which was to be loaded repeatedly. In this case the pier was loaded by 200 gram increments to 1000 grams (2.205 lb) then unloaded and the cycle repeated 11 times.

Upon completion of all dry sand tests the piers were reset, the drain was closed and the bin filled to above the sand surface with water. Due to leaks in the dry wood tub several days passed before
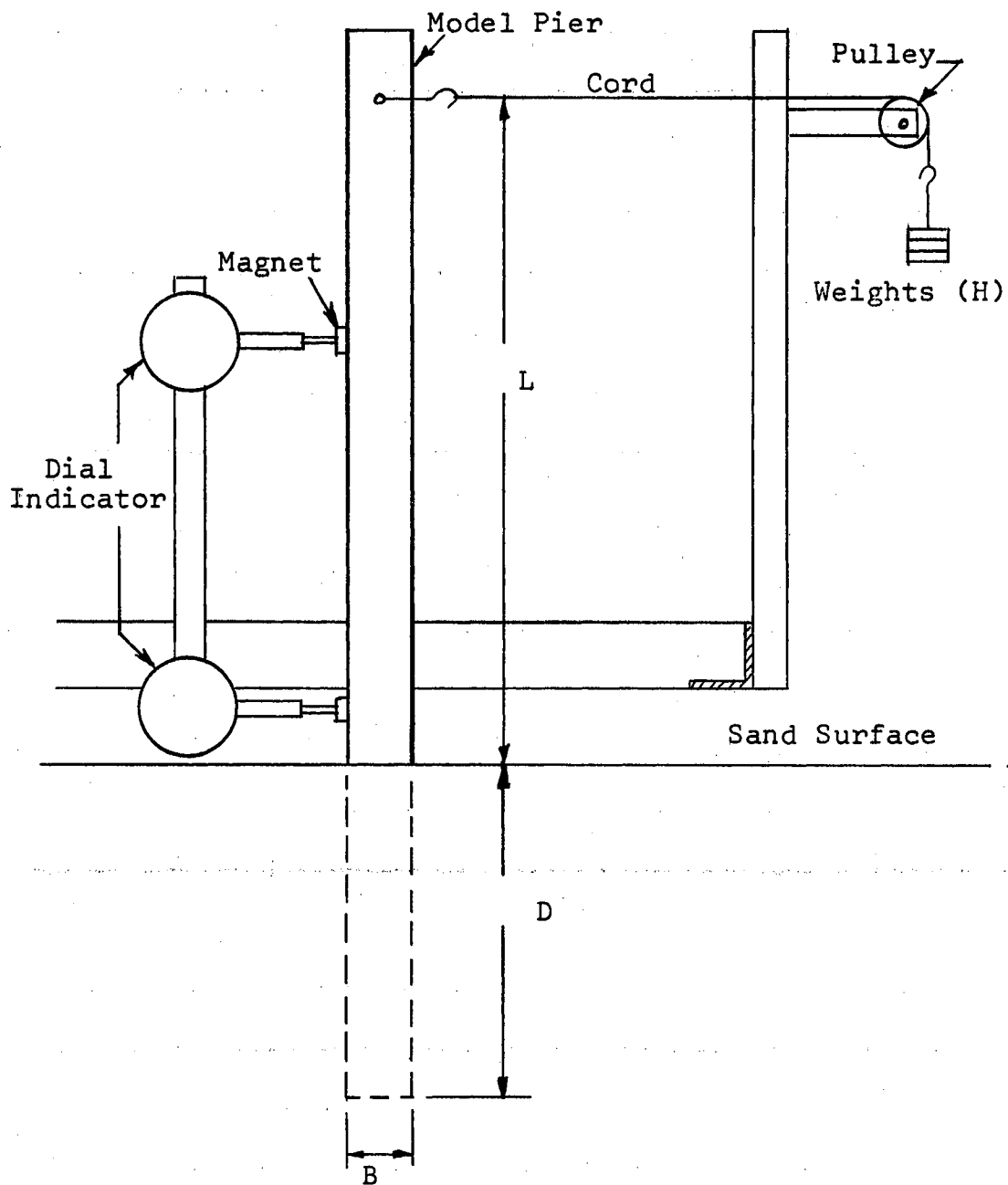
Figure 21. Test Set Up for Model Pier Tests Showing Method of Loading and Measuring Deflection.
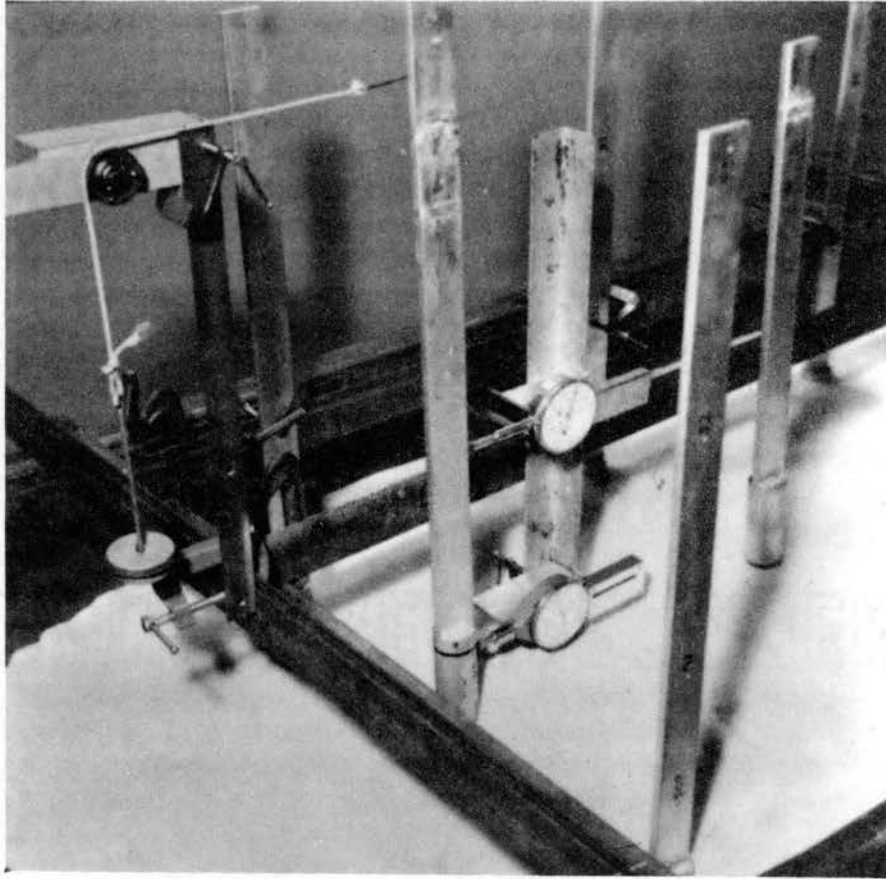
Figure 22. Loading the Model Piers.

testing could be continued. The sand was compacted by a modified vibration cycle: with the reduced effective specific weight of the submerged sand the action of the vibrator caused considerable sand movement, and the final period of vibration after levelling was reduced to about one second in order to minimize further movement. During vibration and testing in the saturated condition the water level was maintained slightly (about 1/4 inch) above the top of the sand. The testing procedure was the same as for the dry sand.

For the final series of tests (drained wet sand) the tank was filled to above the sand level with water after the piers had been clamped in place, and compacted as for the saturated sand tests. Then the drain was opened and water allowed to escape until the water table was below the bottom of the first piers to be tested. Testing was carried out as rapidly as possible to minimize the effects of changing water content. No attempt was made to maintain constant water content during the tests.

Sand Density Tests

A strong possibility existed that the specific weight of the compacted sand in the tub was not uniform throughout the depth. Direct measurement of sand density at different depths was not feasible. As a check on this, sand was placed in a 3 3/4-inch diameter Lucite cylinder closed at the bottom end, which was embedded in the sand in the tank with the cylinder resting on the tank bottom and which remained in the tank through the compaction and testing period. Following completion of the test the cylinder was removed carefully to avoid jarring and placed on a set of scales. The gross weight and the depth of sand was determined. A vacuum cleaner with a small nozzle (1/4-inch OD copper tubing) was
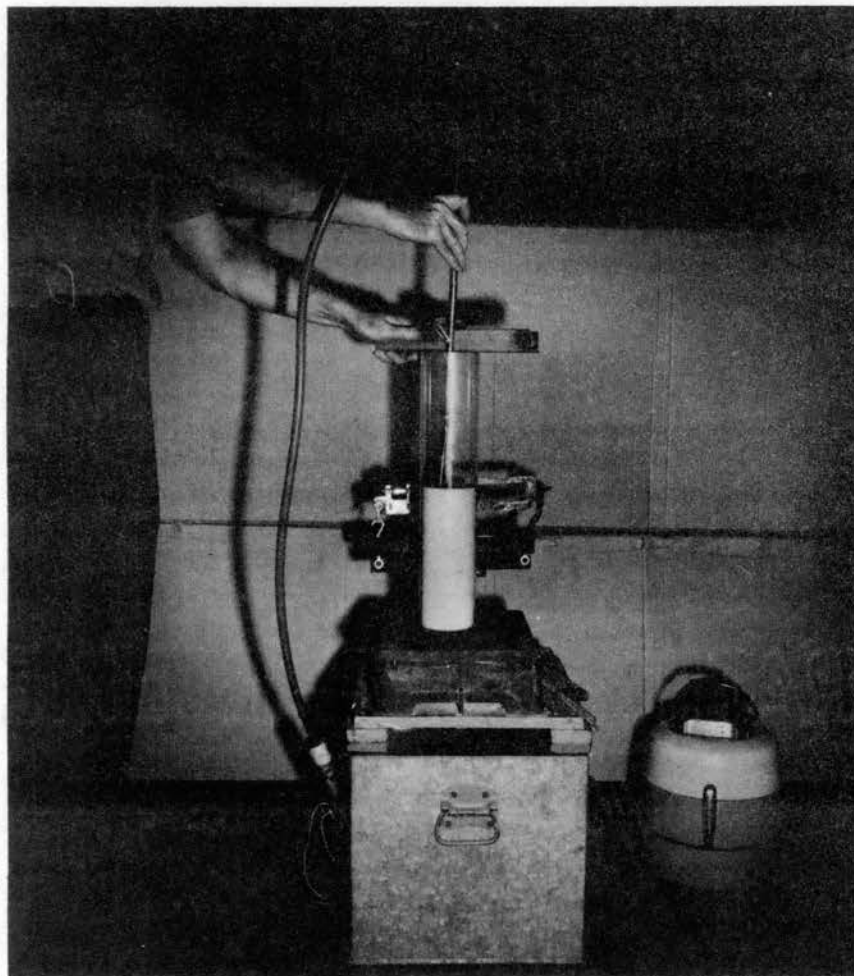
Figure 23.   Measuring the Density Gradient
of the Sand.
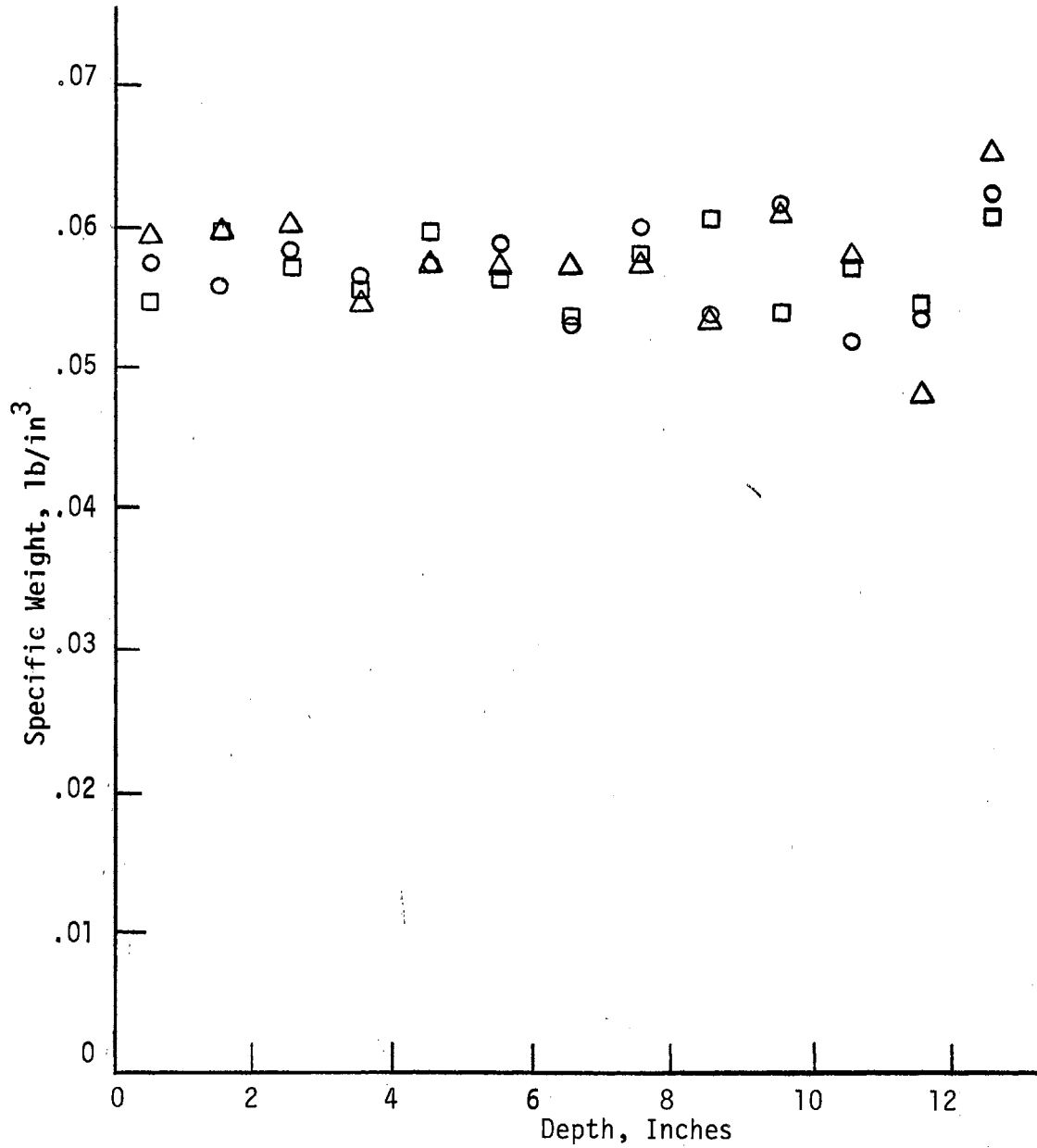
Figure 24. Variation of Specific Weight of Sand With Depth.

used to remove sand from the cylinder by increments of approximately one-inch depth (Figure 23). The weight and height of the sand column was recorded after removal of each increment. Finally the apparent specific weight of each increment was calculated. Although calculated values of specific weight varied considerably between adjacent increments there appeared to be no trend toward an increase in specific gravity with depth (Figure 24). The variation is believed to have been due to errors in measurement, rather than actual changes in specific gravity. The specific gravity of the sand in the cylinder was consistently less than the average in the tub. This is believed to be due to the effect of wall friction in the relatively small diameter cylinder.

CHAPTER VI

ANALYSIS OF THE PIER EXPERIMENT

Development of the Prediction Equations

The experiment had been planned to provide experimental relationships between the dependent dimensionless parameters π_4 and π_6 in terms of each of the independent parameters, π_1, π_2, π_3, π_5, and π_7. (Meanings of the dimensionless parameters are listed in Table IV, p. 68.) However, it was not possible to vary π_5 with the equipment available so that the independent parameters were reduced to four.

In general the experimental procedure was to determine values of the dependent parameters, π_4 and π_6, while one of the independent parameters was varied, the other three being held constant. The resulting relationships were of the form:

$$\pi_4 = F_1(\pi_1, \bar{\pi}_2, \bar{\pi}_3, \bar{\pi}_7)$$

$$\pi_4 = F_2(\bar{\pi}_1, \pi_2, \bar{\pi}_3, \bar{\pi}_7)$$

etc.,

where $F(\pi_1, \bar{\pi}_2, \bar{\pi}_3, \bar{\pi}_7)$ is a function of π_1, with π_2, π_3, π_7 held constant at some predetermined levels. Values of the dependent parameters computed from the deflections recorded during the tests are listed in Appendix B for all levels of the independent parameters.

According to the principles of dimensional analysis (Murphy (66)
pp. 41-44) the resulting component equations may be combined by multi-
plication to form a general prediction equation provided all the com-
ponent equations are similar in form and that auxiliary component
equations developed using different values of the fixed parameters are
related to the primary component equations by the relation:

$$\frac{F(\bar{\pi}_2, \pi_3)}{F(\bar{\pi}_2, \bar{\pi}_3)} = \frac{F(\bar{\bar{\pi}}_2, \pi_3)}{F(\bar{\bar{\pi}}_2, \bar{\pi}_3)}$$

where $F(\bar{\pi}_2, \pi_3)$ is the component equation developed at a fixed value,
$\bar{\pi}_2$, of π_2, and $F(\bar{\bar{\pi}}_2, \pi_3)$ is the auxiliary component equation developed
at a different value, $\bar{\bar{\pi}}_2$, of π_2. $F(\bar{\pi}_2, \bar{\pi}_3)$ and $F(\bar{\bar{\pi}}_2, \bar{\pi}_3)$ are values of
the function at the fixed value of $\bar{\pi}_3$, with π_2 equal to $\bar{\pi}_2$ and $\bar{\bar{\pi}}_2$,
respectively.

In particular, if the component equations meet these tests and plot
as straight lines in logarithmic space, (thereby defining a plane in
logarithmic space) the general prediction equation obtained by multipli-
cation of the component equations, will be of the form:

$$\pi_4 = C_a \, \pi_1^{C_1} \, \pi_2^{C_2} \, \pi_3^{C_3} \, \pi_4^{C_4}.$$

Preliminary analysis of the experimental data consisted of plotting
the data in various coordinate systems--linear, semi-logarithmic, log-
arithmic, and hyperbolic. This indicated that the relationships between
π_4 (and π_6) and π_2 were of the form:

$$\pi_4 = C_1 \, \pi_2^{C_2}.$$

and those of Π_3 were:

$$\Pi_4 = C_3 \, C_4^{\Pi_3}.$$

The data for Π_1 were limited in number and badly scattered, but did approximate a straight line plot on log-log paper, so that relations of the form:

$$\Pi_4 = C_5 \, \Pi_1^{C_6}$$

were considered appropriate.

During preliminary analysis deflections were computed from the initial pier position only, and a relationship relating Π_4 to Π_7, of the form:

$$\Pi_4 = C_7 + C_8 \log \Pi_7$$

was established. It was recognized that this relation could not be introduced into the prediction equation by multiplication, and in consequence this relation was omitted from the early stages of analysis, which used the constant value of $\Pi_7 = 1$.

Following preliminary plotting to establish the forms of relationship, each set of data was fitted by a curve, using the least squares method applied to suitably transformed data (68). The resulting component equations for the dry sand tests are plotted in Figures 25, 26, and 27. These equations were:

$$\Pi_4 = 1.421 \times 10^{-2} \, \Pi_1^{-0.3997} \tag{1a}$$

$$\Pi_6 = 1.610 \times 10^{-2} \, \Pi_1^{-1.236} \tag{1b}$$
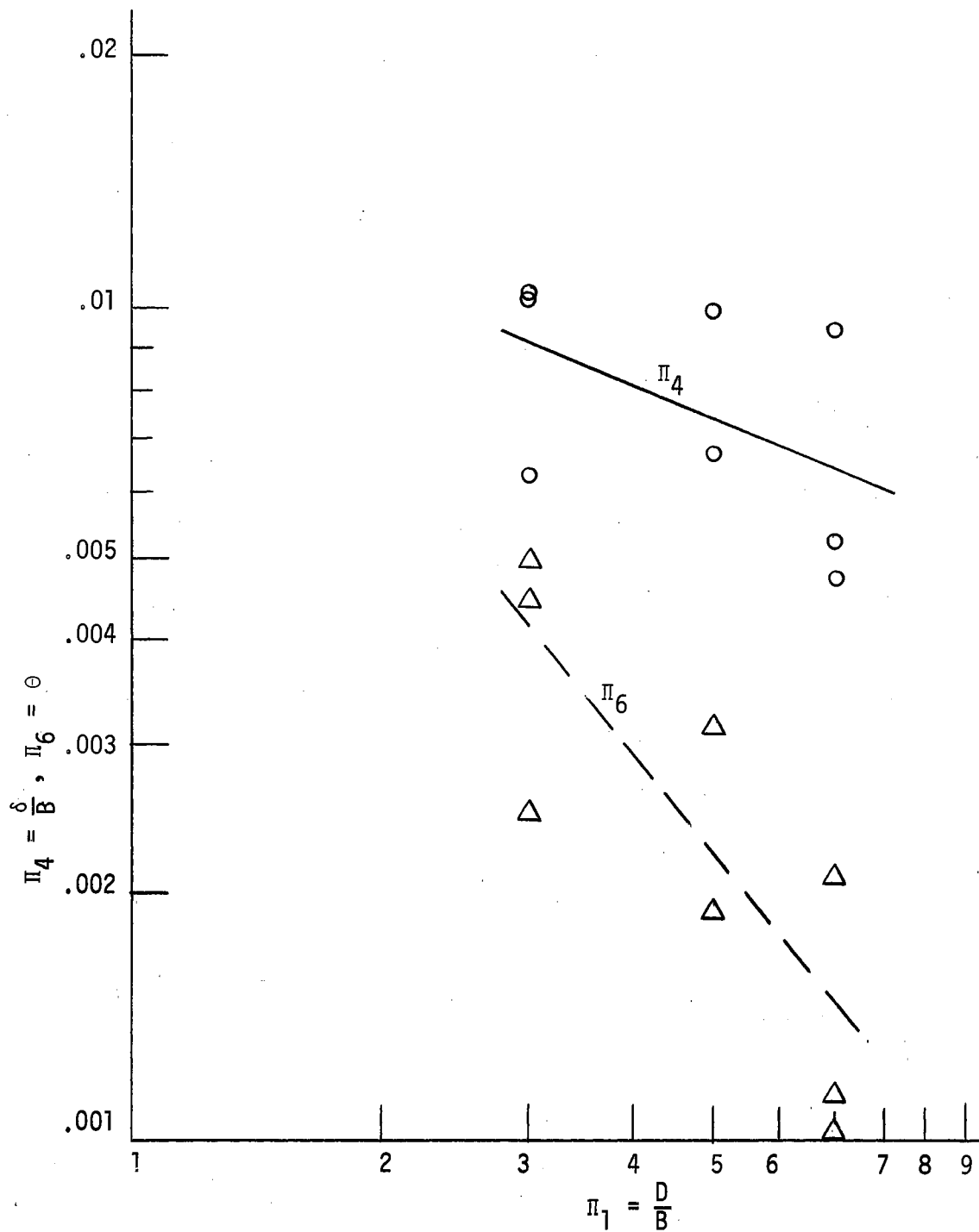
Figure 25. The Relations Between the Dependent Variables, π_4 and π_6, and π_1 When $\pi_2 = 2.096$, $\pi_3 = 2$ and $\pi_7 = 1.4$
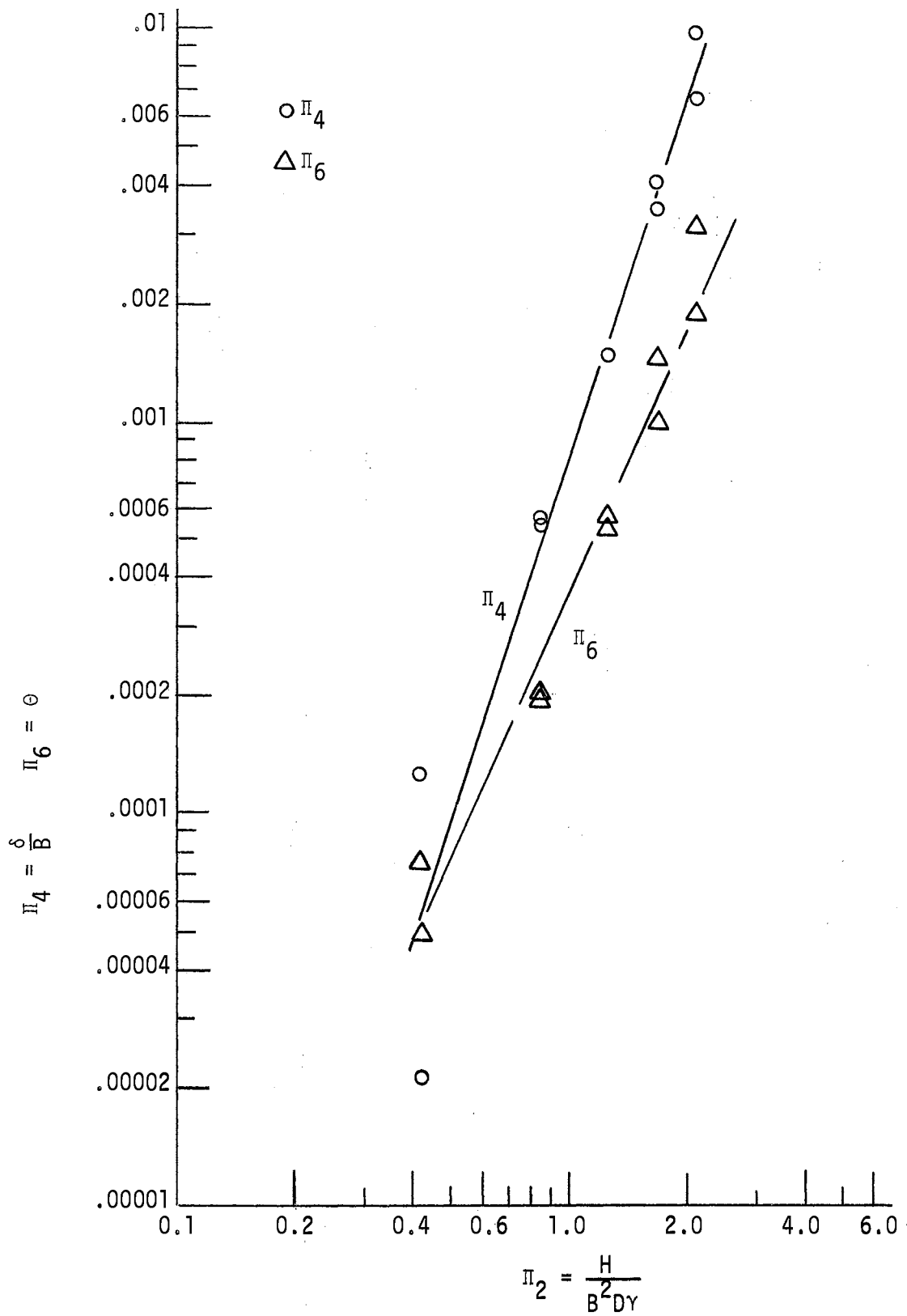
Figure 26. π_4 and π_6 At Various Levels of π_2, When π_1 = 5, π_3 = 2, π_7 = 1.
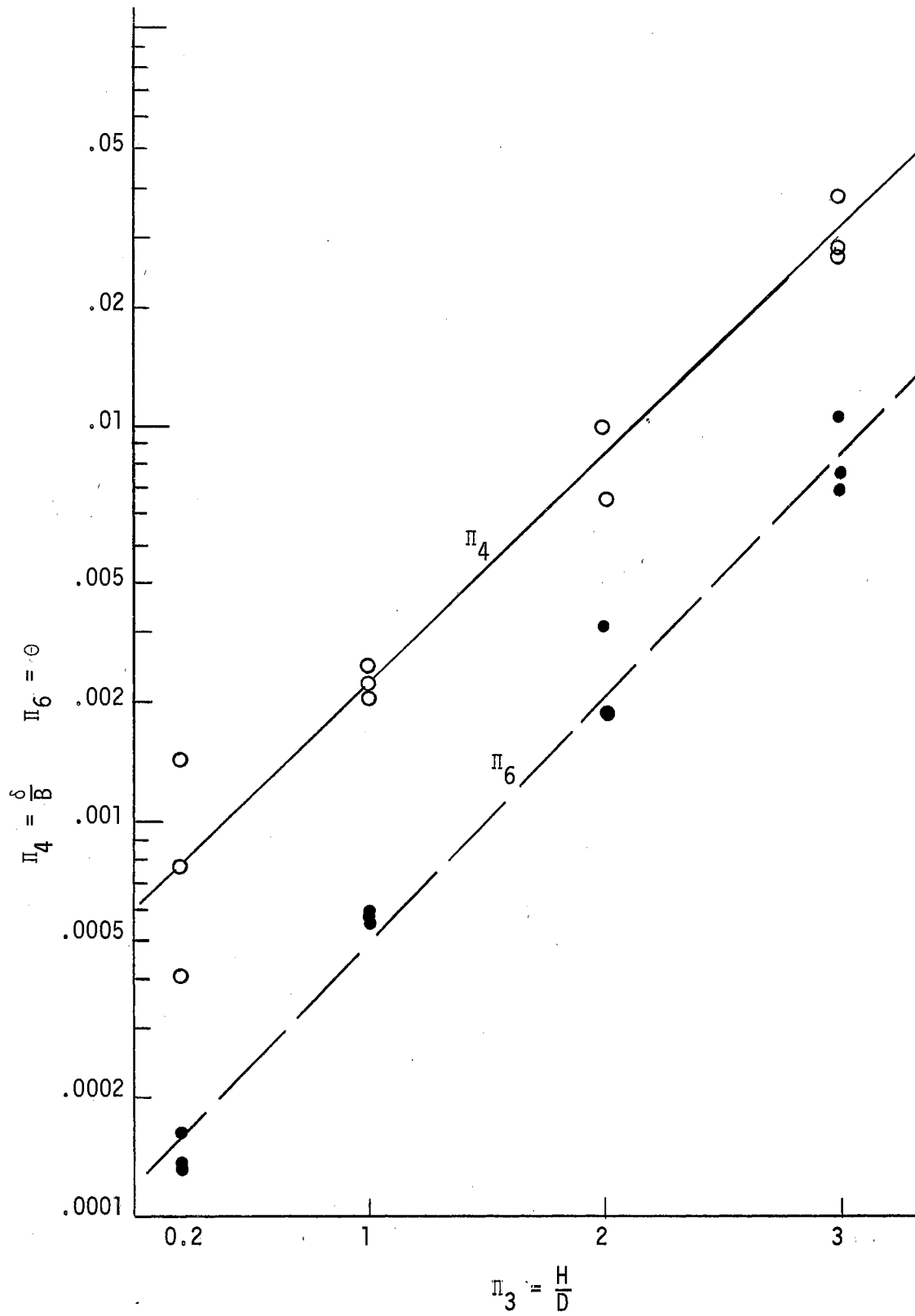
Figure 27. Π_4 and Π_6 at Four Values of Π_3, When $\Pi_1 = 5$, $\Pi_2 = 2.096$, and $\Pi_7 = 1$.

$$\Pi_4 = 8.038 \times 10^{-4} \times \Pi_2^{3.087} \tag{2a}$$

$$\Pi_6 = 3.729 \times 10^{-4} \Pi_2^{2.276} \tag{2b}$$

$$\Pi_4 = 5.93 \times 10^{-4} \times 3.706^{\Pi_3} \tag{3a}$$

$$\Pi_6 = 1.223 \times 10^{-4} \times 4.179^{\Pi_3}. \tag{3b}$$

During the course of the laboratory work it had proved convenient to vary Π_2 in all of the tests. Consequently it was possible to check the relationship between the dependent parameters and Π_2 at other levels of Π_1 and Π_3. These relations are plotted on logarithmic coordinates in Figures 28 and 29. Comparison with these curves indicated some question about the validity of the tests on the type 52 piers (pier types are identified in Figure 18, p. 75), and in order to improve the dependability of the prediction equation the means of the slopes of the six curves in each set were used, resulting in the relations:

$$\Pi_4 = C_3' \, \Pi_2^{3.0245} \tag{2a'}$$

and

$$\Pi_6 = C_4' \, \Pi_2^{3.0022}. \tag{2b'}$$

These component equations, 1a, 2a', and 3a, were combined by multiplication and the values of $Y = \Pi_1^{-0.3997} \times \Pi_2^{3.0245} \times 3.706^{\Pi_3}$ computed. The constant, C, was calculated by the relationship:

$$C = \frac{\Sigma \Pi_4}{\Sigma Y}$$

using all available values of Π_4 and corresponding Y's. This led to the first prediction equation:
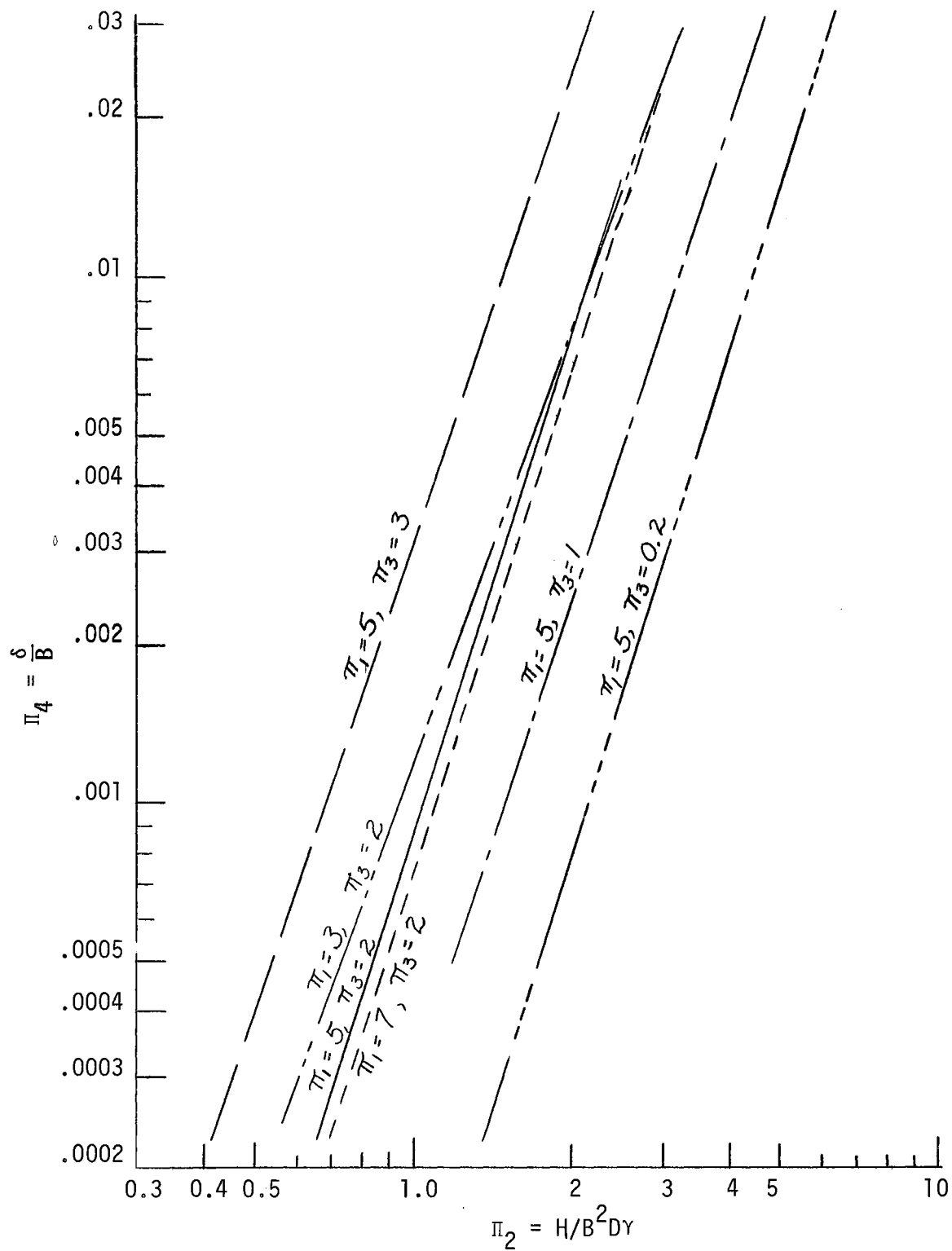
Figure 28. The Relation Between Π_4 and Π_2 at Four Levels of Π_3 and Three Levels of Π_1.
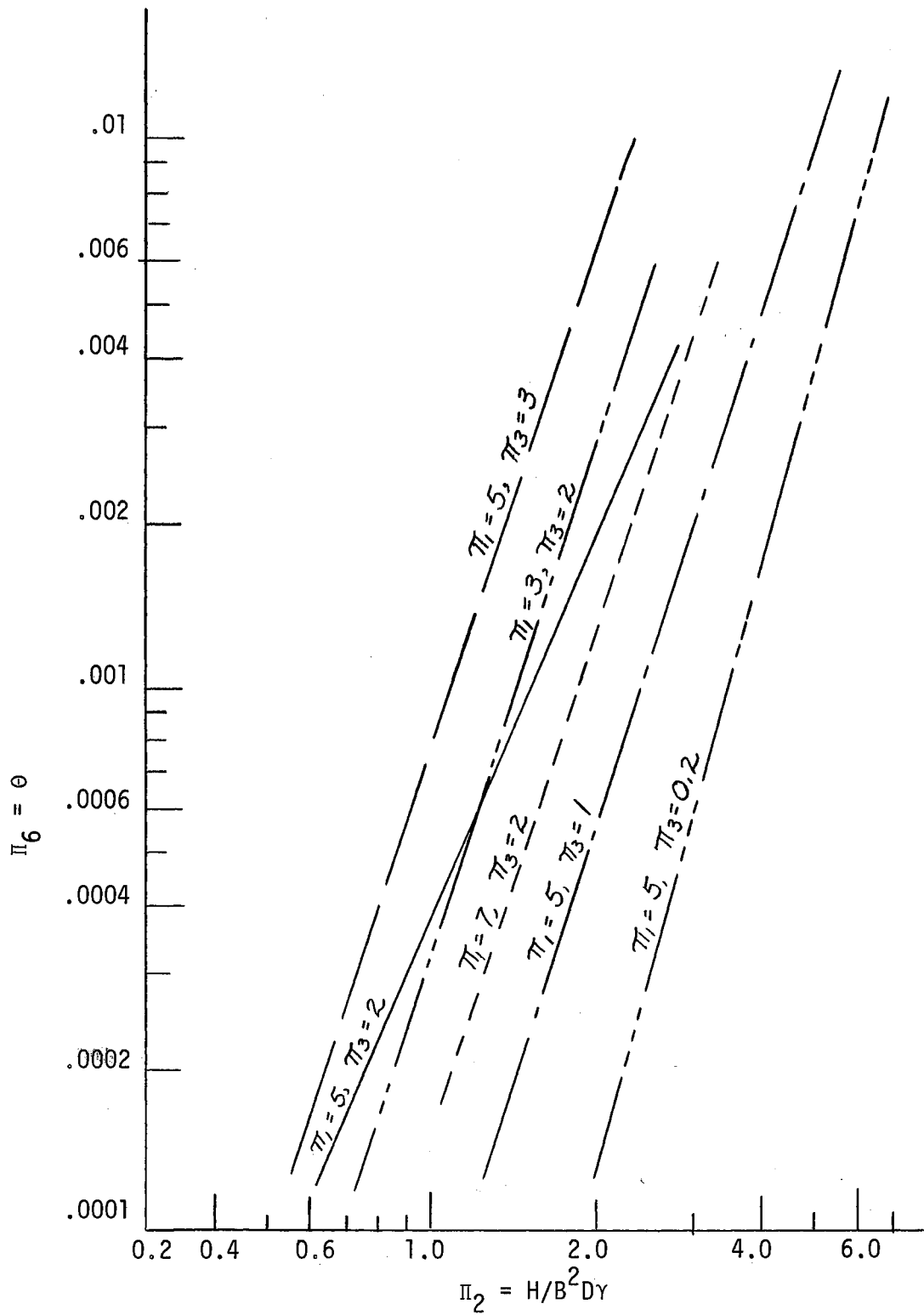
Figure 29. The Relation Between Π_6 and Π_2 at Four Levels of Π_3 and Three Levels of Π_1.

$$\Pi_4 = 1.498 \times 10^{-4} \, (\Pi_1^{-0.3997} \times \Pi_2^{3.0245} \times 3.706^{\Pi_3}). \qquad \text{(4a)}$$

Similarly the prediction equation for Π_6 was determined to be

$$\Pi_6 = 1.265 \times 10^{-4} \, (\Pi_1^{-1.236} \, \Pi_2^{3.0022} \times 4.179^{\Pi_3}). \qquad \text{(4b)}$$

Plots of observed values of Π_4 and Π_6, versus values predicted by equations 4a and 4b, respectively, showed moderately good agreement, but it was observed that the locations of points about the 45 degree line, rather than being random, were related to the values of Π_1 and Π_3. This indicated that the coefficients of Π_1 and Π_3 in the prediction equations were in error. Because of the limited number of scattered data points involved in the development of the component equations involving Π_1, (equations 1a and 1b), this result was not unexpected.

Multiple Regression Analysis

In order to improve the accuracy of the prediction equations, particularly with regard to the coefficients of Π_1 and Π_3, a logarithmic hyperplane was fitted to the transformed data by the method of least squares. This permitted the use of all data points, some of which were not available for development of component equations. The basic assumptions used in the planning and preliminary analysis of the experiment were used in the regression analysis.

These assumptions included:

(a) The X_i ($\log_e \Pi_1$, $\log_e \Pi_2$, Π_3) were independent and without interaction effects.

(b) The deviation was proportional to the expected value.

(c) The form of relationship developed in the preliminary analysis; i.e. $\Pi_4 = C_1 \Pi_1^{C_2} \Pi_2^{C_3} C_4^{\Pi_3}$, was valid.

The assumption of no interaction among the transformed variables is equivalent to the assumption used in developing the first prediction equations, that the transformed data describe a plane. The plots of Π_4 and Π_6 against Π_2 at various levels of Π_1 and Π_3 (Figures 28 and 29) show that interaction between $\log_e \Pi_2$ and $\log_e \Pi_1$, and between $\log_e \Pi_2$ and Π_3, was small or non-existent.

A plot of Π_4 versus Π_2, using non-transformed data, showed the scatter increasing with increasing values of Π_4. This indicated the probability that deviation was proportional to the expected value of Π_4. Similar plots using transformed data (i.e. $\log_e \Pi_4$ versus $\log_e \Pi_2$) showed a moderate decrease in scatter as $\log_e \Pi_4$ increased, indicating that the logarithmic transformation over-corrected the variance. The reason for this was considered to be that there were two basic components of variance; one, involving the experimental unit itself, which increased as the displacement increased, and a second, involving instrument error and errors in reading, which would be expected to be independent of the magnitude of the measurement. The logarithmic transformation linearized the first component, but suppressed the second at high Y values. Although ideal uniformity of scatter was not obtained by the logarithmic transformation, the situation was much improved and it was believed that the analysis of the transformed data would be valid.

The transformed data were fitted by a hyperplane using least squares techniques (68). The form of equation used was

$$Y = b_1 + b_2 X_2 + b_3 X_3 + b_4 X_4$$

or, in terms of the actual variables:

$$\text{Log}_e \; \pi_4 = b_1 + b_2 \log_e \pi_1 + b_3 \log_e \pi_2 + b_4 \pi_3$$

which, cleared of logarithms, becomes:

$$\pi_4 = e^{b_1} \; \pi_1^{b_2} \; \pi_2^{b_3} \; e^{b_4 \pi_3}$$

or, letting $b_1' = e^{b_1}$, $b_4' = e^{b_4}$

$$\pi_4 = b_1' \; \pi_1^{b_2} \; \pi_2^{b_3} \; b_4'^{\pi_3}.$$

Similar reasoning led to the relation for π_6:

$$\pi_6 = B_1' \; \pi_1^{B_2} \; \pi_2^{B_3} \; B_4'^{\pi_3}.$$

(It may be noted that the symbols, b_1, b_2--b_{k+1} are used here in lieu of the more usual b_0, b_1,--b_k, because of the impossibility of using zero as a subscript on the digital computer.)

The plane of best fit for the dependent variable π_4 (in terms of the transformed variables) was:

$$Y = -8.8963 - 0.5015 \; X_1 + 3.1920 \; X_2 + 1.2901 \; X_3 \tag{5}$$

where

$$Y = \log_e \pi_4$$
$$X_1 = \log_e \pi_1$$
$$X_2 = \log_e \pi_2$$
$$X_3 = \pi_3.$$

The estimated standard deviation, in terms of the transformed data, was

$$s = 0.411$$

and the multiple correlation coefficient, used here as an indication of goodness of fit, was

$$R = 0.973.$$

Tests for the significance of the partial regression coefficients, b_i, were conducted using the t test, as outlined by Steel and Torrie, (69, p. 298). These were tests of the null hypotheses; $b_i = 0$, $i = 1, 2, 3, 4$. Results of the tests, shown in Table VII, indicate that all b's are highly significant. That is, the test indicates that the null hypotheses, $b_i = 0$, should be rejected for all i.

TABLE VII

TESTS OF SIGNIFICANCE OF THE REGRESSION COEFFICIENTS
OF EQUATION 5

i	b_i	Standard Deviation of b_i	t_i
1	-8.8962	0.2759	-32.26**
2	-0.5016	0.1577	- 3.180**
3	3.1920	0.0728	43.82**
4	1.2901	0.0517	24.95**

**Indicates t is significant at the 1 percent level ($t_{01,110} = 2.36$).

In terms of the non-transformed parameters, equation 5 becomes:

$$\pi_4 = 1.369 \times 10^{-4} \times \pi_1^{-0.5016} \pi_2^{3.192} \times 3.633^{\pi_3}. \tag{6}$$

Substituting the pertinent quantities into this equation gives:

$$\frac{\delta}{B} = 1.369 \times 10^{-4} \left(\frac{D}{B}\right)^{-0.5016} \left(\frac{H}{B^2 D \gamma}\right)^{3.192} \times 3.633^{\left(\frac{L}{D}\right)} \qquad (6a)$$

and

$$\delta = 1.369 \times 10^{-4} H^{3.192} B^{-4.882} D^{-3.694} \gamma^{-3.192} 3.633^{\left(\frac{L}{D}\right)} . \quad (6b)$$

Similar procedures led to the regression equation for π_6:

$$Y = -9.5087 - 0.8172 X_1 + 3.0298 X_2 + 1.2647 X_3 \qquad (7)$$

where

$$Y = \log_e \pi_6$$
$$X_1 = \log_e \pi_1$$
$$X_2 = \log_e \pi_2$$
$$X_3 = \pi_3$$

Estimated standard deviation was

$$s = 0.409$$

and coefficient of multiple correlation,

$$R = 0.97.$$

Tests for significance of the regression coefficients, B_i, of equation 7 were conducted by the same method (t test) as for the first regression equation. The results, shown in Table VIII, indicate that all B's are highly significant.

In terms of the original variables, equation 7 reduces to:

$$\pi_6 = 7.420 \times 10^{-5} \pi_1^{-0.8172} \pi_2^{3.030} \times 3.5420^{\pi_3}. \qquad (8)$$

This equation, in terms of the pertinent quantities, is:

$$\Theta = 7.420 \times 10^{-5} \left(\frac{D}{B}\right)^{-0.8172} \left(\frac{H}{B^2 D\gamma}\right)^{3.030} 3.542^{\left(\frac{L}{D}\right)} . \tag{8a}$$

which reduces to:

$$\Theta = 7.420 \times 10^{-5} H^{3.030} B^{-5.243} D^{-3.847} \gamma^{-3.030} 3.542^{\left(\frac{L}{D}\right)} . \tag{8b}$$

TABLE VIII

TESTS OF SIGNIFICANCE OF THE REGRESSION COEFFICIENTS
OF EQUATION 7

i	B_i	Standard Deviation of B_i	t_i
1	-9.507	0.2745	-34.64**
2	-0.81715	0.15696	- 5.206**
3	3.0298	0.07249	41.80**
4	1.2647	0.05144	24.59**

In the tests in saturated and in wet sand π_3 and π_7 had not been varied. Consequently the analysis of these tests involved only two independent parameters, π_1 and π_2. Using the same general form of relationship as in the dry sand tests but omitting π_3 the data were fitted by a logarithmic plane of the form:

$$\pi_4 = C_1 \pi_1^{C_2} \pi_2^{C_3}$$

or in terms of the transformed data:

$$\mathrm{Log}_e \pi_4 = C_1' + C_2 \log_e \pi_1 + C_3 \log_e \pi_2$$

As in the dry sand tests, the method of least squares was used to fit a plane to the transformed data, with t tests of the coefficients, standard deviations, and multiple regression coefficient calculated in the transformed scale.

The resulting multiple regression equations for the saturated sand tests were:

$$\pi_4 = 3.5738 \times 10^{-3} \ \pi_1^{-1.185} \ \pi_2^{2.196} \tag{9}$$

with

$$s = 0.426$$

and

$$R = 0.963$$

and

$$\pi_6 = 5.5195 \times 10^{-3} \ \pi_1^{-2.466} \ \pi_2^{2.379} \tag{10}$$

with

$$s = 0.406$$

and

$$R = 0.974.$$

Substituting the pertinent quantities into these equations gives:

$$\frac{\delta}{B} = 3.5738 \times 10^{-3} \ \left(\frac{D}{B}\right)^{-1.185} \left(\frac{H}{B^2 D \gamma}\right)^{2.196} \tag{9a}$$

$$\Theta = 5.5195 \times 10^{-3} \ \left(\frac{D}{B}\right)^{-2.466} \left(\frac{H}{B^2 D \gamma}\right)^{2.379} . \tag{10a}$$

A similar analysis of the data of the wet (drained) sand tests gave:

$$\pi_4 = 8.1835 \times 10^{-4} \ \pi_1^{-0.2092} \ \pi_2^{2.1931} \tag{11}$$

with

$$s = 0.268$$

$$R = 0.983$$

and

$$\Pi_6 = 8.4118 \times 10^{-4} \; \Pi_1^{-0.9499} \; \Pi_2^{2.2485} \tag{12}$$

with

$$s = 0.4785$$

$$R = 0.953.$$

Substituting the pertinent quantities into these equations gives:

$$\frac{\delta}{B} = 8.1835 \times 10^{-4} \; \left(\frac{D}{B}\right)^{-0.2092} \; \left(\frac{H}{B^2 D \gamma}\right)^{2.1931} \tag{11a}$$

and

$$\Theta = 8.4118 \times 10^{-4} \; \left(\frac{D}{B}\right)^{-0.9499} \; \left(\frac{H}{B^2 D \gamma}\right)^{2.2485} . \tag{12a}$$

Tests of the significance of coefficients of the equations 9, 10, 11, and 12 (in terms of the transformed variables) showed all the coefficients to be significant; that is, that the probability of each coefficient being zero, if the experiment were repeated a large number of times, was less than 0.05; and all but one, b_2, the exponent of Π_1 in equation 11, to be highly significant ($p < 0.01$).

Position of the Axis of Rotation

The position of the axis of rotation was calculated for each point in all tests. The location, which is defined for a rigid pier as $Z_0 = \frac{\delta}{\Theta}$, was expressed in dimensionless form as:

$$POZN = \frac{\Pi_4}{\Pi_6 \, \Pi_1} = \frac{\delta}{\Theta D}$$

POZN, a dimensionless parameter, may be substituted for either Π_4 or Π_6 in the set of dimensionless parameters (Appendix A-2) used to describe the system. A prediction equation for POZN may be obtained from equations 6 and 8 by division. This relation is of the same form;

$$POZN = b_1 \, \Pi_1^{b_2} \, \Pi_2^{b_3} \, b_4^{\Pi_3}$$

as the original equations.

In order to reduce fitting errors, the data for the dry sand tests were fitted by a multiple regression equation of this form using the method of least squares on suitably transformed data. All points which resulted in values of POZN equal to or less than zero, or greater than 1, were omitted from the analysis.

The resulting equation was:

$$Y = -0.1598 - 0.3893 \, X_1 + 0.2902 \, X_2 + 0.1055 \, X_3 \tag{13}$$

where

$Y = \log_e POZN$

$X_1 = \log_e \Pi_1$

$X_2 = \log_e \Pi_2$

$X_3 = \Pi_3.$

The multiple correlation coefficient, R, was 0.5615 and a t test of significance of the coefficients showed all but the first to be highly significant ($p < 0.01$). Although the probability that the first coefficient would differ from zero in repeated tests was somewhat less than

0.8, this coefficient was retained in the equation. The resulting equation, in terms of the original dimensionless parameters, is:

$$POZN = 0.8523 \; \pi_1^{-0.3893} \; \pi_2^{0.2902} \; 1.1112^{\pi_3} \qquad (13a)$$

and, in terms of the original pertinent quantities, is:

$$POZN = 0.8523 \; \left(\frac{D}{B}\right)^{-0.3893} \; \left(\frac{H}{B^2 DY}\right)^{0.2902} \; 1.1112^{\left(\frac{L}{D}\right)} \qquad (13b)$$

Effect of Repeated Loads

The component equations for dry sand, developed by consideration of the number of load repetitions, N, as the independent variable π_7, were:

$$\pi_4 = (8.139 + 1.663 \; \log_e \pi_7) \times 10^{-3} \qquad (14)$$

with the coefficient of linear correlation, r, between π_4 and $\log_e \pi_7$ equal to 0.4075, and:

$$\pi_6 = (24.38 + 4.05 \; \log_e \pi_7) \times 10^{-4} \qquad (15)$$

with linear correlation coefficient r = 0.308.

The data used in developing equations 14 and 15, as well as the fitted curves, are plotted in Figures 30 and 31, respectively.

Formation of a general prediction equation by multiplication of either of these equations with the other component equations was not feasible. Such a prediction equation was valid for maximum loads (from which the component equations 14 and 15 were determined) but resulted in extremely erroneous prediction at lesser loads. This behavior was attributed to the fact that equations 14 and 15 are essentially
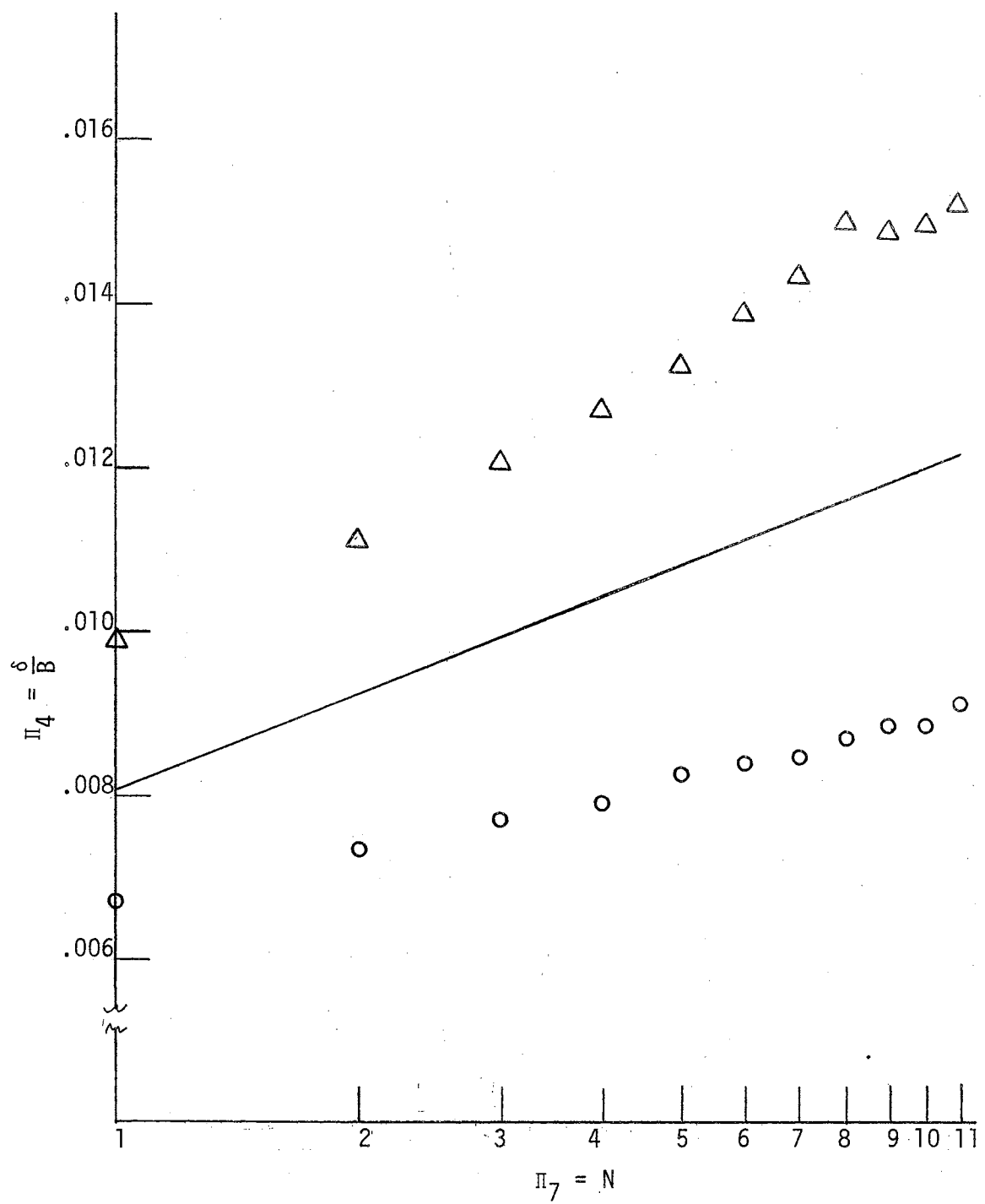
Figure 30. The Effect of the Number of Load Repetitions, N, on Π_4.
$\Pi_1 = 5$, $\Pi_2 = 2.0962$, $\Pi_3 = 2$.
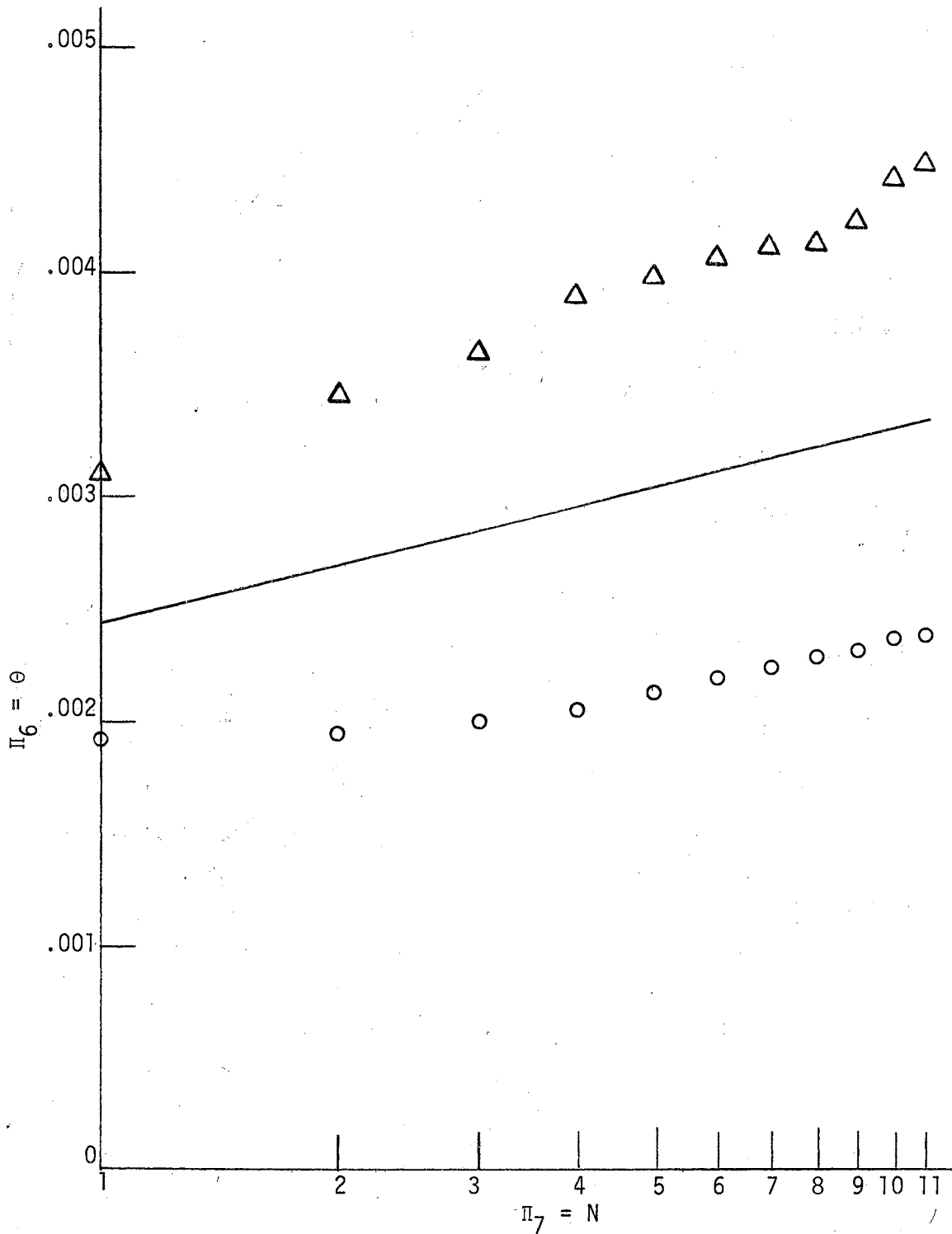
Figure 31. The Effect of the Number of Load Repetitions, N, on Π_6 When Π_1 = 5, Π_2 = 2.0962, Π_3 = 2.

arithmetically additive functions which are undefined in logarithmic space, and hence are not suitable for multiplication with the other component equations.

Since equation 14 was valid for the maximum loads for which it was developed, the equation was adapted to predicting the maximum deflection after N cycles of loading, after the deflection at maximum load at the end of the first cycle had been computed by equation 6. The method used to determine the required constant multiplier follows:

Let π_{41} be the deflection at maximum load in the first loading cycle, and π_{4N} by the deflection at maximum load during the Nth loading cycle, then, considering multiplication valid for the maximum loads only,

$$\pi_{4N} = \pi_{41} \times C \ (8.139 + 1.663 \ \log_e \pi_7) \times 10^{-3} \qquad \text{(a)}$$

$$C = \frac{\pi_{4N}}{\pi_{41} \ (8.139 + 1.663 \ \log_e \pi_7) \times 10^{-3}}$$

Let N = 1, then $\pi_{4N} = \pi_{41}$

$$C = \frac{\pi_{41}}{\pi_{41} \ (8.139 + 1.663 \ \log_e 1) \times 10^{-3}}$$

$$C = \frac{1}{8.447 \times 10^{-3}} = 122.9$$

Substituting in a

$$\pi_{4N} = \pi_{41} (1 + 0.2044 \ \log_e N). \qquad \text{(14a)}$$

Similar reasoning led to:

$$\Pi_{6N} = \Pi_{61} (1 + 0.1661 \log_e \Pi_7).$$ (15a)

It must be emphasized that these equations, 14a and 15a, are valid only for maximum loads and must not be used for predicting displacement or rotation at part loads.

CHAPTER VII

DISCUSSION OF THE PIER EXPERIMENT

The Prediction Equations

Equations to predict the ground-line displacement and rotation of cylindrical piers embedded in dry sand under varying conditions of geometry and loading have been developed as described in Chapter VI. Similar but more restricted prediction equations for piers embedded in wet sand and in saturated sand have also been presented. The methods of dimensional analysis were used in planning, conducting, and analyzing the experiment so that the resulting prediction equations would be valid for similar piers of any scale under conditions similar to those of the test.

The form of component equations was established by plotting the data in various coordinate systems. The forms selected not only fitted the data plots, but are consistent with the expected behavior of a pier at extreme values of the independent parameters.

If π_1 were very small, π_4 would be expected to be very large and to be undefined at $\pi_1 = 0$. For the relation used in developing the component equations,

$$\lim_{\pi_1 \to 0} (\pi_1^{-c}) = \infty$$

and if π_1 were very large, π_4 would be expected to approach zero.

$$\text{Lim } (\pi_1^{-c}) = 0$$
$$\pi_1 \to \infty$$

Similarly, π_4 would be large or undefined at large values of π_2, and would approach zero as π_2 approached zero. For the relation used,

$$\text{Lim } (\pi_2^c) = 0$$
$$\pi_2 \to 0$$

and

$$\text{Lim } (\pi_2^c) = \infty$$
$$\pi_2 \to \infty$$

In the case of the relation between π_4 and π_3, some deflection would be expected when $\pi_3 = 0$ (that is, the thrust is located at the ground line), and deflection would be very large at high values of π_3. For the relationship selected,

$$\text{Lim } (Ce^{\pi_3}) = C$$
$$\pi_3 \to 0$$

and

$$\text{Lim } (Ce^{\pi_3}) = \infty$$
$$\pi_3 \to \infty$$

The prediction equations for the pier in dry sand were:

$$\frac{\delta}{B} = 1.369 \times 10^{-4} \left(\frac{D}{B}\right)^{-0.5016} \left(\frac{H}{B^2 D\gamma}\right)^{3.192} 3.633^{\left(\frac{L}{D}\right)}$$

and

$$\Theta = 7.420 \times 10^{-5} \left(\frac{D}{B}\right)^{-0.8172} \left(\frac{H}{B^2 D \Upsilon}\right)^{3.030} 3.542^{\left(\frac{L}{D}\right)}.$$

The symbols are defined in Table III, p. 68, and in Appendix A1.

Observed values of π_4 and π_6 are plotted in Figures 32 and 33 against values calculated by the above equations for the same values of the independent parameters. All points would be on the line shown if prediction were perfect. It will be noted that there is some non-linearity evident in the logarithmic plots: predicted values tend to be greater than the observed values near the middle of the range, and lower than the observed values near both ends of the range. It will also be noted that the scatter (disregarding the non-linearity) is about uniform throughout the range in these logarithmic plots. In terms of the real (untransformed) variables, the scatter increases greatly toward the high end of the range.

In the region in which a designer would probably be most interested--rotations ranging from 0.0005 to 0.01 radians--the prediction equation tends to over-estimate the rotations. In a few cases the observed value of rotation is barely one-third of the predicted value, but most observed values fall between 50 percent and 150 percent of the predicted values. The rather wide variation between observed and predicted values is ascribed in part to the variability of the material; local variations in the compaction of the sand, slight variation in the method of loading, and errors in estimating the time at which pier movement ceased; all would contribute to variation in the results. A second source of prediction error is due to the failure of the postulated functional relationships to exactly describe the phenomena being investigated. It was noted in Chapter VI that the data on the effect
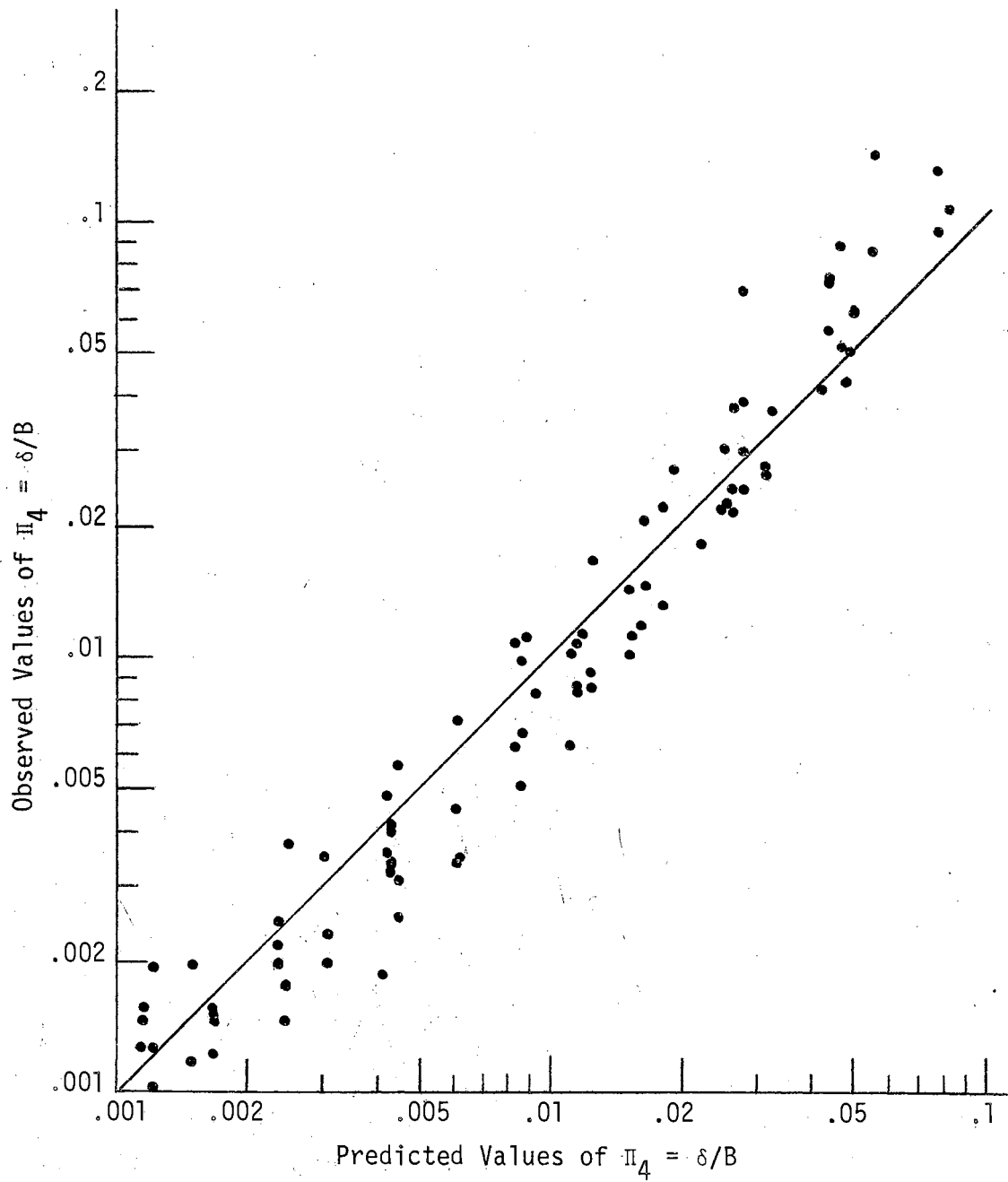
Figure 32. Observed Values of Π_4 Compared to Predicted Values, Dry Sand Tests.
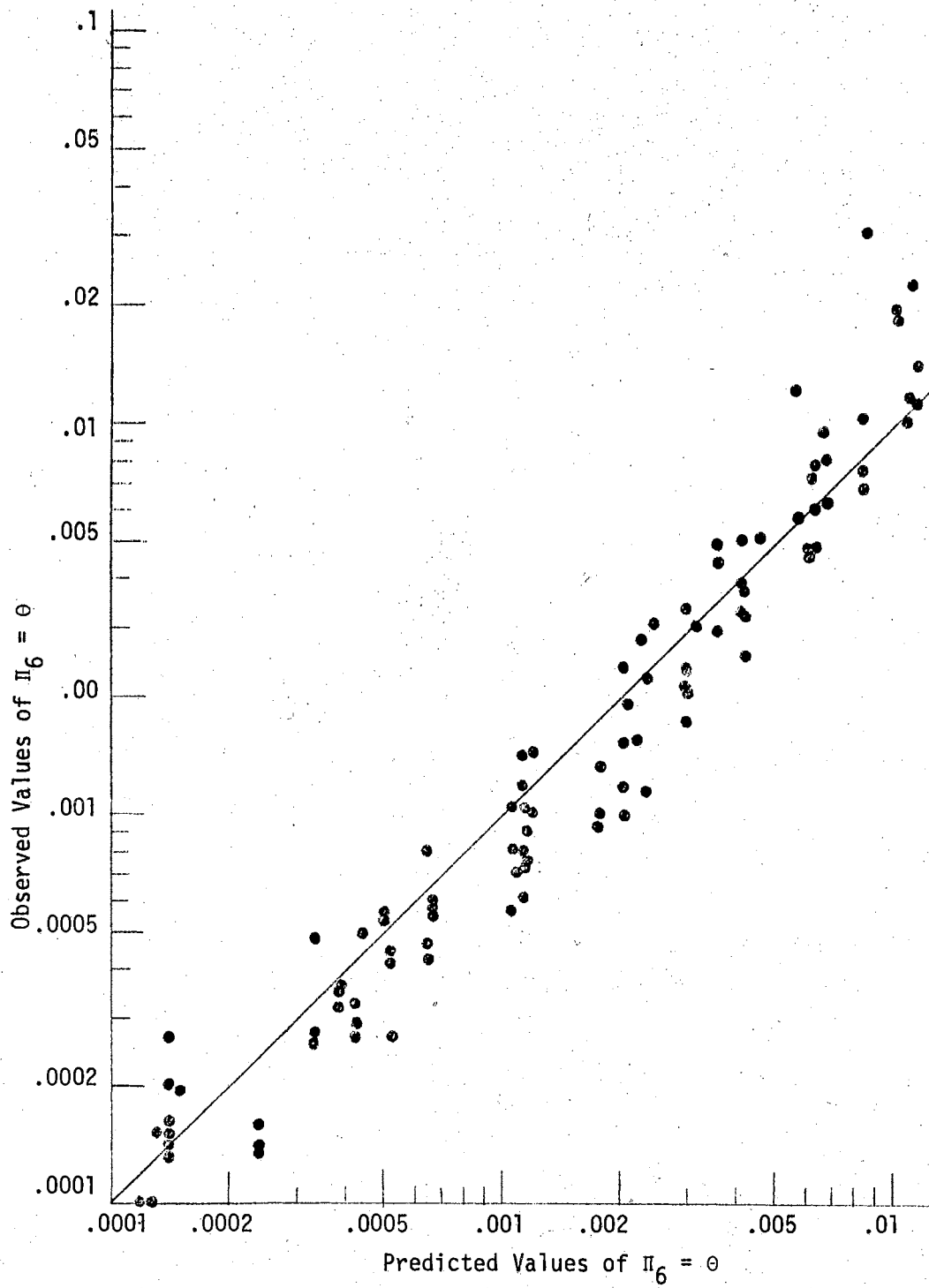
Figure 33. Observed Pier Rotations, Π_6, Compared to Predicted Values, Dry Sand Tests.

of Π_1 on Π_4 and Π_6 were limited and badly scattered. Consequently, the exponent of Π_1 may be subject to rather large error. Certainly some disagreement between the postulated and real functions exists, as is apparent in the curvature of the plots of Figures 32 and 33.

These prediction equations were tested against the data obtained by Beckett (30), by using them to predict horizontal deflection at 0.315 D above the ground line at the same values of the independent variables used by Beckett. The results are plotted in Figure 34. The predicted values of deflection were generally greater than reported [(30) pp. 83, 84, 86], in some cases being four times as great as the observed values. Some over-prediction would be expected because Beckett's tests were conducted in somewhat denser sand presumably with a greater angle of friction, ϕ, than that for which the prediction equations were developed. The effects of internal friction were not investigated in this study. Some difference may have been due to the methods of compaction used--compaction by vibration of the whole mass in the present study, instead of the method of compacting by layers used by Beckett.

Location of Axis of Rotation

The location of the apparent axis of rotation was calculated for each test, using the relationship

$$Z_o = \frac{\delta}{\Theta}$$

where Z_o is the depth of the rotation axis measured from the soil surface. A new parameter, POZN, was defined as the ratio of the depth of the apparent axis of rotation to the embedded depth of the pier:

$$POZN = \frac{Z_o}{D}.$$
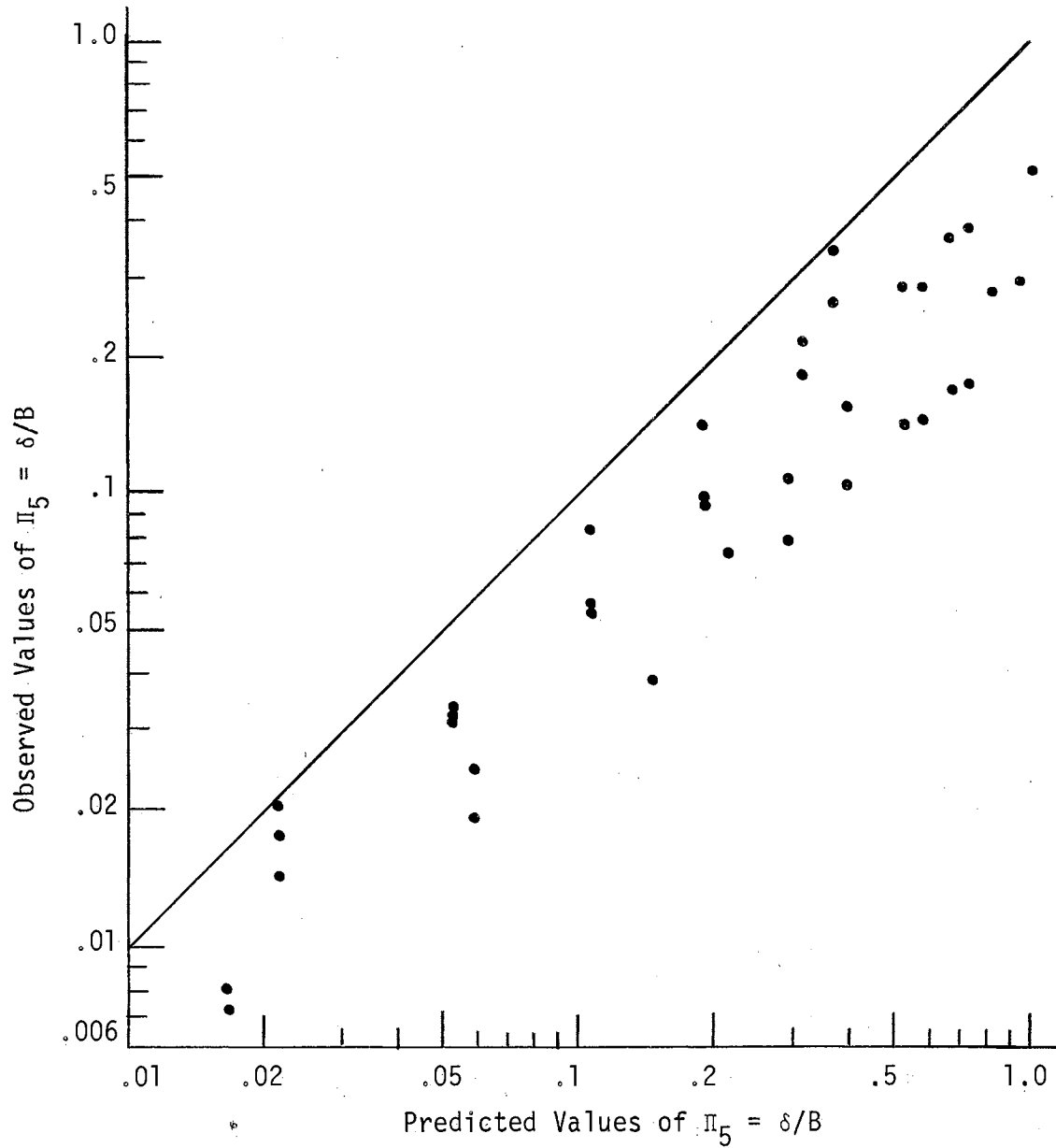
Figure 34. Observed Values of Beckett's (30) Π_5 Compared to Predicted Values, Dry Dense Sand.

Values of POZN are listed in Appendix B.

Mean values of POZN were calculated, from all observations, except for clearly erroneous values, in each series of tests. In the dry sand tests the average depth of the rotation axis was 0.713D; in the saturated sand tests it was 0.746D; and in the wet sand tests it was 0.647D. The mean value of POZN for the dry sand tests, 0.713D, was very close to that predicted by Kent (37), 0.71D, for a value of $\pi_3 = 2$, the average value used in the present study.

The prediction equation for POZN obtained from the dry sand tests was:

$$POZN = 0.8523 \left(\frac{D}{B}\right)^{-0.3893} \left(\frac{H}{B^2 D\gamma}\right)^{0.2902} 1.1112^{\left(\frac{L}{D}\right)}.$$

This indicates that the position of the axis of rotation, POZN, increases as π_2 is increased, decreases as π_1 is increased, and increases as π_3 is increased.

The increase in POZN as π_3 increases is in agreement with the theoretical analyses of Walker and Cox (36), Kent (37) and others. An increase in POZN as the load (corresponding to an increase in π_2, $\frac{H}{B^2 D\gamma}$) increases, was predicted by Prakash (45), although most investigators, such as Kent (37) have reported that the magnitude of the load has no effect on the position of the axis of rotation. The decrease in POZN as π_1, $\frac{D}{B}$, increases is difficult to explain. This effect would occur if the distribution of vertical bearing pressure on the bottom of the pier were trapezoidal in shape, tending to resist overturning. This effect would provide a greater portion of the resistance to overturning in short piers than in long piers, without contributing to thrust resistance, and

consequently would cause the axis of rotation to be relatively deeper for short piers than for longer piers.

The fact that the depth of rotation observed in the wet sand tests was shallower than in the dry sand tests is in agreement with the Rankine-Coulomb theory of soil strength. The wetting of the sand is considered to add a cohesive character to the otherwise purely frictional sand. The cohesive strength may be considered to be independent of depth, whereas the frictional strength increases linearly with depth. The effect of the added cohesion is to increase the strength of the soil a uniform amount in absolute terms at all depths, but in terms of the frictional strength the relative increase in strength is much greater near the surface than at greater depths. The effect of this relatively greater increase in strength at shallow depths is to raise the theoretical point of rotation. Analyses of pier overturning (36), based on the Rankine-Coulomb active and passive pressure theories, predict that the axis of rotation of a pier subjected to an overturning moment only will be at 0.667D below the surface in purely granular material (C = 0) and at 0.5D in purely cohesive material ($\phi = 0$).

Resistance to Overturning

The experiment was planned to obtain information on the deflection-load relationships of piers, and no attempt was made to determine the maximum thrusts or moments that the piers could withstand. Except for eight piers which were inadvertently loaded to failure, loading was discontinued before failure occurred. It was noted, however, that the resistance of the piers to overturning was much greater than could be accounted for by the assumption of the Rankine passive pressure acting

on the front and the Rankine active pressure acting on the back of the pier; considerably greater even than would be predicted by passive pressure acting alone. Such a result is in general agreement with the mechanism proposed by Hansen (70) in which the overturning resistance is attributed to the passive resistance of the soil wedge directly ahead of the pier and of the shearing resistance on two vertical planes in the direction of motion containing the sides of the pier.

Effect of Repeated Loads

The equations developed to relate π_4 and π_6 to π_7, the number of repetitions of load, were

$$\pi_{4N} = \pi_{41} (1 + 0.2044 \log_e \pi_7)$$

and

$$\pi_{6N} = \pi_{61} (1 + 0.1661 \log_e \pi_7)$$

with π_{4N} being the value of π_4 at maximum load after N cycles of loading; π_{41} the value at maximum load in the first load cycle. These equations are not valid for deflections and rotations at less than the maximum loads.

If the probable loading on a pier foundation supporting a rigid frame building with roof loads or grain loads is considered, it appears improbable that maximum loads would occur more often than once per year. A building designed for a 50-year life could be expected to be fully loaded not more than 50 times: N may reasonably be taken as 50 or less. If the building is to be designed for a 20-year life, N will probably not be greater than 20. The maximum rotation, then, to be expected

during the life of the structures, subject to the conditions of the experiment, will be:

$$\Pi_{6(50)} = \Pi_{61} (1 + 0.1661 \log_e 50) = 1.65 \Pi_{61}$$

and

$$\Pi_{6(20)} = \Pi_{61} (1 + 0.1661 \log_e 20) = 1.50 \Pi_{61}$$

respectively.

Welch (64), working with a saturated sand-clay mixture, obtained the relation:

$$\text{Tan } \Theta = \frac{N}{9.7529 + 14.274 N}$$

for the effect of repeated loading. When this relation is evaluated at $N = 1$ and at $N = 20$ and $N = 50$, the effect of load repetition may be written:

$$\text{Tan } \Theta_{(20)} = 1.558 \tan \Theta_I$$

and

$$\text{Tan } \Theta_{(50)} = 1.589 \tan \Theta_I$$

which agrees remarkably well with the above relations when the difference in soils is considered.

CHAPTER VIII

A METHOD OF ANALYSIS OF RIGID FRAMES ON YIELDING FOUNDATIONS

A method for analyzing rigid frames on yielding foundations was developed, utilizing the unit load method of frame deflection analysis in conjunction with iteration to solve the non-linear deflection equations resulting from the non-linear foundation displacements. The procedure was incorporated in a program written in Fortran IV for the IBM 7040 digital computer. The computer program is presented in Appendix C.

The Unit Load Method

The unit load method, as described by Wang (49) and others, is a means of determining deflections in an elastic structure due to bending, in which the deflection, δ_A, of a determinate structure at a point A is expressed by:

$$\delta_A = \int \frac{Mmds}{EI} \tag{1a}$$

where

M is the moment throughout the structure due to applied loading

m is the moment throughout the structure caused by a unit load at A acting in the direction of deflection

s is distance along the centroidal axes of the structural members.

Similarly, a rotation, Θ_A, is expressed by:

$$\Theta_A = \int \frac{Mm'ds}{EI} \qquad (1b)$$

where

m' is the moment caused by a unit moment applied at A.

In applying the unit load method to an n-fold indeterminate structure, the structure is first considered to be made determinate by releasing n restraints. The n actions--forces and moments--corresponding to these restraints are considered as the "redundant actions" or simple "redundants".

Each of the n deflections or rotations corresponding to each of the released restraints will be the sum of the effects of the applied load and of each of the redundants. Thus it is possible, if the actual deflection or rotation at each restraint is known, to write n deflection equations of the form:

$$\delta_{1,p} + \delta_{1,1} + \delta_{1,2} - - - \delta_{1,n} = \Delta_1 \qquad (2)$$

$$\delta_{n,p} + \delta_{n,1} + \delta_{n,2} - - - \delta_{n,n} = \Delta_n$$

where

$\delta_{1,p}$ is the computed deflection at the first restraint, due to the applied load

$\delta_{1,1}$ is that due to the first redundant, and so on; and

Δ_1 is the known deflection at that restraint of the actual indeterminate structure.

(In the above system of equations no distinction is made between deflections and rotations; the procedure is the same for both.)

Each of the $\delta_{i,j}$ is a linear function of the redundant j, and the system of equations may be solved for the n redundants, provided the Δ_i are known.

A major disadvantage of the unit load method of analysis is the amount of work involved in setting up and formally integrating to determine each of the $(n^2 + n)$ deflections. Its advantage is the ease with which variations in section properties and structural geometry may be accommodated.

The hingeless single-bay gable frame is a third-order indeterminate; three supporting reactions are redundant to static equilibrium. The reactions considered redundant in this analysis are H_R, M_R, and M_L, identified in Figure 35. In computation, the three restraints corresponding to these redundant reactions are removed, and deflections and rotations due to the applied load and to each redundant reaction are computed by the unit load method. If the supports are considered fixed, the sum of all components of a given deflection or rotation (for example, the rotation at the base of the left leg,Θ_L) must equate to zero. By this means three deflection equations, in terms of the known load and the three unknowns, H_R, M_R, and M_L, are written. These equations are of the form:

$$\delta(P) + \delta(H_R) + \delta(M_R) + \delta(M_L) = 0 \qquad (3)$$

$$\Theta_R(P) + \Theta_R(H_R) + \Theta_R(M_R) + \Theta_R(M_L) = 0$$

$$\Theta_L(P) + \Theta_L(H_R) + \Theta_L(M_R) + \Theta_L(M_L) = 0$$

where $\delta(P)$ is the horizontal movement of the base of the right leg (relative to the left leg) due to the applied load, P; $\delta(H_R)$ that due to the redundant horizontal thrust H_R, etc.
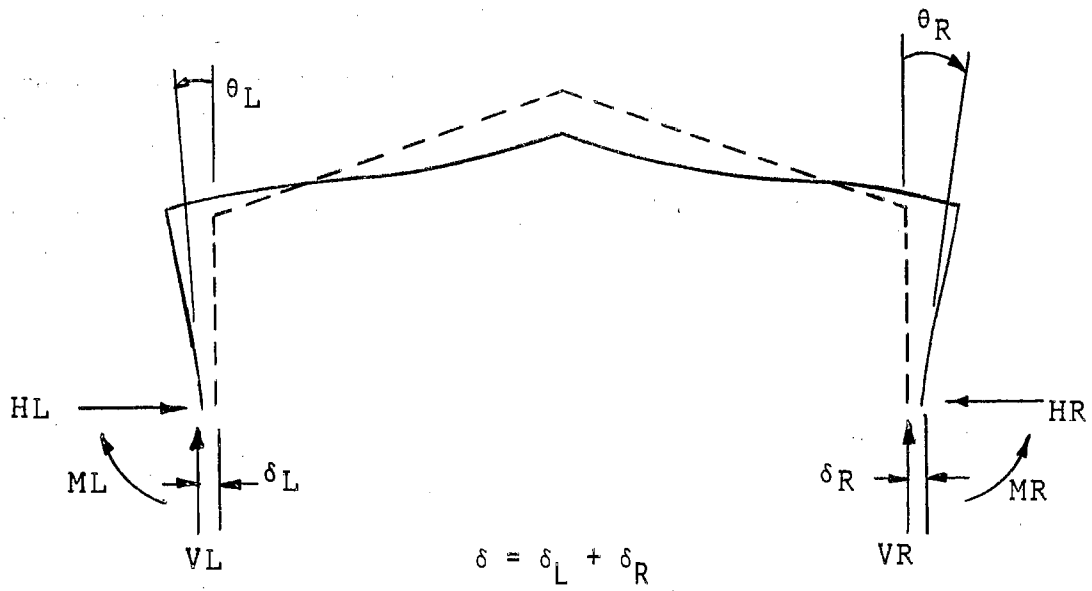
Figure 35. Deflections and Reactions, Hingeless Frame
with Foundation Yielding.

This set of simultaneous equations can be solved for the three unknowns, H_R, M_R, M_L, and the remaining reactions determined by the methods of statics.

If, instead of being fixed, the supports deflect a known amount, so that the final horizontal deflection of the right support with respect to the left is Δ_1, the rotation of the right support is Δ_2, and the rotation of the left support is Δ_3, the deflection equations may be rewritten, equating to the known deflections, Δ, as follows:

$$\delta(P) + \delta(H_R) + \delta(M_R) + \delta(M_L) = \Delta_1 \qquad (4)$$

$$\Theta_R(P) + \Theta_R(H_R) + \Theta_R(M_R) + \Theta_R(M_L) = \Delta_2$$

$$\Theta_L(P) + \Theta_L(H_R) + \Theta_L(M_R) + \Theta_L(M_L) = \Delta_3$$

These, still linear, simultaneous equations may also be readily solved for H_R, M_R, and M_L as before.

If, however, the deflection of the supports is unknown, but a function of H_R, M_R, M_L, and H_L, then the equations may become non-linear, of the general form:

$$\delta(P) + \delta(H_R) + \delta(M_R) + \delta(M_L) = f_1(H_R, H_L, M_R, M_L) \qquad (5)$$

$$\Theta_R(P) + \Theta_R(H_R) + \Theta_R(M_R) + \Theta_R(M_L) = f_2(H_R, M_R)$$

$$\Theta_L(P) + \Theta_R(H_R) + \Theta_R(M_R) + \Theta_L(M_L) = f_3(H_L, M_L)$$

where $f(H_R$, etc.) are relations describing the displacement and rotation of the piers when subjected to applied loads or moments.

In general, such a set of non-linear simultaneous equations are not solvable by direct methods. Iterative methods may lead to a solution, but convergence is not assured (71).

The Iterative Method of Solution

The method adopted for solution of the rigid frame on yielding foundations uses an iterative procedure. This procedure consists of the following steps:

Step 1: Compute the reactions of the frame with fixed supports, using equation 3.

Step 2: Using the values of reactions obtained in Step 1, compute displacements and rotations of each support, using appropriate equations relating foundation movement to applied actions.

Step 3: Insert the values of total horizontal displacement (Δ_1) and rotation of the right (Δ_2) and left (Δ_3) supports obtained in Step 2, into equation 4. Solve equation 4 for new values of H_R, M_R, and M_L and obtain H_L by statics.

Step 4: Repeat Step 2 using the new values of the reactions. Repeat Steps 3 and 4 until sufficiently close approximation is obtained.

It appears that the process will converge unless the piers are inadequate to withstand the thrusts involved; that is, that the calculated deflections of the piers are comparable to those of the pin-and-roller supported frame.

Once the three redundant reactions have been determined, the remaining reactions and internal actions may be determined by statics.

The Approximate Solution By Digital Computer

Development of the deflection equations by formal integration is rather laborious, particularly if a number of changes in frame geometry and section properties are to be considered. The digital computer program developed to reduce this problem makes use of approximate integration over a series of finite intervals to establish each of the deflections, δ_{ij}, by use of the approximate relation:

$$\delta = \int \frac{Mm \, ds}{EI} \doteq \sum \frac{M_k m_k \Delta s_k}{E_k I_k} \tag{5}$$

where M_k, m_k, E_k, I_k are the mean values of M, m, E, and I respectively over the kth interval Δs_k The program as written uses ten equal intervals, Δs, for each member with a maximum of four members. This makes possible the inclusion of variable section, and the application of loads at any of the 41 grid points of the structure.

Complete details of the computer program, including instructions for preparing input information, are presented in Appendix C.

Operation of the program is as follows:

1. The deflection matrix is computed using finite integration, to form a system of equations which, in matrix form, is:

$$[\delta] [R] = [-\delta_p] \tag{7}$$

which corresponds to the set of equations 3. This equation is solved for the reactions, R, which result from the fixed base condition.

2. These reactions are used to predict the resulting pier movement, and the corresponding movements of the frame bases, Δ.

3. The revised matrix equation,

$$[\delta]\ [R] = [\Delta - \delta_p]\ \ \ \ \ \ \ \ \ \ \ (8)$$

is solved for new values of R.

Steps 2 and 3 are repeated until a satisfactory degree

of convergence has been achieved. If the process diverges,

the operation is halted.

In the form in which the program is presented in Appendix C, the subroutine PIER uses the prediction equations developed in Chapter VI, equations 6 and 8, to predict pier rotation. Other prediction equations, if such are available, which may be suitable for more general types of soil, may be readily incorporated in the subroutine in place of these.

Use of the Computer Program in Design

The frame analysis program determines, with reasonable accuracy, the actions--shears, moments, and axial thrusts--in a hingeless rigid frame with any system of loading, corrected for anticipated foundation movement. As presented here, it is useful in design only as a method of analyzing a specific design. The user must still assume specific section properties and foundation geometry, test his design by the analysis program, then correct either section properties or foundation geometry or both, and repeat the process as many times as may be needed.

In order to provide an initial estimate of pier size for the design process, the curves of Figures 36 and 37 have been developed. These curves are solutions of the prediction equation for π_6 (Θ)--equation 8a of Chapter VI, page 103 for constant values of π_6, of 0.005 and 0.01 radians, respectively. The dimensionless parameters used in these
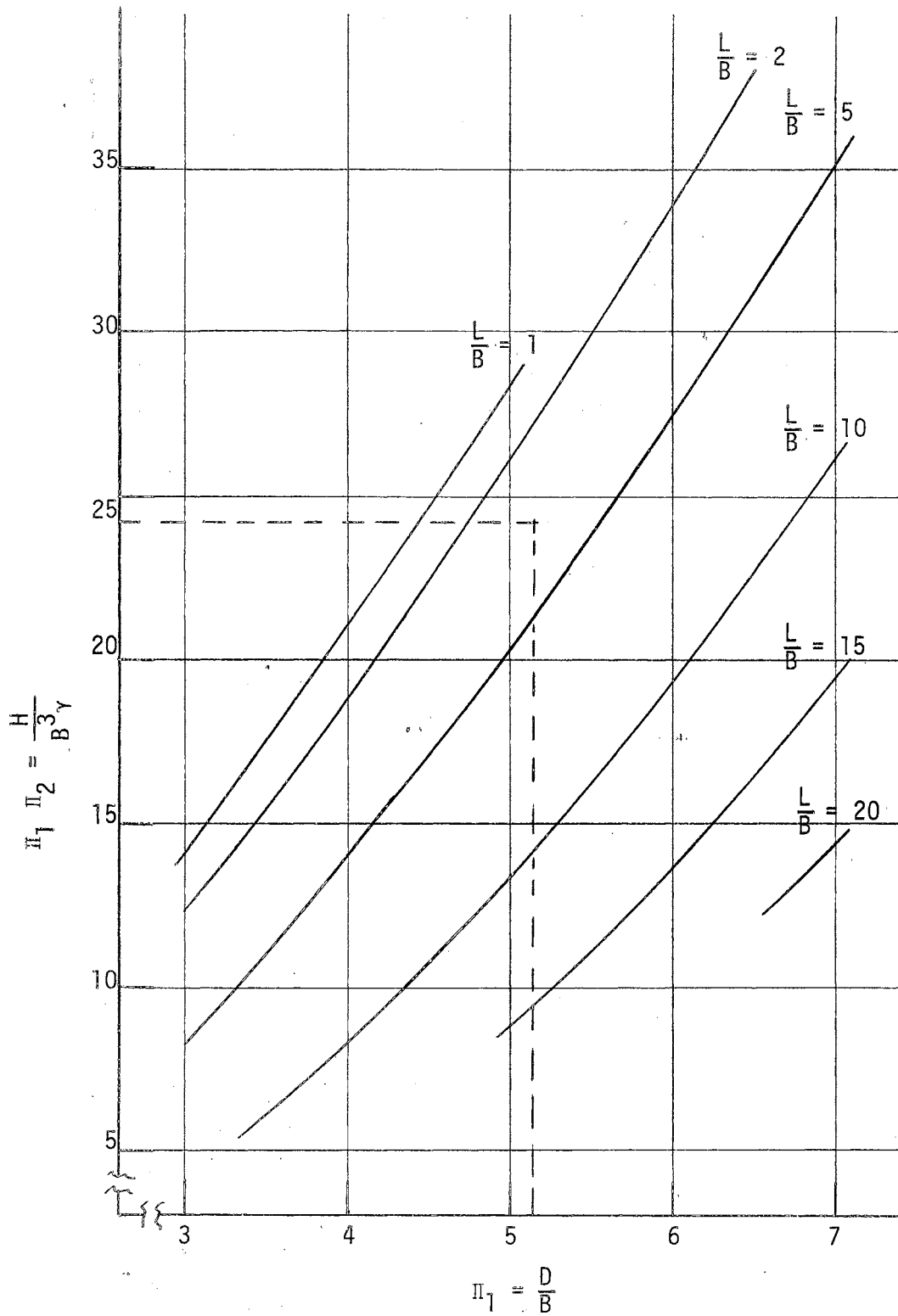
Figure 36. The Relation Between Thrust, Depth and Moment
Parameters When $\Pi_6 = 0.005$.
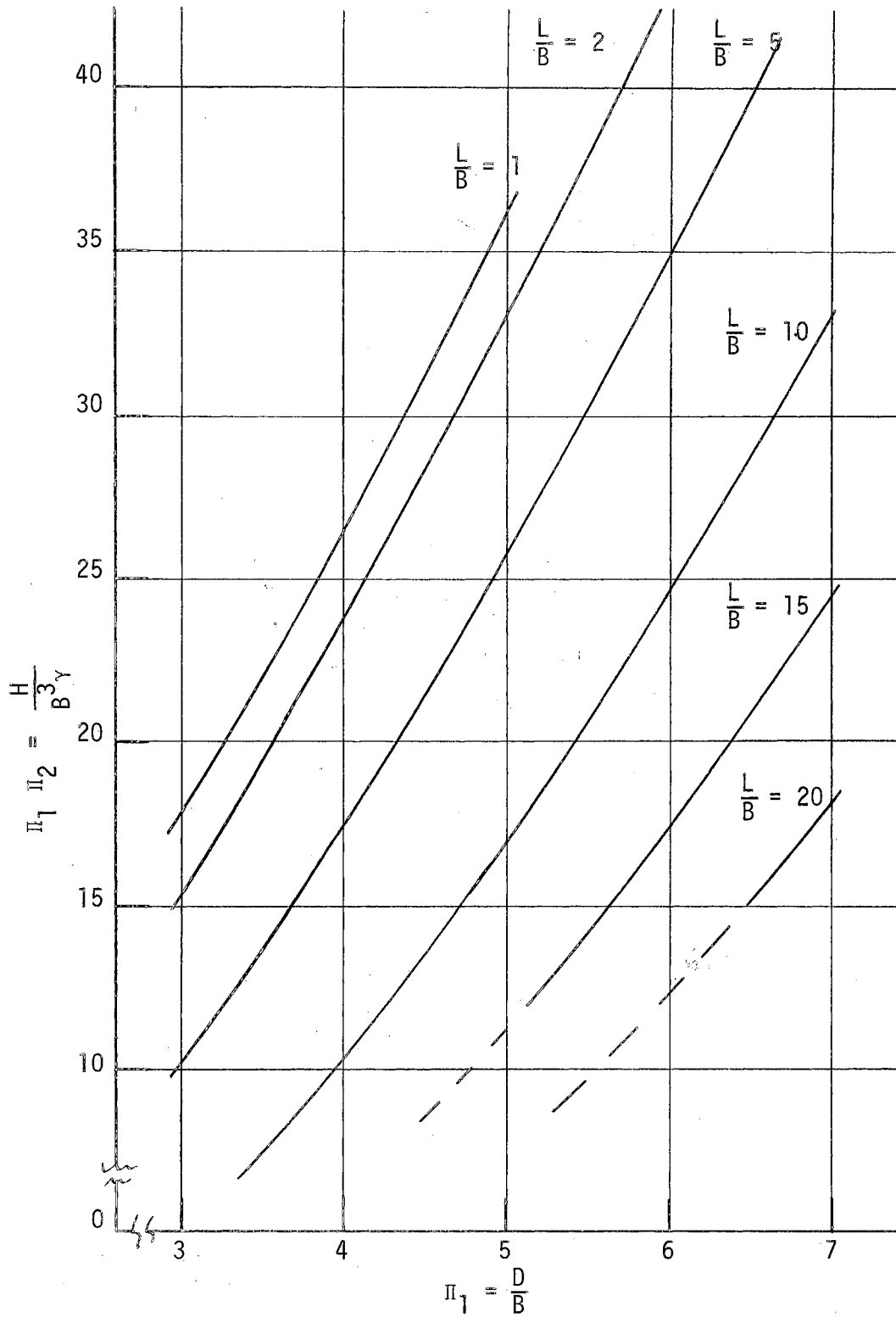
Figure 37. The Relation Between Thrust, Depth and Moment
Parameters When $\pi_6 = 0.01$.

figures are redefined, by multiplying, in order to eliminate the
quantity, D--the embedded depth of the pier--from the thrust and moment
parameters. These sets of curves predict the depth of pier embedment
(expressed as the dimensionless parameter $\Pi_1 = \frac{D}{B}$) required to restrict
pier rotation to 0.005 and 0.01 radians, respectively, when known combi-
nations of thrust and moment are applied. Application of these curves
is restricted to the conditions of the pier experiment conducted in dry
sand from which the prediction equation was developed. The values of the
dimensionless parameters used in the experiment are shown in Table V,
page 72. An example of the use of these curves follows.

Example Problem - Selection of Pier Dimensions

Consider the frame and loading system of Figure 10, page 49.
The frame is to be continuous with cylindrical piers embedded
in dry sand which has a bulk specific weight of 107.7 pounds
per cubic foot. An initial estimate of suitable pier dimen-
sions is required, to limit pier rotation to 0.005 radians.

From Figure 10 and given conditions

$$H = 6171 \text{ lb}$$
$$M = 351,000 \text{ lb-in}$$
$$\gamma = 107.7 \text{ lb-ft}^{-3} = 0.0624 \text{ lb-in}^{-3}$$
$$L = \frac{M}{H} = 56.88 \text{ in}$$

Assume pier diameter, B = 16 in

$$\frac{H}{B^3\gamma} = \frac{6171}{16^3 \times 0.0624} = 24.14, \quad \frac{L}{B} = \frac{56.88}{16} = 3.56$$

Entering Figure 36 at $\frac{H}{B^3\gamma} = 24.14$ read horizontally to

$\frac{L}{B}$ = 3.56, interpolating between the curves for $\frac{L}{B}$ = 2 and $\frac{L}{B}$ = 5. Reading vertically downward from this point to the bottom scale,

$$\pi_1 = \frac{D}{B} = 5.15$$

$$D = 16 \times 5.15 = 82.4 \text{ inches}$$

The required pier dimensions are 16 inches diameter by 82 inches embedded depth.

The computation above does not consider the reduction in moment and thrust caused by pier movement. In actual selection of the initial trial pier dimensions the designer may anticipate these reductions and reduce the pier length accordingly. Once trial values of the pier dimensions have been established, they may be used in the computer program to obtain a first analysis of the frame-pier system. The results of the first analysis may be used in the same fashion to further refine the pier dimensions.

There is no reason the computer program could not be modified to carry out the iterative procedure involved in design, if it were desired. However, as selection of section properties and foundation geometry, and the relationships between the two, is so involved with subjective judgment, availability of equipment and materials, and economic factors, it appeared that inclusion of such a procedure would, unless the program were greatly expanded, cause a greater loss in terms of general applicability than the gain in convenience would justify.

CHAPTER IX

PROCEDURE OF THE FRAME EXPERIMENTS

In order to check on the accuracy of the frame analysis program in predicting pier deflections, a series of load tests of a scale model rigid frame with pier foundations was conducted in the sand tank in the laboratory. Also, several years previously, three full-size wooden rigid frames with pier foundations had been load-tested by Friesen (72) and these data were available for correlation. Unfortunately, the wooden frames had been tested in a very different soil from that used in developing the prediction equations so that it was not possible to correlate the results of the full-scale tests with the model tests. The tests of the full-scale wooden frames are included here primarily for information on observed deflections of full-sized frames tested in a real soil, and no attempt has been made to relate these results to those of the model.

Tests of the Model Frame

The Frame Model

The frame model was designed to model the prototype frame discussed in Chapter III. The model was built of hot-rolled steel, with a basic length scale of twelve. The problems involved in constructing and handling a true model of this scale led to the adoption of a model design in which the frame cross-sectional area was distorted. In the final model frame design 1 1/4 x 1/8 inch steel bar was used, with the major axis

perpendicular to the plane of the frame. This arrangement practically eliminates deflection due to axial or shear strain, while maintaining normal flexural behavior, and has the merit of needing no restraint against buckling out of plane.

The piers of this frame consisted of round steel bar, 1 7/16 inches diameter by 10 inches long. The piers were bronze-welded to the frame legs. Arms of 3/4 by 1/8 inch angle were brazed to the piers to permit pier movement to be measured. Details of the model frame and piers are shown in Figure 38.

Procedure

The model frame was set up in the same sand tank which had been previously used for the pier tests. Methods of setting the model in place and compacting the sand were similar to those used for piers. Dial gauges, with springs removed, were attached to the frame by magnets at five points to measure deflections. One gauge was located two inches above the sand surface in contact with the left pier arm with a second gauge located eight inches above this also in contact with the left pier arm, in order to measure movement of the left pier. A third gauge was located at the peak of the frame to measure vertical deflection of the frame peak. The remaining two gauges were located at the right pier arm, symmetrical with the first two, in order to measure movement of the right pier. The load was applied at the peak of the frame by the use of weights. The arrangement for testing is shown diagrammatically in Figure 38, and a photograph of the test arrangement in Figure 39.

After setting the frame and gauging equipment in position and obtaining initial dial readings, a load of one pound was applied, and the readings of the dials recorded; an added load of two pounds was applied
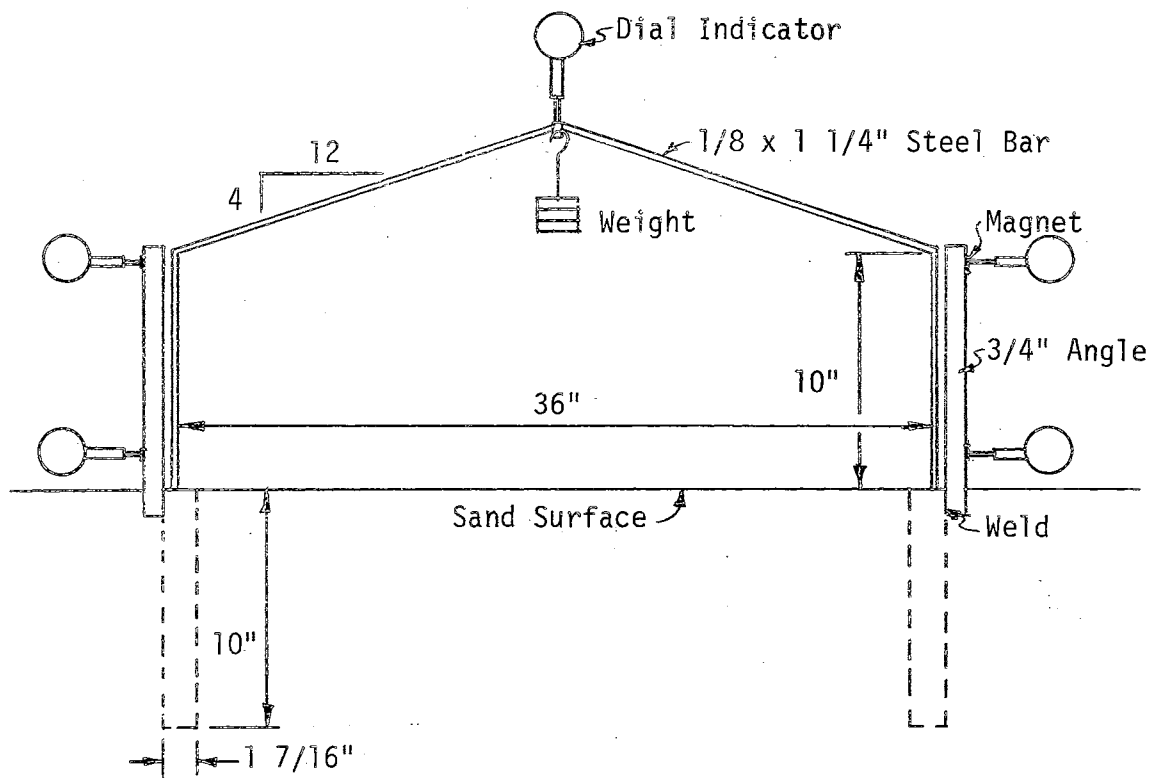
Figure 38. Model Frame, Showing Method of Loading and Measuring Deflections.
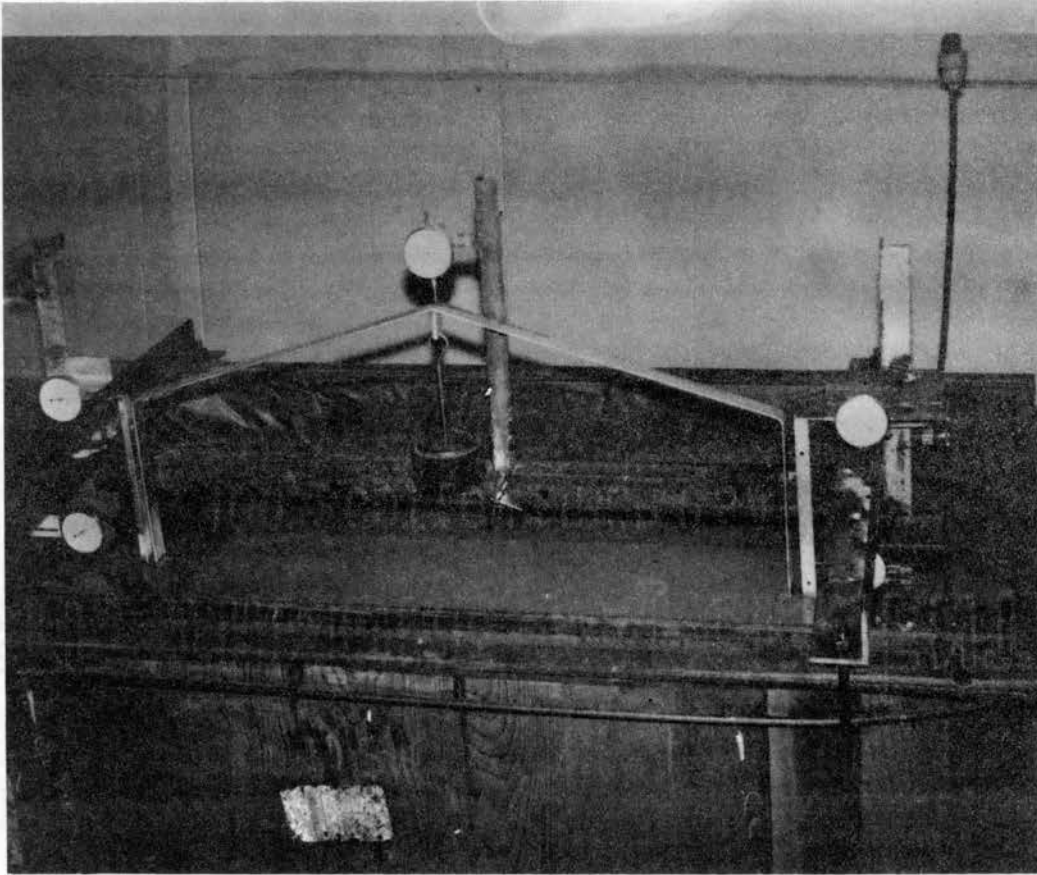
Figure 39. Testing the Model Frame.

and the dials read, then another two pound increment of load was added.
Following recording of deflection readings the load was removed and the
cycle repeated through a total of nine cycles.

In the tenth loading cycle the load was increased by two pound
increments to a maximum of nine pounds. Following the completion of
the tenth load cycle the frame was removed from the sand tank, the sand
was loosened, and the frame replaced, the sand compacted and the test
repeated. Three tests were made with the frame in dry sand and three in
saturated sand.

Upon completion of the tests the model was altered to a two-hinged
configuration, with lateral support movement prevented, and retested by
applying a load at the peak, with the peak deflection measured. The
results of this test were used to compute the value of EI for the model.
The value of EI so determined was 6006.3 pound-square-inches, compared
to a value of 5898.6 pound-square-inches calculated from the section
dimensions and using a value of 29 x 10^6 pounds per square inch for the
modulus of elasticity.

Tests of Full-Sized Wooden Frames

Three full-sized wooden frames were tested at Oklahoma State
University by James A. Friesen (72) in 1963 (Figures 40, 41). Each
frame spanned 23 feet between leg centers. These frames were built of
jarrah wood, with glued fir plywood gussets. The frame legs extended
five feet into the ground, with concrete piers 16 inches in diameter cast
around them. The soil was Bethany or Kirkland silt loam, typically 40
to 40 per cent clay in the B horizon. Testing was conducted following
an extended period of dry weather. No soil moisture data are available.
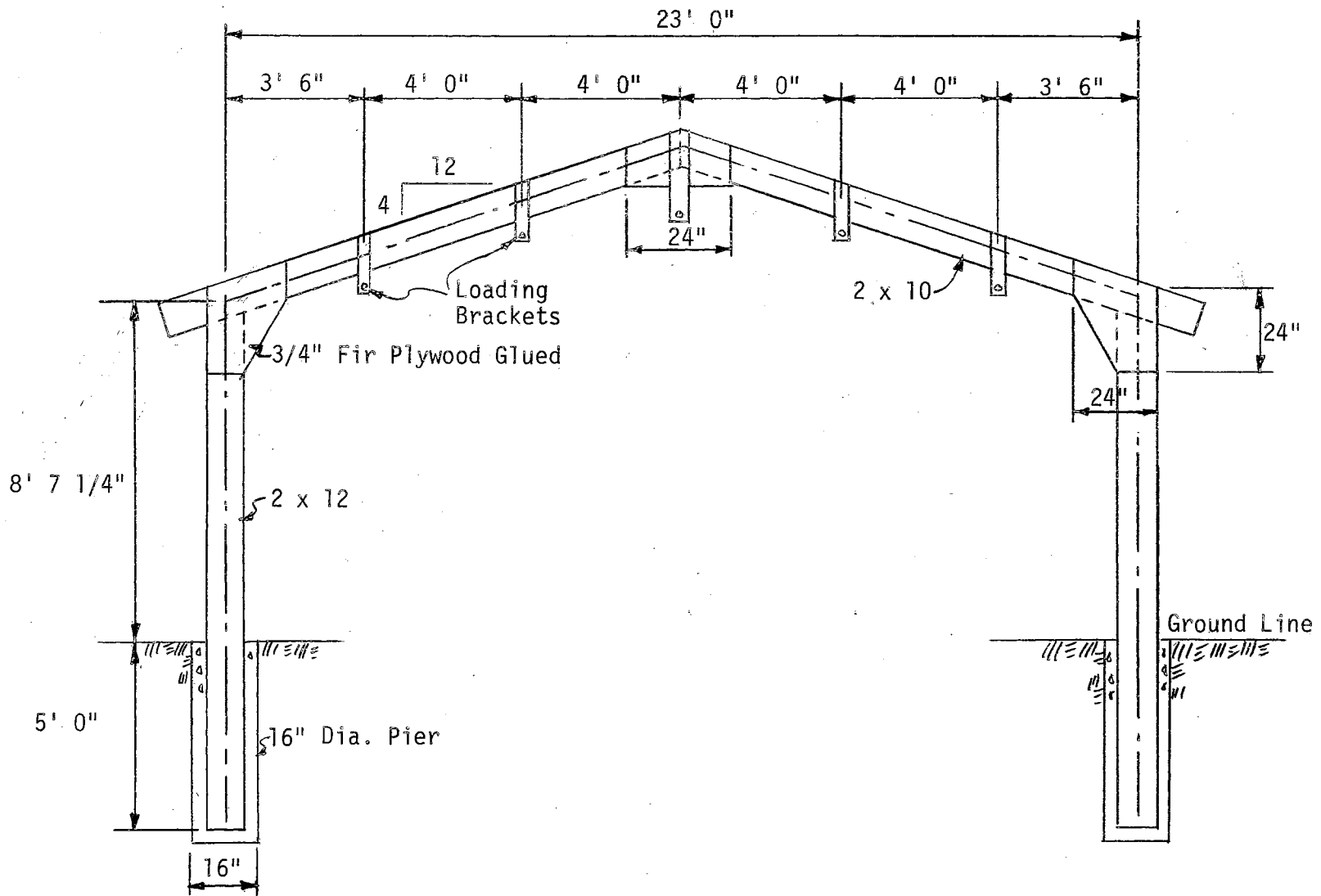
Figure 40. Construction Details and Dimensions of the Full-Size Wooden Frame.
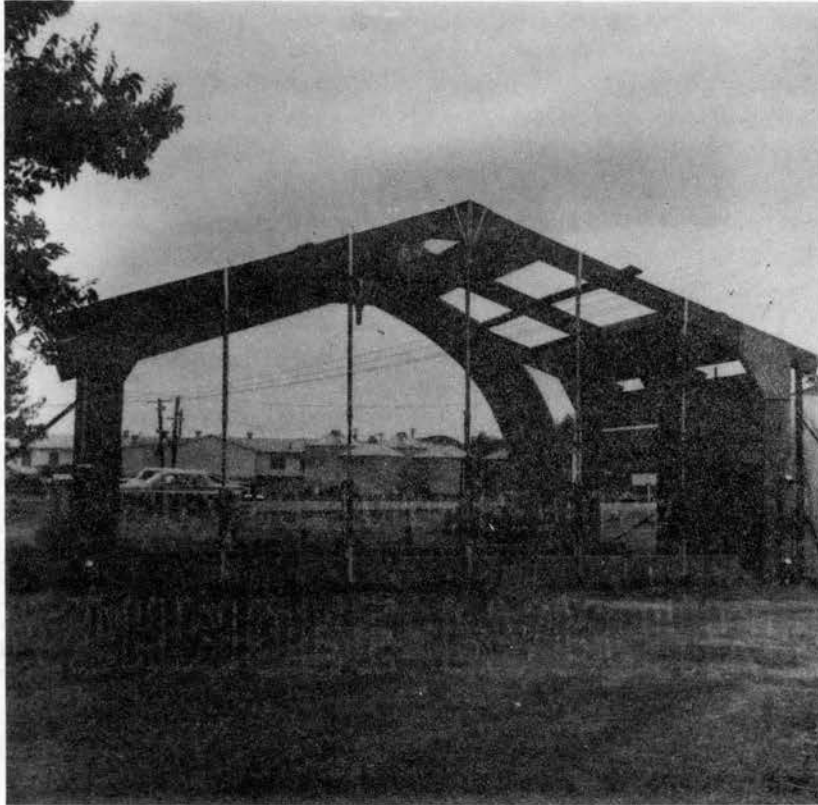
Figure 41. Load Testing the Full-Size
Wooden Frames.

The frames were tested individually by applying vertical loads at five points; 3.5 and 7.5 feet horizontally from the centerline of each leg, and at the center. The loads were applied by means of hydraulic cylinders attached to piers embedded in the soil. Details of the frame and the locations of the loading points are shown in Figure 40. The test arrangement is shown in Figure 41.

Deflections were measured by dial indicators at nine points, shown in Figure 42. Dial gauges 2 and 3 measured the deflection of a steel bar attached to the lower end of the left leg. Gauges 7 and 8 measured similar deflections at the right leg. Movement of the bases of the frames was computed from the readings of these four gauges.

The frames were tested with four loading cycles, each consisting of seven increments of load. After each cycle the load was completely removed before commencing the next load cycle.

Moments of inertia, I, for the nominal 2 x 12 leg members and the 2 x 10 rafter members were calculated from the dimensions of the cross sections, using the average values for all members of each nominal size. Modulus of elasticity, E, was determined by loading sections of the wood approximately 1 inch by 2 inches by 40 inches long, as simple beams and measuring the deflection of the mid-point. The elastic modulus so determined was 2.4 x 10^6 pounds per square inch (average of two samples).
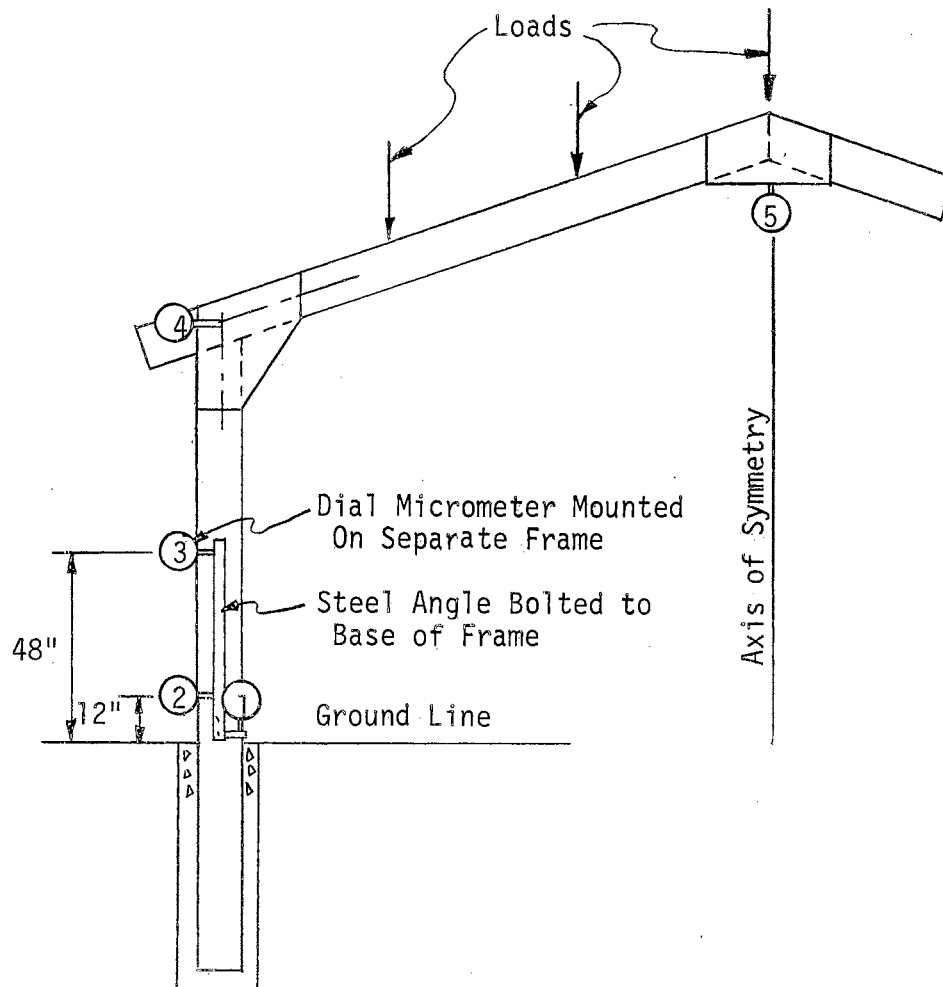
Figure 42. Method of Measuring Deflection in Tests of Full-Sized Wooden Frames.

CHAPTER X

RESULTS OF THE FRAME EXPERIMENTS

Model Frame Test

Analysis

Ground line deflections and rotations of the piers supporting the model frame in the tests in dry sand were computed from the dial gauge readings. These are listed in Appendix D-1 and are plotted against the load on the frame in Figures 43 and 44. Predicted deflections and rotations, computed by the frame analysis program described in Chapter VIII using the prediction equation for dry sand, are also shown. It will be noted that the predicted values agree well with the observations at the five pound load, but are considerably higher than the observed values at the nine pound load, and are low at the three pound load. Due to the very small deflections at the one pound load, this load was omitted from the analysis.

In terms of the dimensionless parameters used in the pier experiment, π_1 was 6.96, π_3 was approximately 0.5, and the value of π_2, corrected for the predicted deflection, was 2.214 at the five pound load. These values were within the ranges used in the pier experiment.

Deflections observed in the experiment are plotted against predicted deflections in Figure 45. Logarithmic coordinates were used for convenience because of the wide range of values. As a measure of the accuracy of prediction, a linear regression equation passing through

144
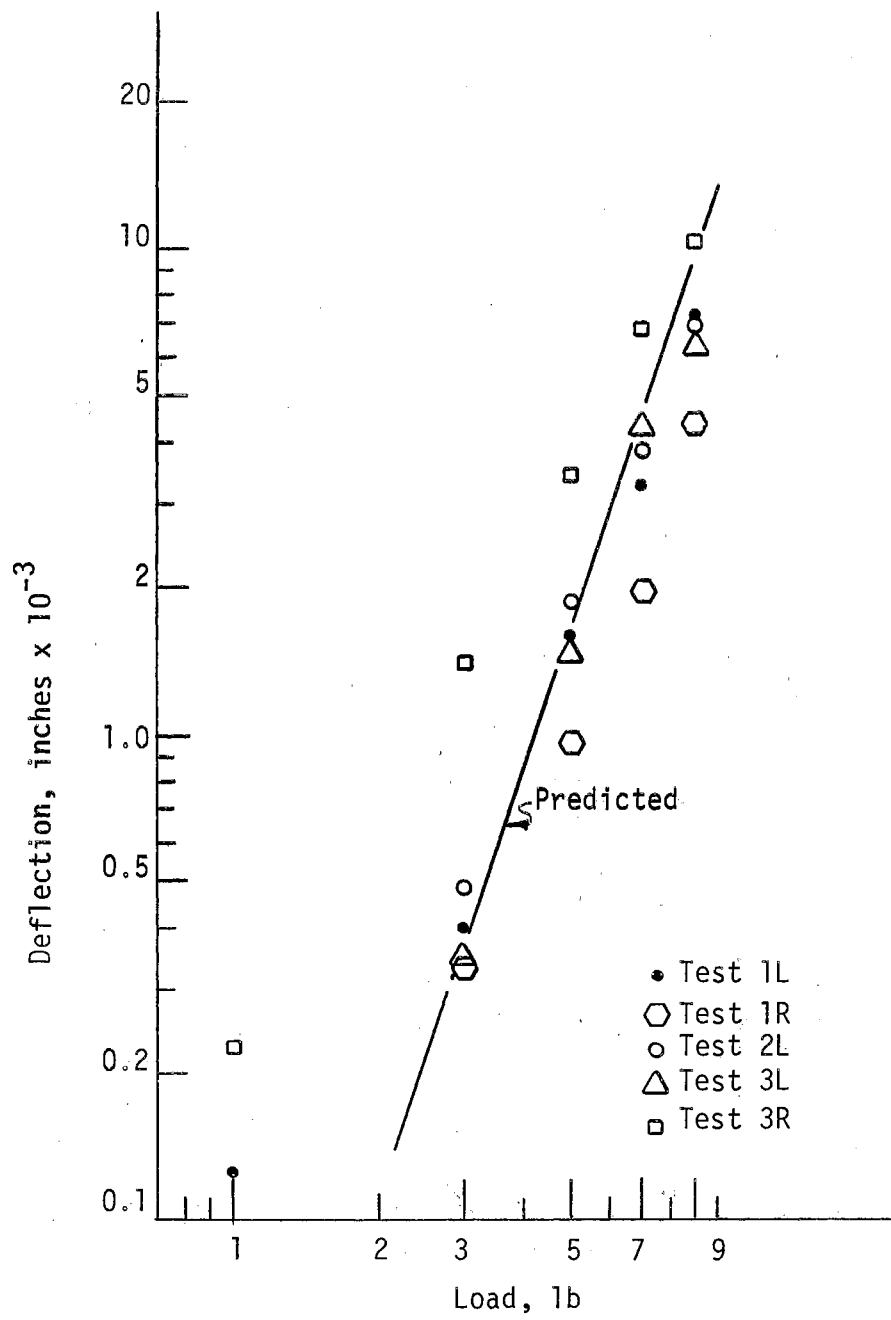
Figure 43. Deflections of Model Frame Piers at Five Loads.
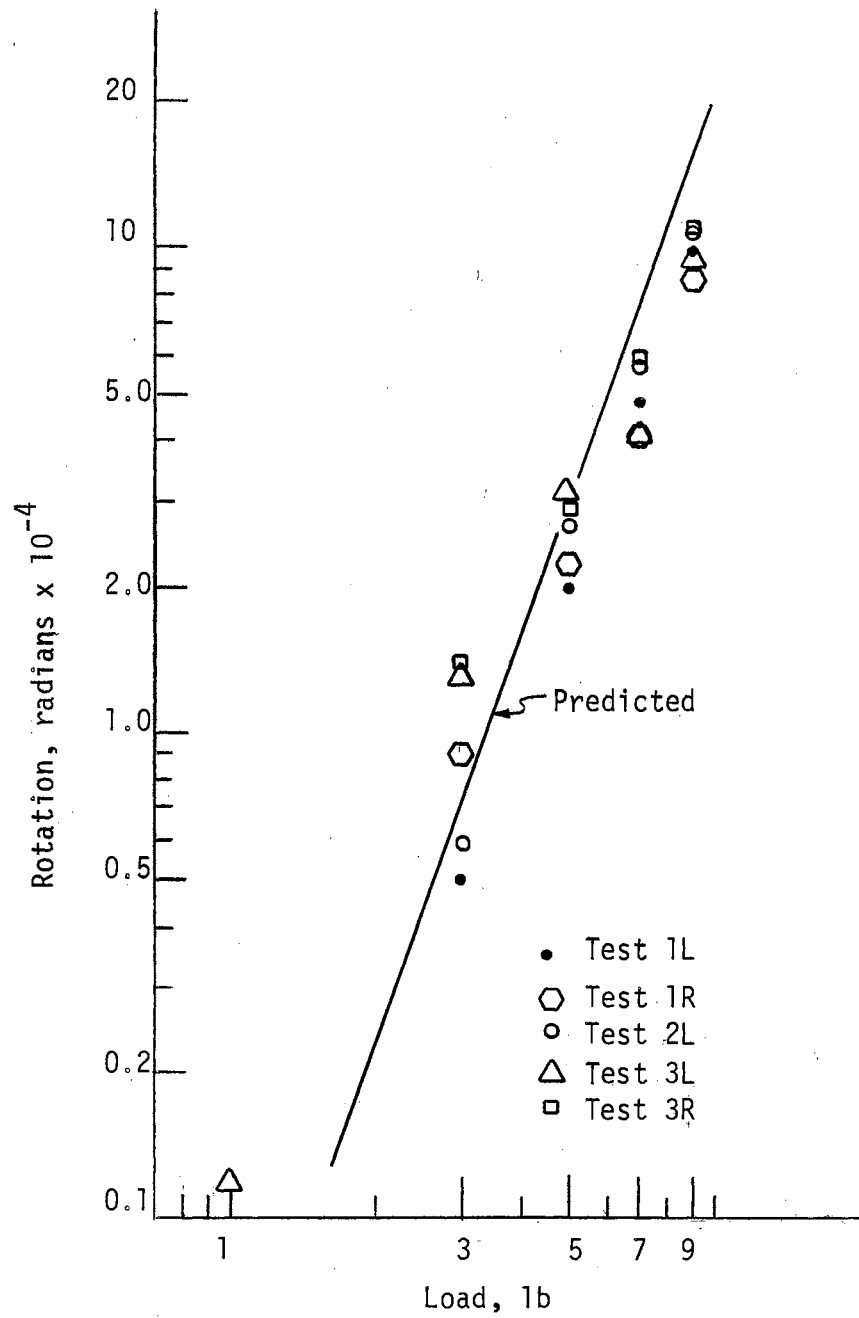
Figure 44. Rotations of Model Frame Piers at Five Loads.
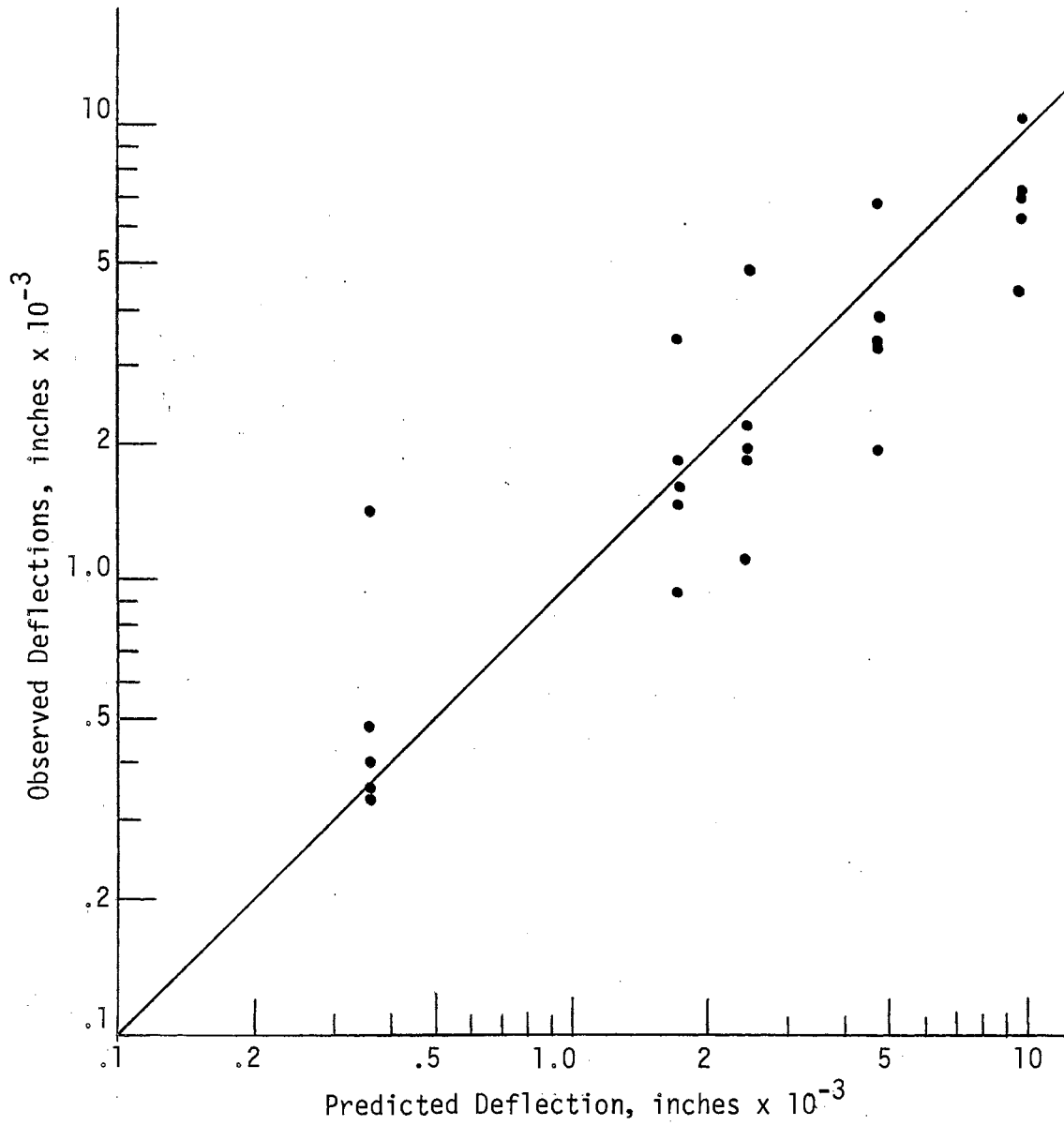
Figure 45. Observed Deflections of Model Frame Piers Compared to Predicted Deflections.

the origin was fitted to these (non-transformed) data. The equation was:

$$\delta_o = 0.777 \; \delta_p \tag{1}$$

where

δ_o = observed deflection

δ_p = predicted deflection

The coefficient of linear correlation, r, between δ_o and δ_p was 0.857.

A similar plot of observed versus predicted rotations is shown in Figure 46. The regression equation was:

$$\Theta_o = 0.644 \; \Theta_p \tag{2}$$

with coefficient of linear correlation, r, equal to 0.980.

Vertical deflections of the peak observed during the tests are compared in Table IX and Figure 47 with the deflections predicted for a fixed end condition and with those predicted by the frame analysis program which corrects for the predicted foundation movement. Observed deflections in the dry sand tests agreed very closely with those predicted when foundation movement was considered, and were about 8 per cent greater than predicted for the fixed end case. Deflections observed during loading of the frame in the two-hinged configuration are also shown in Figure 47. Peak deflections observed in the tests in saturated sand were about 4 per cent greater than in the dry sand tests.

Discussion

The differences between observed and predicted pier movements are believed to be attributable to two factors. One is the variability of the material, in which small changes in compaction technique may have
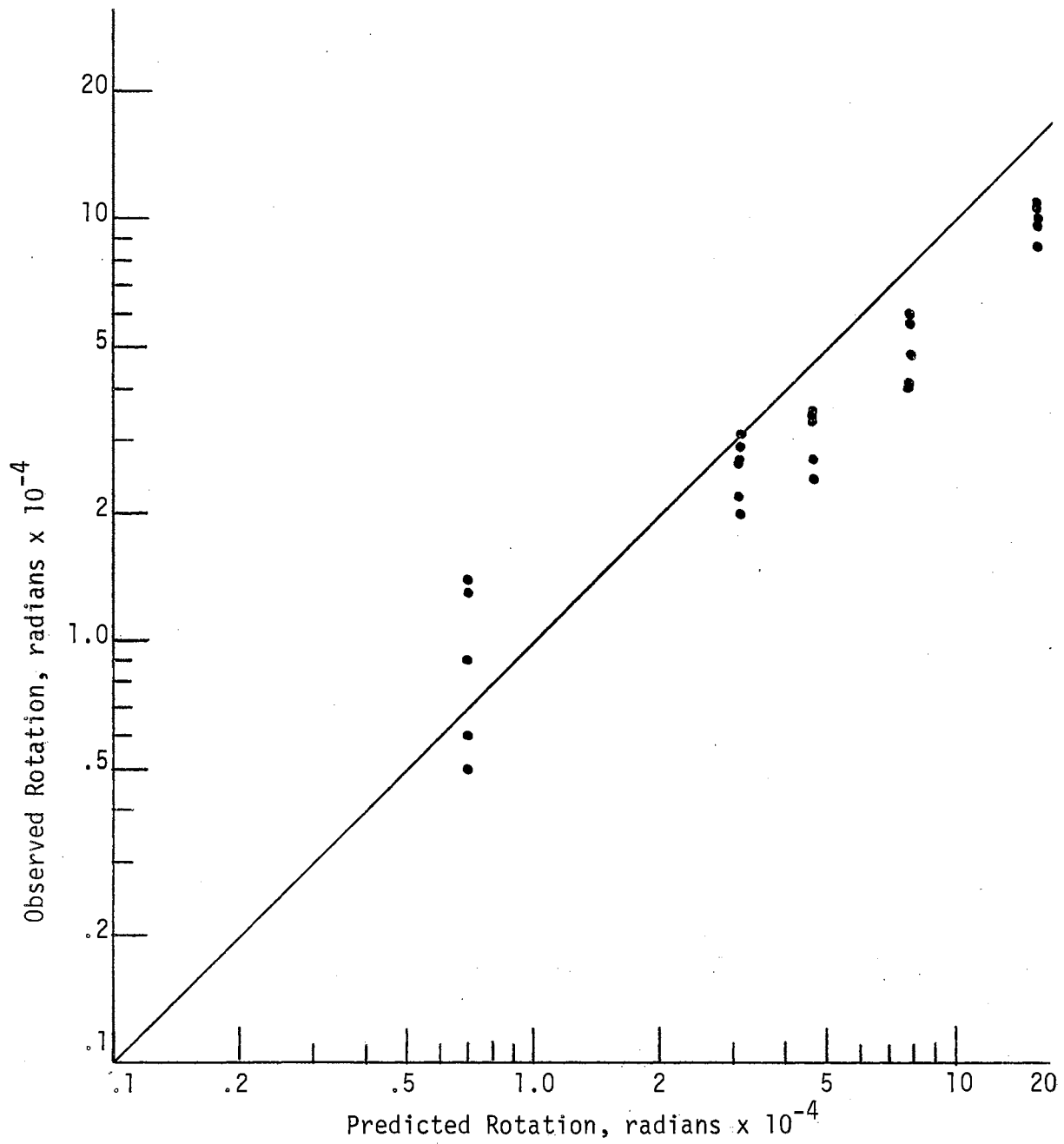
Figure 46. Observed Rotations of Model Frame Piers Compared to Predicted Rotation.

TABLE IX

OBSERVED AND PREDICTED DEFLECTIONS AT THE PEAK OF THE MODEL FRAME
DRY SAND TESTS

Load lb	Predicted Deflection Fixed End in	Predicted Deflection Foundation Movement Considered in	Observed Deflection, in			
			Test 1	Test 2	Test 3	Mean
1	0.02545	0.02549	0.0259	0.0254	0.0253	0.0255
3	0.07635	0.07921	0.0799	0.0794	0.0794	0.0796
5	0.12725	0.14010	0.1349	0.1350	0.1361	0.1353
7	0.17815	0.19806	0.1969	0.1974	0.1981	0.1975
9	0.22905	0.26133	0.2589	0.2589	0.2604	0.2594
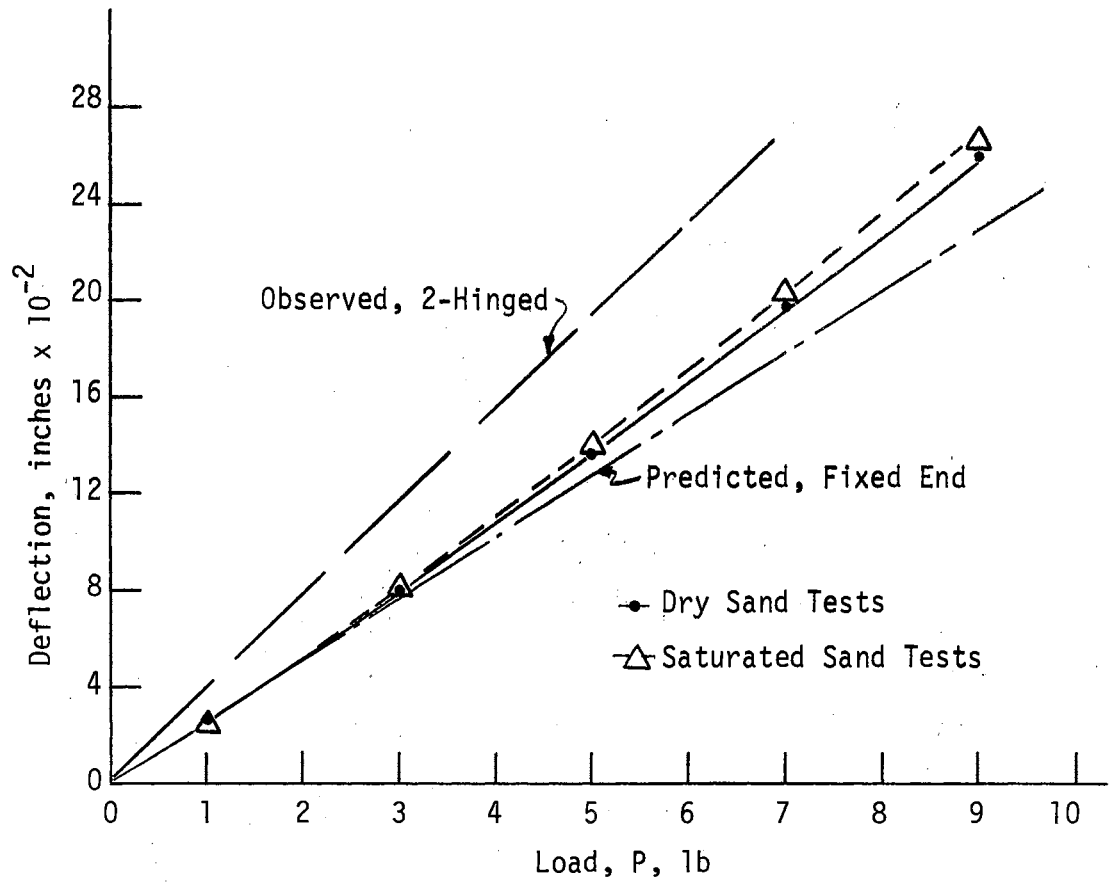
Figure 47. Deflection at the Peak of the Model Frame, Means of
Three Tests.

resulted in fairly large changes in response to load; this variation
is apparent in the deflection of the fifth pier listed in Appendix D-1,
which was almost double that of the other four piers. The second factor
is the location of these tests with respect to the logarithmic hyperplane
of equations 6 and 8, Chapter VI. The test location was near a "corner"
of the hyperplane; that is, $\pi_1 = 6.96$ and $\pi_3 = 0.506$ were near the
extreme values used in the pier experiment, of $\pi_1 = 7$, $\pi_3 = 0.2$. At such
a location on the prediction equation surface the expected accuracy of
prediction would be less than near the midpoint of the surface. The
situation is analogous to the broadening of confidence intervals in
simple regression as extreme values are approached.

As applied to the calculation of moments in the frame, the error
in predicting pier movement at high loads (predicted movement being
greater than the actual movement) would result in the predicted changes
in frame moment being greater than the actual changes. In particular,
predicted changes in moment at the base, haunch, and peak would be
larger than the actual changes, resulting in underestimating the final
moment at the base and the peak, and overestimating the moment at the
haunch. The actual error in predicted moments at the critical regions
would depend on the error in prediction of support movement and on the
magnitude of the predicted change as compared to that of the predicted
fixed end moment. For the model, at the nine pound load, the computed
moment at the support, assuming the fixed support condition, is 26.36
pound-inches. The predicted change in moment due to movement of the
foundation is -3.16 pound-inches, giving a final predicted moment of
23.19 pound-inches. If the observed pier movement and resulting moment
change is taken to be 0.7 times the predicted value--approximately the

average value from equations 1 and 2--then the actual change in moment would be

$$0.7 \times 3.16 = -2.21 \text{ pound-inches}$$

for a final moment of 24.15 pound-inches. This represents an error in the final predicted moment of about 4 per cent which is much less than the expected variation due to differences among different piers. On the other hand, if less firmly supported foundations were used, the error in predicted moment might be greater than 10 per cent.

It appears from the results of this experiment that the frame analysis program incorporating the prediction equations from Chapter VI, may be used in analyzing moments in hingeless frames on pier foundations embedded in dry sand, with relatively small errors. It must be recognized that under the test conditions the analytic method may tend to underestimate final moments at the bases of the frame and at the peak, and overestimate the moment at the haunch.

Tests of Full-Sized Wooden Frames

Analysis and Discussion

Loads applied to the frames had been recorded from the readings of two separate instruments; a load cell at one loading point, and a pressure gauge in the hydraulic loading system. When loads were computed from these readings, it was evident that serious error existed. It was impossible to determine the source or magnitude of the error. The haunch deflections predicted for a fixed end condition at the average load shown by the two instruments agreed closely with the observed haunch

deflections at low values of load, so the average of the two instruments was used in the analysis.

Because of the possibility of error in the load data, and various inconsistencies in the deflection data, the analysis was limited to computing deflections at the ground line, haunches, and peak, and computing the rotation of the frame at the ground line. Means of the haunch deflections, ground line rotations, and the ground line deflections at each load are plotted against total load on the frame in Figures 48, 49, and 50. Deflections at the peak were omitted from further consideration due to inconsistency between the observed deflections and those predicted by the observed haunch deflections and frame geometry. Loads, deflections, and rotations are listed in Appendix D-2.

In Figure 48 the mean values of the haunch deflections observed in the tests of the three frames are plotted against load through the four cycles of loading. For comparison, the haunch deflection predicted for fixed supports is also shown in the first cycle. The line representing predicted deflection is approximately tangent to the lower end of the observed deflection curve: this is an indication that the method used to compute the loads is reasonably accurate.

In the first cycle of loading, haunch deflection increases more rapidly as the load is increased. In a linearly elastic structure with fixed supports this relationship would be linear. The curvature is presumed to be due to support displacement and possibly in part also due to a non-linear response of the wooden structure. Friesen reported some cracking sounds coming from the gussets at high loads--such noises indicate the occurrence of irrecoverable deformation in the gussets.
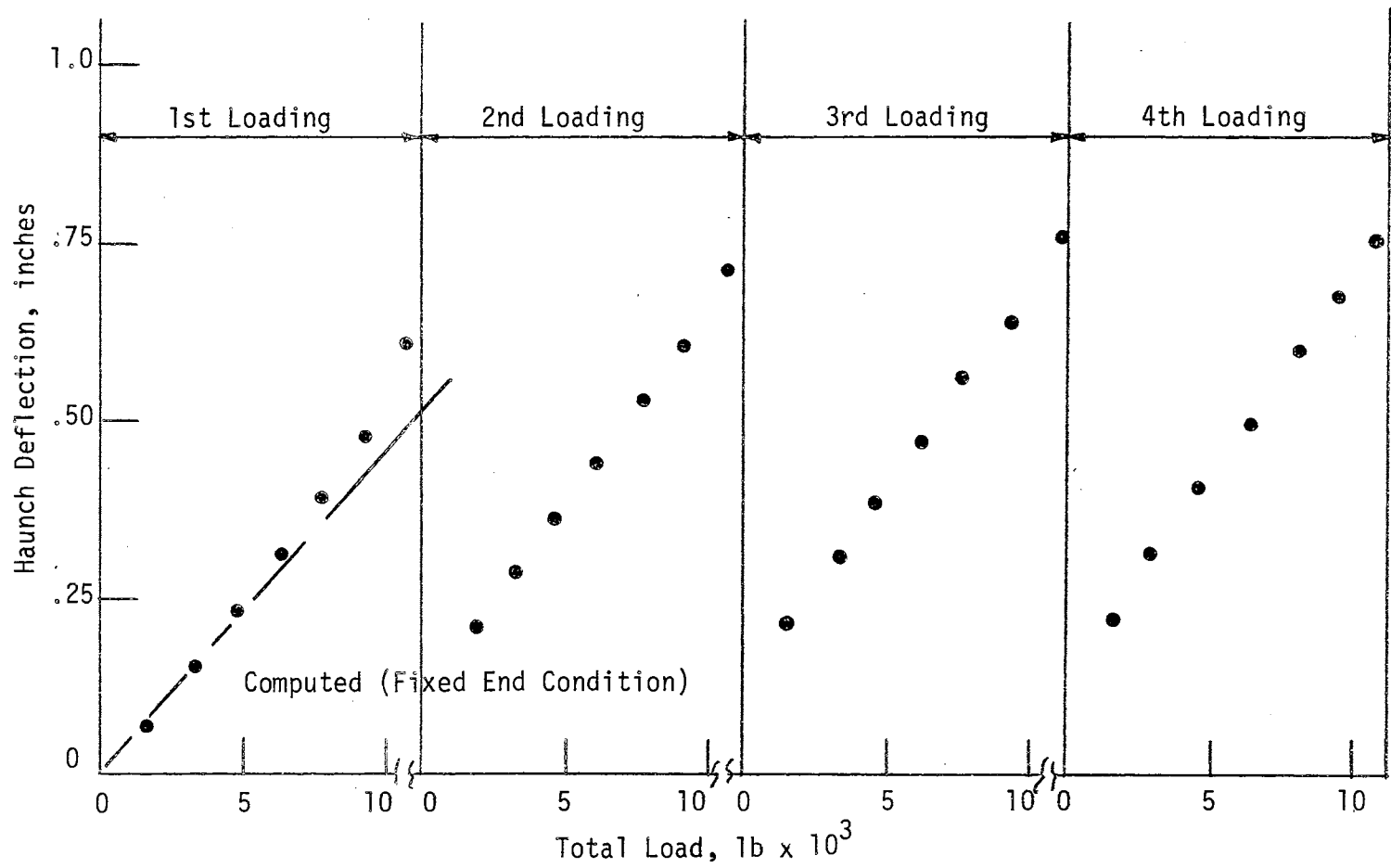
Figure 48. Haunch Deflections of Full-Sized Wood Frames, Means of Six Observations.
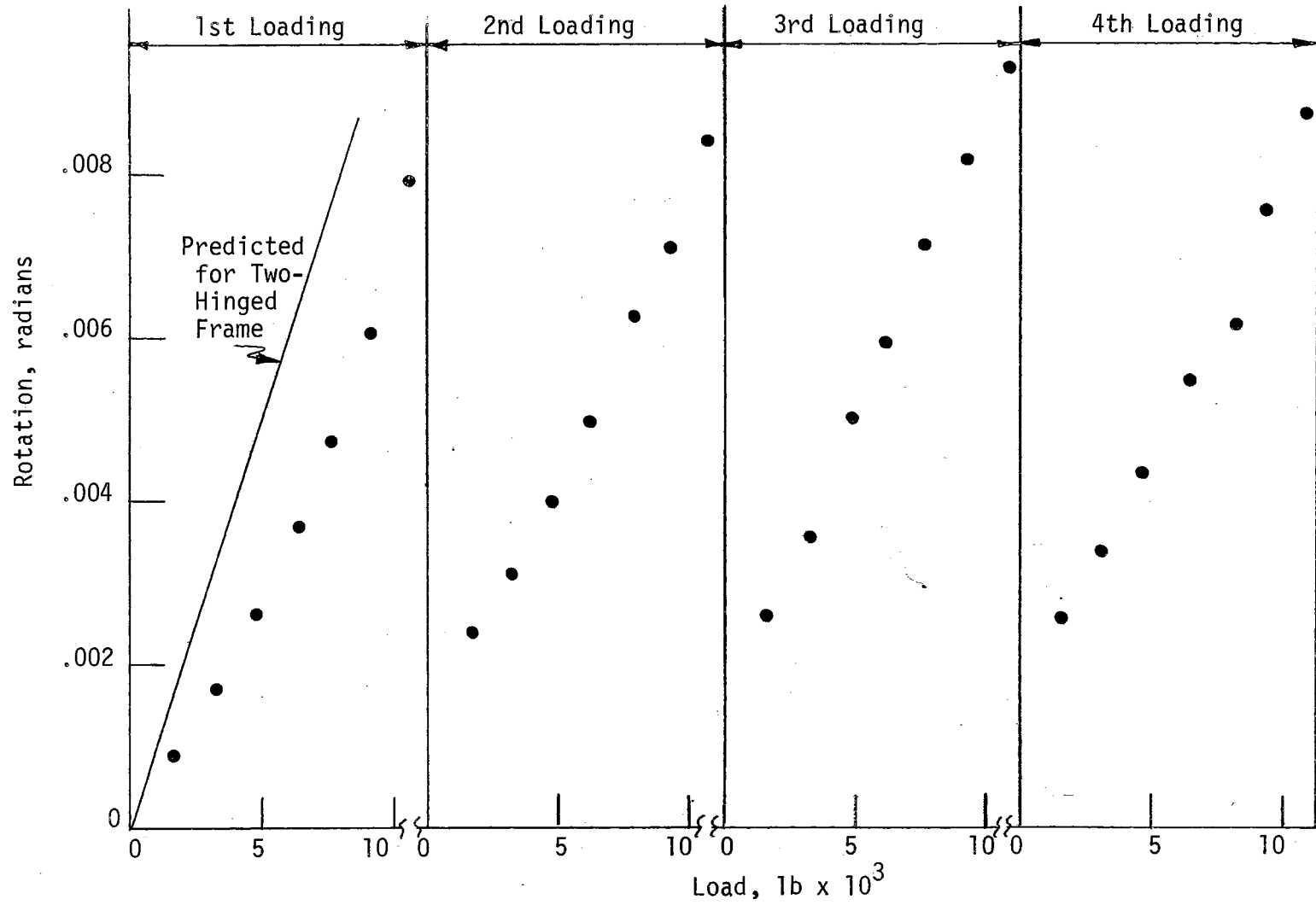
Figure 49. Rotation of Bases of Wooden Frames, Means of Five Bases.
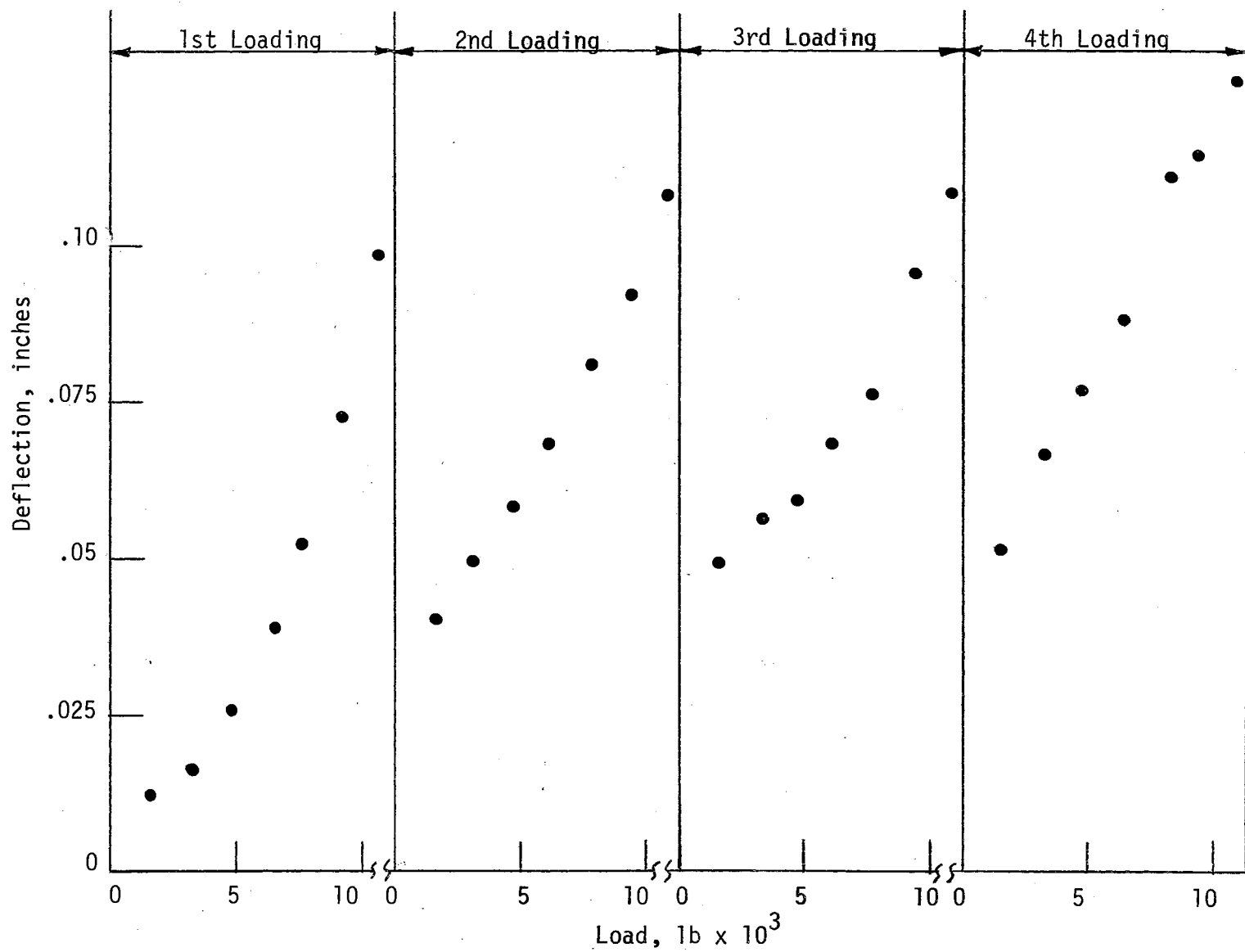
Figure 50. Ground Line Deflection of Wooden Frames, Means of Five Frame Bases.

Following the first cycle the frame was unloaded and reloaded, using similar loads, for a total of four loading cycles. Figure 48 shows that in the second and subsequent cycles much greater haunch deflections occurred than in the first, particularly at low loads. The apparent linearity of the deflection-load curves in the second and subsequent cycles suggest that the non-linear component of the deformations occurring in the first cycle was irrecoverable, so that in subsequent cycles the frame, and presumably the foundations, exhibit a linear response to load. Deflections in subsequent cycles were very little greater than in the second cycle.

The rotational response of the frame legs at ground line to loading, and to load cycling, shown in Figure 49, was very similar to the haunch deflection response. In the first cycle rotation increased more rapidly as load was increased. In subsequent cycles the relationship appears to be linear. Very little additional rotation occurred during the third and fourth cycles. The mean maximum rotation observed was 0.0112 radians; the maximum rotation of any one frame base was 0.0171 radians occurring at the left pier of frame 3 during the third load cycle at the maximum load of 11000 pounds. Variations among frame legs were large; the rotation of the left bases was consistently greater than that of the right. The reason for this is unknown, but a possible explanation lies in the nature of the site--a former barnyard. It is possible that in its earlier use excavation had disturbed the soil in which the left piers were set, and reduced its lateral bearing capacity.

The rotations of the frame legs in the first cycle were compared with the rotation which would be expected if the frame had been tested in a two-hinged configuration. The rotation of one frame leg--the left

leg of frame 3--consistently exceeded the predicted value. The means
of the rotations of the six legs, however, were less than the predicted
two-hinged rotations, as shown in Figure 49. The mean rotation ranged
from 53 per cent of the predicted value at small loads to 73 per cent
at the maximum load, and averaged 61 per cent.

The moment at the ground line, assuming linearly elastic action of
the frame, was computed for each observation. The computed values varied
widely from a maximum of 4332 pound-feet to negative values. The
existence of negative moment at the base of the frame is inconsistent
with the observed deflection and rotation, so it must be assumed that
some or all of the computed base moments are in error. This error is
attributed to permanent deformation in the frame itself which occurred
during the first cycle of loading.

Stresses in the haunch gussets were computed, assuming a linear
stress-strain response, for the maximum calculated haunch moment with
the frame in a two-hinged and in a hingeless configuration. In the two-
hinged configuration the calculated value of the maximum shear at the
glue line, due only to moment, was 230 pounds per square inch. This is
more than three times the allowable stress in rolling shear, 72 pounds
per square inch, recommended by Perkins (73). The maximum bending
stresses in the gussets, assuming the plys perpendicular to the direc-
tion of stress to be ineffective, were 4085 pounds per square inch,
compared to an allowable stress of 2000 pounds per square inch (73). In
the hingeless configuration the calculated stresses were about 10 per
cent less than listed above.

A stress of 4085 pounds per square inch would be unlikely to exist
at the unsupported compression edge of the gusset; buckling would be

expected to occur before such a stress developed. (The ratio of
unsupported length to the least dimension of the compression edge of
the plywood gussets was 34.) When the probability of buckling and
stress concentration in the joint are considered it seems very probable
that localized failure occurred in the plywood gussets, most likely as
shear failure at the extremities of the glue area and as compression
failure at the unsupported inner edges of the gussets. The sounds which
were heard during loading indicate that some such failure was occurring.

Localized failure at the haunches would invalidate moment
computations based on linearly elastic action of the frame. Such failure
would have increased the moment at the peak and bases of the frame.
Consequently, it is believed that the computed base moments at large
loads in the first cycle, and at all loads in subsequent cycles, are
considerably less than actually existed.

No such failure should have occurred at the small loads used at the
beginning of the first cycle, so that computed base moments should be
reasonably correct for this part of the test sequence. Computed base
moments and observed rotations are listed in Table X for the first four
loads of the first load cycle. Frame 3 is omitted from the table because
of the abnormal behavior of the left leg. Considering the probable be-
havior of the haunch joints, it would appear that the moments shown are
the minimum moments which could have existed. Any relaxation or failure
in a joint would cause the actual moment to exceed the values of Table X.
Comparison of these calculated base moments with those predicted for the
frame if the ends were completely fixed (the last column of Table X)
shows that the moments developed at the frame bases were approximately
half--and possibly more than half--of the fixed end moments in each case.

TABLE X

COMPUTED MOMENTS AND OBSERVED ROTATIONS OF THE BASES OF THE WOOD FRAMES
FIRST LOAD CYCLE

Load No.	Frame No.	Load lb	Left Leg Moment lb-ft	Left Leg Rotation rad	Right Leg Moment lb-ft	Right Leg Rotation rad	Means Moment lb-ft	Means Rotation rad	Fixed End Moments lb-ft
1	1	1750	1133	0.00085	1240	0.000512			
	2	1450	962	0.000695	989	0.00061			
							1081	0.000667	2132
2	1	3430	2247	0.00168	2545	0.00111			
	2	3150	2332	0.00134	2421	0.00106			
							2356	0.00130	4385
3	1	4960	3114	0.00252	3372	0.00170			
	2	4720	2992	0.00252	3268	0.00165			
							3187	0.002098	6450
4	1	6510	3606	0.00363	3980	0.00244			
	2	6110	3546	0.00352	3965	0.00219			
							3774	0.00295	8409

The ground line deflection of the frame legs, shown in Figure 50, behaved similarly to the rotation. The deflection-load relation was nonlinear during the first cycle, but approaches linearity in subsequent cycles.

The apparent depth, Z_0, to the axis of rotation, computed by the relation

$$Z_0 = \frac{\delta}{\theta}$$

was consistently less than expected throughout these tests; in only four cases in the 168 observations did it reach thirty inches (0.5 D) which is theoretically the minimum possible depth if a purely cohesive soil, with resistance independent of depth, is assumed. This behavior could be explained if the upper soil layers were stiffer than the deeper layers, which appears improbable when the previous history of the site (an old barnyard) is considered. It appeared more probable that the effect was due to bending of the extended frame legs within the encasing concrete pier. Such bending could involve crushing of the wood on the compression side near the top of the pier, and would be increased if the frame legs were loose in the pier socket as a result of dehydration after the piers were cast. (When the site was inspected several years after the test, radial cracking of the piers from the corners of the frame legs was observed, but it was reported that this cracking was not evident during the test.) The probable bending of the frame below the top of the concrete encasement would permit the frame base to rotate and displace more than the pier. Such an effect should be considered in design.

Although it was impossible, due to permanent deformation of the frame, to compute the actual moments and thrusts exerted by the frame on the piers for the whole test sequence, base moments calculated for the first few loads of the first cycle (before the haunch gussets had been subjected to excessive stress) indicate that the piers resisted moments at least as large as 4300 pound-feet, and probably considerably larger. For these particular loads the computed base moments were approximately half those computed for full base fixity.

No attempt was made to relate the results of this test to those of the model frame and model pier tests because of the differences in the soils. Rotations and horizontal displacements of up to 0.0143 radians and 0.171 inch, respectively, were observed at the bases of the frame legs at loads which would produce moments of 14,500 pound-inches and thrusts of 3660 pounds if the bases were fixed.

A material having accurately predictable elastic behavior should be used in future studies of this type. If such a material were to be used, and strain instrumentation applied at the main points of interest, it should be possible to determine accurately the degree of support provided by the foundation piers, and to account for inelastic as well as elastic behavior of the frame and the piers. Although no cracking of the piers was observed during the test, the cracking noted later indicates the necessity of providing circumferential reinforcement of the concrete piers.

CHAPTER XI

SUMMARY AND CONCLUSIONS

Summary

Hingeless rigid frames offer some advantage over the more conventional two-hinged conformation, in that moment due to roof loads is more uniformly distributed throughout the frame, thus making more efficient use of a constant section, and erection procedures for small span frames are simplified. By extending the legs of the frame into holes bored in the earth, then casting concrete piers around the legs, foundations may be constructed without forming, and bolts or other fastenings are not required to attach the frame to the foundation.

Movement of the foundations, due to forces and moments transmitted to them by the frame, or from other causes, affects the action of the frame.

Objectives of this study were:

1. To evaluate the effect of foundation movements on frame action.

2. To evaluate the stability of cylindrical piers used as foundations for rigid frames.

3. To determine criteria for the design of cylindrical piers as rigid frame foundations.

Analysis of a single design of frame, the "prototype frame", subjected to various types of loading and to foundation movements which

were consistent with the reactions of the frame on the foundations, showed that foundation movement reduced the efficiency of the frame when vertical loads (and large haunch moments) were present, but increased the efficiency of the frame when large base moments, due to wind loads or internal grain bin loading, existed.

An experimental program was conducted in which the rotation and horizontal ground line deflection of model cylindrical piers subjected to overturning forces were evaluated. The principles of dimensional analysis were applied in the design of the experiment so that the resulting prediction equations would be valid regardless of scale. Prediction equations were developed to define the ground line deflection and the rotation of piers embedded in dry sand for a wide range of geometrical parameters. More restricted equations were also developed for piers embedded in saturated and in wet sand.

A method for analyzing hingeless single-bay gable frames, supported by piers which deflect and rotate in response to the actions of the frame, was developed. This method of analysis, incorporated in a computer program written in Fortran IV, consists of an approximate solution of the hingeless frame by the unit load method, followed by computation of the pier deflections and rotations in response to the frame reactions. The process is repeated until a satisfactory solution is obtained.

A test of the analysis method consisted of load-testing a model frame supported by piers embedded in sand. The observed pier movements agreed fairly well with those predicted by the analysis. Observed deflections of the peak of the model were very close to those predicted.

Data from a series of tests of full-sized wooden hingeless frames, which had been conducted earlier at Oklahoma State University, were

analyzed. Inelastic action of the gussets of these frames prevented accurate analysis, but it was clear that a considerable degree of restraint was supplied by the foundations. The precise degree of restraint could not be determined, but it appeared that the moments developed at the base of the frame were about half--and possibly more than half--of the predicted fixed end moments.

Conclusions

The following conclusions are based on the analytical and experimental studies described in earlier chapters:

1. Movement of the supporting piers of a "hingeless" rigid frame, caused by forces and moments transmitted to the piers by the frame, reduce the capacity of the frame to support common types of vertical load.

2. Movement of the supporting piers of a hingeless rigid frame loaded by wind load or grain bin load, which produce large moments at the ground line, increases the ability of the frame to withstand the loads by redistributing moments throughout the frame.

3. The movement of cylindrical piers embedded in dense dry sand and acted upon by a horizontal thrust may be described by two dimensionless equations:

$$\frac{\delta}{B} = 1.369 \times 10^{-4} \left(\frac{D}{B}\right)^{-0.5016} \left(\frac{H}{B^2 D\gamma}\right)^{3.192} 3.633^{\left(\frac{L}{D}\right)}$$

$$\Theta = 7.420 \times 10^{-5} \left(\frac{D}{B}\right)^{-0.8172} \left(\frac{H}{B^2 D\gamma}\right)^{3.030} 3.542^{\left(\frac{L}{D}\right)}$$

(The pertinent quantities involved in these equations are defined in Table III, p. 68 and Appendix A-1.)

4. The movement of cylindrical piers embedded in saturated sand and subjected to a horizontal thrust located at 2D above the ground line may be described by two dimensionless equations:

$$\frac{\delta}{B} = 3.5738 \times 10^{-3} \left(\frac{D}{B}\right)^{-1.185} \left(\frac{H}{B^2 D\gamma}\right)^{2.196}$$

$$\Theta = 5.5195 \times 10^{-3} \left(\frac{D}{B}\right)^{-2.466} \left(\frac{H}{B^2 D\gamma}\right)^{2.379}$$

5. The movement of cylindrical piers embedded in drained wet sand and subjected to a horizontal thrust located at 2D above the ground line may be described by two dimensionless equations:

$$\frac{\delta}{B} = 8.1835 \times 10^{-4} \left(\frac{D}{B}\right)^{-0.2092} \left(\frac{H}{B^2 D\gamma}\right)^{2.1931}$$

$$\Theta = 8.4118 \times 10^{-4} \left(\frac{D}{B}\right)^{-0.9499} \left(\frac{H}{B^2 D\gamma}\right)^{2.2485}$$

6. The depth, relative to D--the embedded depth of the pier-- of the axis of rotation of a cylindrical pier embedded in dry sand averaged 0.71 D which is somewhat greater than predicted by classical pressure theory. This depth increased as the thrust and moment parameters increased, and decreased as the length parameter increased.

7. The average depth, relative to D, of the axis of
    rotation of piers embedded in drained wet sand was
    0.65 D. This was noticeably less than the value
    for piers in dry sand. This effect is consistent
    with the existence of cohesion in the wet sand, and
    is in general agreement with classical earth pressure
    theory for a soil exhibiting both frictional and
    cohesive resistance.

8. The resistance of the piers to overturning was much
    greater than that computed for the assumption of
    passive pressure alone acting to oppose the motion
    of piers.

9. An iterative method of solving for reactions and
    pier displacements of hingeless single-bay rigid
    frames was developed. The prediction equations
    developed from the pier tests in dry sand were
    incorporated in the computer program written to
    solve this problem. The program may be modified
    to incorporate any other suitable equations re-
    lating pier movement to actions developed at the
    base of the frame.

10. In tests of a model hingeless frame supported by
    cylindrical piers embedded in sand, observed pier
    movement was reasonably close to that predicted
    by the analysis.

11. The results of tests of full-sized wooden frames
    supported by cylindrical piers 16 inches in

diameter and 60 inches deep embedded in clay soil,
indicated that the resisting moments developed by
the piers were at least half of those predicted for
a completely fixed end condition, for frame loads
less than those at which permanent deformation of
the frame was expected to occur.

12. Concrete piers in which structural members are
embedded to transmit moment from the member to
the pier require circumferential reinforcement
to prevent radial cracking.

Suggestions for Further Research

A major limitation to the application of the method of frame
analysis is the lack of generally applicable information on the response
of piers to overturning actions. Soils are extremely varied, and the
few prediction equations available (including those presented herein) are
restricted to a very few soil conditions. A more general method of
determining pier response is needed.

Although Walker and Cox (36) reported that Anderson's (74) device
for determining the relation between lateral pressure and strain in
holes drilled in the soil was not effective in predicting the overturning
resistance of the piers they tested, it would seem that some such device
could be developed for on-site determinations, or possibly the results of
the Anderson device could be correlated with tests of piers and suitable
conversions developed.

It would also be desirable to be able to predict the lateral
pressure response from laboratory tests of the soil. Possibly the

stress-strain response determined in a laboratory triaxial test could be related to a lateral pressure function, or could be used to characterize the soil response for a method of solution similar to that developed by Mindlin (47) for an elastic solid.

Further tests of full-scale frames should be conducted in order to study long-term effects, and the effects of a variety of load systems such as would occur in a real building subjected to various wind, snow and internal loads. For detailed investigation, the use of steel frames would assure essentially linear elastic action and such frames could be fitted with strain gauge instrumentation to determine actions with a fair degree of reliability.

In order to permit satisfactory analysis of wood frames with plywood gussets, a study of the deflection of plywood gussets in response to moment and shear loads is needed. Both glued and nailed gussets should be investigated.

A SELECTED BIBLIOGRAPHY

1. Terzaghi, K. and R. B. Peck. _Soil Mechanics in Engineering Practice._ Wiley, New York, 1948.

2. Terzaghi, K. "A Fundamental Fallacy in Earth Pressure Computation," _Journal of the Boston Society of Civil Engineers._ April, 1936 (Reprinted in _Contributions to Soil Mechanics._ Boston Society of Civil Engineers, Boston, 1940).

3. Tschebotarioff, G. P. "Large Scale Model Earth Pressure Tests on Flexible Bulkheads," _Proc. American Society of Civil Engineers._ Vol. 74, No. 1, January, 1948.

4. Terzaghi, K. "Evaluation of Coefficients of Subgrade Reaction," _Geotechnique._ Vol. 5, pp. 297-326, December, 1955.

5. Collin, A. _Landslides in Clays._ Tr. W. R. Schriever, University of Toronto Press, Toronto, 1956.

6. Vesic, A. B. "Beams on an Elastic Subgrade and the Winkler's Hypothesis," _Proc. Fifth Intl. Conf. on Soil Mechanics and Foundation Engineering._ Vol. 1, Paris, 1961.

7. Matlock, H. and L. A. Reese. "Foundation Analysis of Offshore Pile-Supported Structures," _Proc. Fifth Intl. Conf. on Soil Mechanics and Foundation Engineering._ Vol. 2, Paris, 1961.

8. Davisson, M. T. and H. L. Gill. "Laterally Loaded Piles in a Layered Soil System," _Proc. Am. Soc. of Civil Engineers._ Vol. 89, No. SM3, May, 1963.

9. Kondner, R. L. "Hyperbolic Stress-Strain Response, Cohesive Soils," _Proc. Am. Soc. of Civil Engineers._ Vol. 89, No. SM1, January, 1963.

10. Kondner, R. L. and R. J. Krizek. "Correlation of Load-Bearing Tests on Soils," _Proc. Highway Research Board._ Vol. 41, 1962.

11. Wilson, S. D. and R. J. Dietrich. "Effect of Consolidation Pressures on Elastic and Strength Properties of Clay," _Proc. Am. Soc. of Civil Engineers, Research Conf. on Shear Strength of Cohesive Soils._ Boulder, Colo., 1960.

12. Denisov. N. J. and B. F. Reltov," Elastic and Structural Deformations of Clayey Soils," _Proc. Fourth Intl. Conf. on Soil Mechanics and Foundation Engineering._ Vol. 1, London, 1957.

13. Murayama, S. and T. Shibata. "Rheological Properties of Clays," Proc. Fifth Int. Conf. on Soil Mechanics and Foundation Engineering. Vol. 1, Paris, 1961.

14. Buisman, A.S.K. "Results of Long-Term Settlement Tests," Proc. Intl. Conf. on Soil Mechanics and Foundation Engineering. Cambridge, Mass., 1936.

15. Vialov, S. S. and A. M. Skibitsky. "Rheological Processes in Frozen Soils and Dense Clays," Proc. Fourth Intl. Conf. on Soil Mechanics and Foundation Engineering. Vol. 1, London, 1957.

16. Vialov, S. S. and A. M. Skibitsky. "Problems of the Rheology of Soils," Proc. Fifth Int. Conf. on Soil Mechanics and Foundation Engineering, Vol. 1, Paris, 1961.

17. Mitchell, J. K., H. B. Seed, and J. Paduana. "The Creep Deformation and Strength Characteristics of Soils Under the Action of Sustained Stress." Report No. TE65-8 to the U.S. Bureau of Reclamation. Dept. of Civil Engineering, University of California, Berkeley, October, 1965.

18. Chen, Liang-Sheng. "An Investigation of Stress-Strain and Strength Characteristics of Cohesionless Soils by Triaxial Compression Tests," Proc. Second Intl. Conf. on Soil Mechanics and Foundation Engineering. Vol. 5, Rotterdam, 1948.

19. Whitman, R. V. "The Behavior of Soils Under Transient Loadings," Proc. Fourth Intl. Conf. on Soil Mechanics and Foundation Engineering. Vol. 1, London, 1957.

20. Lenoe, E. M. "Deformation and Failure of Granular Media Under Three-Dimensional Stresses," Experimental Mechanics. Vol. 6, No. 2, Feb., 1966.

21. Abbett, R. W. American Civil Engineering Practice. Vol. 2, Wiley, New York, 1956.

22. Lee, Donovan H. Deep Foundations and Sheet Piling. Concrete Publications Ltd., London, 1961.

23. Seiler, J. F. "Effects of Depth of Embedment on Pole Stability," Wood Preserving News. Vol. X, No. 11, Nov., 1932.

24. Feagin, L. B. "Lateral Pile Loading Tests," Proc. Am. Soc. of Civil Engineers, Vol. 61, No. 9, Nov., 1935.

25. Raes, Paul E. "Theory of Lateral Bearing Capacity of Piles," Proc. Int. Conf. on Soil Mechanics and Foundation Engineering. Cambridge, Mass., 1936.

26. Wilkins, R. J. "The Bending of a Vertical Pile Under Lateral Forces," Civil Engineering (London). Vol. 46, p. 539, May, 1951.

27. Shilts, W. L., L. D. Graves, and G. G. Driscoll. "A Report of Field and Laboratory Tests on the Stability of Posts Against Lateral Loads," Proc. Second Int. Conf. on Soil Mechanics and Foundation Engineering. Vol. 5, Rotterdam, 1948.

28. Nelson, G. L., G.W.A. Mahoney, and J. Fryrear. "Stability of Poles Under Tilting Moments, Part I," Agricultural Engineering. Vol. 39, No. 3, March, 1958.

29. Nelson, G. L. "Stability of Poles Under Tilting Moments, Part II," Agricultural Engineering. Vol. 39, No. 4, April, 1958.

30. Beckett, F. E. "An Experimental Study of Model Poles Under Lateral Loads." unpub. Ph.D. Thesis, Oklahoma State University, 1958.

31. Lazard, A. "Moment Limite de Renversement des Fondations Isolées," Proc. Fourth Int. Conf. on Soil Mechanics and Foundation Engineering. Vol. 1, London, 1957

32. Kondner, R. L. and G. E. Green. "Lateral Stability of Rigid Poles Subjected to a Ground Line Thrust." 41st Annual Meeting, Highway Research Board, Jan., 1962.

33. Anderson, W. C. "Pole Foundations to Resist Tilting Moments," Electric Light and Power. Vol. 26, No. 10, Oct., 1948.

34. Anderson, W. C. "Foundations to Resist Tilting Moments Imposed on Upright Cantilevers Supporting Highway Signs," Highway Research Board Bulletin. No. 247, Washington, 1960.

35. Behn, F. E. "Tests of Tilting Moment Resistance of Cylindrical Reinforced Concrete Foundations for Overhead Sign Supports," Highway Research Board Bulletin. No. 247, Washington, 1960.

36. Walker, J. N. and E. H. Cox. "Design of Pier Foundations for Lateral Loads." American Society of Agricultural Engineers, Paper No. 64-408, St. Joseph, Michigan, 1964.

37. Kent, B. P. "A Pole Stability Theory Supported by a Model Study," unpub. M.S. Thesis, University of Arizona, 1961.

38. Broms, Bengt B. "Design of Laterally Loaded Piles," Proc. Am. Soc. of Civil Engineers. Vol. 91, No. SM3, May, 1965.

39. Cummings, A. E. "Discussion on Feagin, Lateral Pile Loading Tests," Proc. Am. Soc. of Civil Engineers. Vol. 61, No. 9, Nov., 1935.

40. Palmer, L. A. and J. B. Thompson. "The Earth Pressure and Deflection Along the Embedded Length of Piles Subjected to Lateral Thrust," Proc. Second Int. Conf. on Soil Mechanics and Foundation Engineering. Vol. 5, Rotterdam, 1948.

41. Hopkins, D. A. "Discussion on McNulty, Thrust Loading of Piles," Proc. Am. Soc. of Civil Engineers. Vol. 82, No. SM4, October, 1956.

42. McClelland, B. and J. A. Focht. "Soil Modulus for Laterally Loaded Piles," Proc. Am. Soc. of Civil Engineers. Vol. 82, No. SM4, October, 1956.

43. Radosavljevic, Z. "Calcul et Essais des Pieux en Groupe," Proc. Fourth Int. Conf. on Soil Mechanics and Foundation Engineering. Vol. 2, London, 1957.

44. Bergfelt, A. "The Axial and Lateral Load Bearing Capacity and Failure by Buckling of Piles in Soft Clay," Proc. Fourth Int. Conf. on Soil Mechanics and Foundation Engineering. Vol. 2, London, 1957.

45. Prakash, S. "A Review of the Behavior of Partially Embedded Poles Subjected to Lateral Loads." unpub. M.S. Thesis, University of Illinois, 1960.

46. Matlock, H. and L. C. Reese. "Generalized Solutions for Laterally Loaded Piles," Proc. Am. Soc. of Civil Engineers. Vol. 86, No. SM5, October, 1960.

47. Mindlin, R. D. "Force at a Point in the Interior of a Semi-Infinite Solid," Physics. Vol. 7, pp. 195-202, 1936.

48. Milne, C. M., A. C. Dale, and S. K. Suddarth. "Analysis of Structural Frames with Semi-Rigid Ground Connections." American Society of Agricultural Engineers Transcript No. 67-416, St. Joseph, Mich., 1967.

49. Wang, C. Statically Indeterminate Structures. McGraw-Hill, New York, 1953.

50. Kleinlogel, A. Rigid Frame Formulas. 2nd ed. Frederick Ungar Pub. Co., New York, 1958.

51. Bonnicksen, L. W. "Rigid Pillar Construction," Agricultural Engineering. Vol. 36, No. 4, April, 1955.

52. Polshin, D. E. and R. A. Tokar. "Maximum Allowable Non-Uniform Settlement of Structures," Proc. Fourth Int. Conf. on Soil Mechanics and Foundation Engineering. Vol. 1, London, 1957.

53. Roscoe, K. H. "A Comparison of Tied and Free Pier Foundations," Proc. Fourth Int. Conf. on Soil Mechanics and Foundation Engineering. Vol. 1, London, 1957.

54. Rodda. E. D. and M. L. Paul. "An Investigation of a Reinforced Concrete Rigid Frame for Farm and Light Industrial Structures." University of Illinois Engineering Experiment Station Bulletin 467, 1963.

55. Wagner, W. V. and E. D. Rodda. "Development of an All-Precast Concrete Rigid Frame Building for Farm and Agri-Business." American Society of Agricultural Engineers Paper No. 64-921, St. Joseph, Michigan, 1964.

56. Friesen, J. A. "Evaluation of Theoretical Stresses in Two-Hinged and Hingeless Frames." unpub. report, Agricultural Engineering Department, Oklahoma State University, 1961.

57. Friesen, J. A. and G. L. Nelson. "Performance of Light-Gage Cold-Rolled Steel Frames for Light Building Construction." American Society of Agricultural Engineers Paper No. 63-435, St. Joseph, Mich., 1963.

58. Nelson, G. L., et al. "A One-Hinged Frame for Light Building Construction," Transactions of American Society of Agricultural Engineers. Vol. 5, No. 1, 1962.

59. Baracos, A. and M. Bozozuk. "Seasonal Movements in Some Canadian Clays," Proc. Fourth Int. Conf. on Soil Mechanics and Foundation Engineering. Vol. 1, London, 1957.

60. Schriever, W. R. and R. F. Leggett. "Performance of Concrete Foundation Slabs on Canadian Clays," Proc. Fifth Int. Conf. on Soil Mechanics and Foundation Engineering. Vol. 1, Paris, 1961.

61. Griffin, J. G. "Engineers Study Movement of Foundation on Heavy Clay," Mississippi Farm Research. Vol. 25, No. 6, June, 1962.

62. "Designing Buildings to Resist Snow and Wind Loads." American Society of Agricultural Engineers Recommendation R288T, St. Joseph, Mich., 1965.

63. Rice, C. E. "A Model Study of Anchorage Types for Fixed-End Arches." unpub. report, Agricultural Engineering Department, Oklahoma State University, 1959.

64. Welch, G. B. "Experimental Analysis of Rotation in a Vertical Plane of Shallow Pier Foundations Subjected to a Couple." unpub. Ph.D. Thesis, Oklahoma State University, 1965.

65. Buckingham, E. "On Physically Similar Systems," Physical Review. Vol. 4, p. 345, 1914.

66. Murphy, Glenn. Similitude in Engineering. Ronald Press, New York, 1950.

67. Tschebotarioff, G. P. Soil Mechanics, Foundations, and Earth Structures. McGraw-Hill, New York, 1951.

68. Natrella, M. G. Experimental Statistics. National Bureau of Standards Handbook 91. U.S. Govt. Printing Office, Washington, 1963.

69. Steel, R.G.D. and J. H. Torrie. Principles and Procedures of Statistics. McGraw-Hill, New York, 1960.

70. Hansen, J. B. "The Ultimate Resistance of Rigid Piles Against Transversal Forces," Danish Geotechnical Inst. Bulletin 12. Copenhagen, 1961.

71. Nielsen, K. L. Methods in Numerical Analysis. MacMillan, New York, 1964.

72. Friesen, J. A. "Jarrah Wood Frame Tests." unpub. report, Agri. Engr. Dept., Oklahoma State University, 1964.

73. Perkins, N. S. Plywood Properties, Design and Construction. Douglas Fir Plywood Assn., Tacoma, Wash., 1962.

74. Anderson, W. C. "A Device for Evaluating Horizontal Soil Resistance for Overhead Sign Supports," Highway Research Board Bulletin 247. Washington, 1960.

APPENDIX A

NOTATION

APPENDIX A-1

NOTATION

Symbol		Dimensions
B	Diameter of pier	L
C	A constant	-
D	Depth of pier embedment	L
E	Modulus of elasticity	FL^{-2}
F	The force dimension	F
H	Horizontal thrust	F
h	Height of frame leg	L
I	Moment of inertia	L^4
L	Height of thrust line above soil surface	L
L	The length dimension	L
ℓ	Span of frame	L
M	Moment	FL
N	Number of load cycles	-
n	Model scale	-
P	Concentrated load	F
V	Vertical force	F
Z	Depth below soil surface	L
Z_0	Depth of axis of rotation	L
α	Angle of rafter, measured from horizontal	-
γ	Effective specific weight of soil	FL^{-3}
$\Delta\ \delta$	Deflection	L
Θ	Rotation	-

Symbol		Dimensions
λ	Length	L
Π	A dimensionless parameter	-
ϕ	Angle of friction of soil	-

APPENDIX A-2

DIMENSIONLESS PARAMETERS USED IN THE PIER EXPERIMENT

Π_1 $\dfrac{D}{B}$ The depth parameter

Π_2 $\dfrac{H}{B^2 D \gamma}$ The load parameter

Π_3 $\dfrac{L}{D}$ The moment arm parameter

Π_4 $\dfrac{\delta}{B}$ The deflection parameter (dependent)

Π_5 ϕ The angle of friction of the soil

Π_6 Θ The rotation of the pier (dependent)

Π_7 N The number of load cycles

$POZN = \dfrac{\Pi_4}{\Pi_6 \, \Pi_1} = \dfrac{\delta}{\Theta D}$ Depth of axis of rotation (dependent)

APPENDIX B

DATA FROM THE PIER EXPERIMENT

APPENDIX B-1

DATA FROM THE PIER EXPERIMENT - DRY SAND TESTS

PI7	PI2	PI4	PI6	POZN
	TYPE 50 PI1 = 5.0 PI3 = 0.2			
	RUN 1 POSITION 1			
1	1.2577	0.000646	0.000012	10.333334
1	1.6769	0.001050	0.000050	4.200000
1	2.0961	0.001437	0.000137	2.090909
1	2.5153	0.001992	0.000325	1.225641
1	3.4711	0.004800	0.001200	0.800000
1	4.3871	0.011092	0.002825	0.785251
1	5.3104	0.020917	0.005050	0.828383
1	6.2747	0.039012	0.009512	0.820237
1	7.2368	0.073083	0.018550	0.787960
	TYPE 50 PI1 = 5.0 PI3 = 0.2			
	RUN 2 POSITION 9			
1	1.6770	0.000583	0.000050	2.333333
1	2.0963	0.000771	0.000138	1.121212
1	2.5156	0.001187	0.000287	0.826087
1	3.4798	0.003200	0.000800	0.800000
1	4.4357	0.008383	0.002250	0.745185
1	5.3517	0.014371	0.003938	0.729947
1	6.2751	0.030087	0.008188	0.734962
1	7.2374	0.073883	0.019550	0.755840
	TYPE 50 PI1 = 5.0 PI3 = 0.2			
	RUN 2 POSITION 3			
1	1.2577	0.000121	0.000050	0.483333
1	1.6770	0.000175	0.000100	0.350000
1	2.0961	0.000409	0.000162	0.503846
1	2.5155	0.000631	0.000275	0.459091
1	3.4389	0.001892	0.000700	0.540476
1	4.3550	0.005059	0.001563	0.647600
1	5.3109	0.011903	0.003387	0.702768
1	6.2751	0.024240	0.006375	0.760457
1	7.2374	0.057918	0.014663	0.790011
	TYPE 51 PI1 = 5.0 PI3 = 1.0			
	RUN 1 POSITION 7			
1	1.2577	0.000605	0.000137	0.880303
1	1.6769	0.001273	0.000325	0.783333
1	2.0961	0.002203	0.000562	0.783333
1	2.5153	0.003374	0.000913	0.739498
1	3.4386	0.008489	0.002338	0.726292

APPENDIX B-1 (Continued)

PI7	PI2	PI4	PI6	POZN
1	4.4029	0.022316	0.004813	0.927403
1	5.3587	0.043774	0.011312	0.773904

TYPE 51 PI1 = 5.0 PI3 = 1.0
RUN 1 POSITION 4

1	1.2577	0.000700	0.000200	0.700000
1	1.6769	0.001475	0.000350	0.842857
1	2.0961	0.002004	0.000575	0.697101
1	2.5153	0.003390	0.000762	0.889071
1	3.4313	0.008442	0.002150	0.785271
1	4.3874	0.022115	0.006013	0.735620
1	5.3513	0.052202	0.014087	0.741112

TYPE 51 PI1 = 5.0 PI3 = 1.0
RUN 2 POSITION 7

1	1.2577	0.000848	0.000125	1.356667
1	1.6769	0.001520	0.000312	0.972667
1	2.0961	0.002350	0.000600	0.783333
1	2.5153	0.003940	0.001025	0.768699
1	3.0603	0.007476	0.001937	0.771720
1	3.4795	0.010728	0.003012	0.712241
1	4.4028	0.028707	0.007862	0.730233
1	5.3189	0.085265	0.023125	0.737423

TYPE 52 PI1 = 5.0 PI3 = 2.0
RUN 1 POSITION 8

1	0.4192	0.000125	0.000050	0.500000
1	0.8384	0.000567	0.000200	0.566667
1	1.2577	0.001479	0.000525	0.563492
1	1.6769	0.003481	0.001012	0.687654
1	2.0961	0.007808	0.001150	1.357971
1	0.0000	0.005535	0.001288	0.859871
2	0.4192	0.005573	0.001262	0.882838
2	0.8384	0.005725	0.001250	0.916000
2	1.2577	0.005837	0.001575	0.741270
2	1.6769	0.006394	0.001738	0.735971
2	2.0961	0.007331	0.001912	0.766667
2	0.0000	0.006510	0.001438	0.905797
3	0.4192	0.006454	0.001475	0.875141
3	0.8384	0.006229	0.001625	0.766667
3	1.2577	0.006508	0.001750	0.743810
3	1.6769	0.006892	0.001850	0.745045
3	2.0961	0.007667	0.002000	0.766667
3	0.0000	0.007008	0.001550	0.904301
4	0.4192	0.006933	0.001600	0.866667

APPENDIX B-1 (Continued)

PI7	PI2	PI4	PI6	POZN
4	0.8384	0.006831	0.001713	0.797810
4	1.2577	0.007033	0.001800	0.781481
4	1.6769	0.007398	0.001912	0.773638
4	2.0961	0.007887	0.002075	0.760241
4	0.0000	0.007133	0.001600	0.891667
5	0.4192	0.007040	0.001662	0.846867
5	0.8384	0.006937	0.001775	0.781690
5	1.2578	0.007435	0.001888	0.787859
5	1.6769	0.007619	0.001987	0.766667
5	2.0961	0.008223	0.002163	0.760501
5	0.0000	0.007469	0.001688	0.885185
6	0.4192	0.007394	0.001738	0.851079
6	0.8384	0.007358	0.001850	0.795495
6	1.2577	0.007437	0.001975	0.753165
6	1.6769	0.007992	0.002050	0.779675
6	2.0961	0.008396	0.002225	0.754682
6	0.0000	0.007756	0.001763	0.880142
7	0.4192	0.007790	0.001800	0.855556
7	0.8384	0.007579	0.001925	0.787446
7	1.2577	0.007848	0.002012	0.779917
7	1.6769	0.008242	0.002150	0.766667
7	2.0961	0.008417	0.002300	0.731884
7	0.0000	0.008015	0.001813	0.884368
8	0.4192	0.007977	0.001838	0.868254
8	0.8384	0.007875	0.001950	0.807692
8	1.2577	0.007954	0.002075	0.766667
8	1.6769	0.008356	0.002163	0.772832
8	2.0961	0.008675	0.002350	0.738298
8	0.0000	0.008244	0.001838	0.897279
9	0.4191	0.008169	0.001887	0.865563
9	0.8384	0.007962	0.002025	0.786420
9	1.2577	0.008231	0.002112	0.779290
9	1.6769	0.008377	0.002238	0.748790
9	2.0961	0.008819	0.002388	0.738743
9	0.0000	0.008283	0.001900	0.871930
10	0.4192	0.008208	0.001950	0.841880
10	0.8384	0.008050	0.002100	0.766667
10	1.2577	0.008356	0.002163	0.772832
10	1.6769	0.008635	0.002288	0.755009
10	2.0961	0.008810	0.002437	0.722906
10	0.0000	0.008512	0.001925	0.884416
11	0.4192	0.008523	0.001963	0.868577
11	0.8384	0.008335	0.002088	0.798603
11	1.2577	0.008415	0.002213	0.760640
11	1.6769	0.008760	0.002337	0.749554
11	2.0961	0.009125	0.002450	0.744898
11	2.5153	0.013894	0.001937	1.434194
11	2.6411	0.015229	0.002425	1.256014

APPENDIX B-1 (Continued)

PI7	PI2	PI4	PI6	POZN
11	2.8507	0.019208	0.005550	0.692192
11	3.0603	0.033960	0.009538	0.712145

TYPE 52 PI1 = 5.0 PI3 = 2.0
RUN 1 POSITION S

1	0.4192	0.000021	0.000075	0.055556
1	0.8384	0.000567	0.000200	0.566667
1	1.2577	0.001490	0.000563	0.529630
1	1.6769	0.004025	0.001450	0.555172
1	2.0961	0.009912	0.003125	0.634400
1	0.0000	0.007762	0.002425	0.640206
2	0.4192	0.007706	0.002462	0.625888
2	0.8384	0.008185	0.002588	0.632689
2	1.2577	0.008827	0.002738	0.644901
2	1.6769	0.009604	0.002975	0.645658
2	2.0961	0.011110	0.003437	0.646424
2	0.0000	0.009485	0.002787	0.680568
3	0.4192	0.009533	0.002800	0.680952
3	0.8384	0.009775	0.002950	0.662712
3	1.2577	0.010150	0.003100	0.654839
3	1.6769	0.010965	0.003313	0.662013
3	2.0961	0.012069	0.003687	0.654576
3	0.0000	0.010627	0.003137	0.677424
4	0.4192	0.010552	0.003187	0.662091
4	0.8384	0.010973	0.003262	0.672669
4	1.2577	0.011281	0.003412	0.661172
4	1.6769	0.011808	0.003550	0.665258
4	2.0961	0.012721	0.003875	0.656559
4	0.0000	0.011069	0.003287	0.673384
5	0.4192	0.011042	0.003350	0.659204
5	0.8384	0.011481	0.003412	0.672894
5	1.2577	0.011875	0.003550	0.669014
5	1.6769	0.012327	0.003737	0.659643
5	2.0961	0.013237	0.003975	0.666038
5	0.0000	0.011806	0.003462	0.681949
6	0.4192	0.011883	0.003500	0.679048
6	0.8384	0.012029	0.003625	0.663678
6	1.2577	0.012394	0.003738	0.663211
6	1.6769	0.012854	0.003875	0.663441
6	2.0961	0.013869	0.004087	0.678593
6	0.0000	0.012344	0.003638	0.678694
7	0.4192	0.012392	0.003650	0.678995
7	0.8384	0.012604	0.003775	0.667770
7	1.2577	0.012921	0.003875	0.666882
7	1.6769	0.013333	0.004000	0.666667
7	2.0961	0.014327	0.004138	0.692548
7	0.0000	0.012642	0.003750	0.674222

APPENDIX B-1 (Continued)

PI7	PI2	PI4	PI6	POZN
8	0.4192	0.012652	0.003787	0.668097
8	0.8384	0.012958	0.003850	0.673160
8	1.2577	0.013390	0.003962	0.675815
8	1.6769	0.013858	0.004050	0.684362
8	2.0961	0.014994	0.004137	0.724773
8	0.0000	0.012958	0.003850	0.673160
9	0.4192	0.013006	0.003863	0.673463
9	0.8384	0.013379	0.003925	0.681741
9	1.2577	0.013762	0.004025	0.683851
9	1.6769	0.014194	0.004137	0.686103
9	2.0961	0.014835	0.004288	0.692031
9	0.0000	0.013369	0.003888	0.687781
10	0.4192	0.013417	0.003900	0.688034
10	0.8384	0.013752	0.003987	0.689760
10	1.2577	0.014087	0.004075	0.691411
10	1.6769	0.014519	0.004187	0.693433
10	2.0961	0.014933	0.004400	0.678788
10	0.0000	0.013694	0.003937	0.695556
11	0.4192	0.013704	0.003975	0.689518
11	0.8384	0.013973	0.004062	0.687897
11	1.2577	0.014394	0.004138	0.695770
11	1.6769	0.014844	0.004238	0.700590
11	2.0961	0.015240	0.004462	0.683007
11	2.5153	0.018815	0.005413	0.695227
11	2.6411	0.021687	0.006475	0.669884
11	2.8507	0.045560	0.012737	0.715375

TYPE 53   PI1 =   5.0   PI3 =   3.0
RUN 1   POSITION 3

1	0.4192	0.000325	0.000050	1.300000
1	0.8384	0.001254	0.000275	0.912121
1	1.2577	0.003679	0.000925	0.795495
1	1.6771	0.010271	0.002575	0.797735
1	1.8864	0.018304	0.004775	0.766667
1	2.0961	0.026490	0.006963	0.760922
1	2.3057	0.041625	0.011450	0.727074

TYPE 53   PI1 =   5.0   PI3 =   3.0
RUN 2   POSITION 8

1	0.4192	0.000335	0.000087	0.766667
1	0.8384	0.001229	0.000425	0.578431
1	1.2578	0.003415	0.001012	0.674486
1	1.6770	0.011392	0.003250	0.701026
1	2.0963	0.027723	0.007562	0.733168
1	2.5155	0.086737	0.022975	0.755060

APPENDIX B-1 (Continued)

PI7	PI2	PI4	PI6	POZN
		TYPE 53 PI1 = 5.0 PI3 = 3.0		
		RUN 2 POSITION 6		
1	0.4192	0.000281	0.000075	0.750000
1	0.8384	0.001554	0.000450	0.690741
1	1.2577	0.004455	0.001312	0.678889
1	1.6770	0.014578	0.003888	0.750000
1	2.0963	0.037447	0.010413	0.719268
		TYPE 32 PI1 = 3.0 PI3 = 2.0		
		RUN 1 POSITION 5		
1	0.6987	0.000308	0.000150	0.685185
1	1.3973	0.002310	0.001037	0.742303
1	2.0962	0.010908	0.004950	0.734568
		TYPE 32 PI1 = 3.0 PI3 = 2.0		
		RUN 1 POSITION 6		
1	0.6987	0.000469	0.000088	1.785714
1	1.3973	0.001981	0.000813	0.812820
1	1.7467	0.003494	0.001537	0.757453
1	2.0962	0.006337	0.002975	0.710084
1	2.4454	0.013215	0.005813	0.757826
		TYPE 32 PI1 = 3.0 PI3 = 2.0		
		RUN 2 POSITION 4		
1	0.6987	0.000517	0.000100	1.722222
1	1.0479	0.001269	0.000487	0.867521
1	1.3973	0.003490	0.000563	2.067901
1	1.7467	0.007100	0.001000	2.366667
1	2.0962	0.010392	0.004450	0.778402
		TYPE 72 PI1 = 7.0 PI3 = 2.0		
		RUN 1 POSITION 2		
1	0.8984	0.000343	0.000162	0.301282
1	1.1979	0.000765	0.000275	0.397186
1	1.4972	0.001468	0.000462	0.453346
1	1.7966	0.002519	0.000725	0.496305
1	2.4853	0.008507	0.002038	0.596480
1	3.1449	0.021758	0.004700	0.661348
1	3.7992	0.050774	0.010037	0.722632

APPENDIX B-1 (Continued)

PI7	PI2	PI4	PI6	POZN

TYPE 72 PI1 = 7.0 PI3 = 2.0
RUN 2 POSITION 1

1	0.8984	0.001031	0.000275	0.535714
1	1.1978	0.001981	0.000475	0.595865
1	1.4972	0.003733	0.000800	0.666667
1	1.7966	0.005657	0.001438	0.562215
1	2.1859	0.010933	0.002400	0.650794
1	2.4853	0.016636	0.003388	0.701590
1	2.8402	0.026532	0.005138	0.737777
1	3.1396	0.037306	0.007175	0.742782

TYPE 72 PI1 = 7.0 PI3 = 2.0
RUN 2 POSITION 5

1	0.8984	0.000508	0.000150	0.484127
1	1.1978	0.001006	0.000263	0.547619
1	1.4973	0.001762	0.000425	0.592437
1	1.7968	0.003081	0.000612	0.718659
1	2.1861	0.006237	0.001175	0.758359
1	2.4855	0.009175	0.001750	0.748980
1	3.1399	0.024310	0.004637	0.748877

APPENDIX B-2

DATA FROM THE PIER EXPERIMENT - SATURATED SAND TESTS

PI7	PI2	PI4	PI6	POZN
	TYPE 32 PI1 = 3.0 PI3 = 2.0			
	RUN 3 POSITION 9			
1	0.8311	0.000612	0.000175	1.166667
1	1.6620	0.003196	0.001275	0.835512
1	2.4933	0.007712	0.003575	0.719114
1	3.3245	0.016281	0.007337	0.739637
1	4.1557	0.030948	0.014537	0.709611
1	4.9865	0.071550	0.035300	0.675637
	TYPE 32 PI1 = 3.0 PI3 = 2.0			
	RUN 3 POSITION 5			
1	0.8312	-0.000000	-0.000013	-2.416667
1	1.6620	0.001500	0.000400	1.250000
1	2.4933	0.005084	0.002112	0.802268
1	3.3241	0.014381	0.006375	0.751961
1	4.1557	0.036854	0.017050	0.720512
	TYPE 32 PI1 = 3.0 PI3 = 2.0			
	RUN 3 POSITION 4			
1	0.8312	0.000173	-0.000087	0.658730
1	1.6617	0.001802	0.000762	0.787796
1	2.4933	0.005383	0.002700	0.664609
1	3.3241	0.013190	0.006187	0.710550
1	4.1557	0.028577	0.012813	0.743469
	TYPE 52 PI1 = 5.0 PI3 = 2.0			
	RUN 3 POSITION 7			
1	0.9972	0.000491	0.000062	1.570000
1	1.9945	0.002258	0.000500	0.903333
1	2.9919	0.006420	0.001513	0.848898
1	3.9894	0.011014	0.002887	0.762843
1	4.9868	0.018223	0.004825	0.755354
1	5.9841	0.029457	0.007663	0.768869
1	8.2780	0.084234	0.021238	0.793261
	TYPE 52 PI1 = 5.0 PI3 = 2.0			
	RUN 3 POSITION 3			
1	0.9972	0.000805	0.000188	0.858889
1	1.9945	0.003315	0.000925	0.716667
1	2.9919	0.007681	0.002125	0.722941
1	3.9894	0.014808	0.004300	0.688760

APPENDIX B-2 (Continued)

PI7	PI2	PI4	PI6	POZN
1	4.9868	0.024486	0.007113	0.688547
1	5.9843	0.041265	0.011925	0.692068

TYPE 52 PI1 = 5.0 PI3 = 2.0
RUN 3   POSITION 2

1	0.9972	0.000451	0.000112	0.801852
1	1.9945	-0.001023	0.001125	-0.181852
1	2.9919	0.007293	0.001413	1.032596
1	3.9894	0.013389	0.002963	0.903868
1	4.9868	0.021849	0.005088	0.858927
1	5.9843	0.034493	0.008613	0.800992

TYPE 72 PI1 = 7.0 PI3 = 2.0
RUN 3   POSITION 1

1	0.7123	0.000130	0.000037	0.494048
1	1.4246	0.000569	0.000088	0.929422
1	2.1372	0.001202	0.000213	0.807773
1	3.5620	0.003428	0.000625	0.783571
1	4.2743	0.004995	0.000963	0.741419
1	5.8309	0.009268	0.001812	0.730501
1	7.4694	0.015615	0.003050	0.731362
1	9.0387	0.025015	0.004650	0.768497

TYPE 72 PI1 = 7.0 PI3 = 2.0
RUN 3   POSITION 8

1	0.7123	0.000666	-0.000037	-2.535714
1	1.4246	0.001446	0.000050	4.130952
1	2.1371	0.002541	0.000263	1.382653
1	2.8495	0.004502	0.000475	1.354010
1	3.5620	0.006753	0.000712	1.354010
1	4.2743	0.009366	0.001163	1.150922
1	5.8434	0.016157	0.002463	0.937334
1	7.4820	0.027147	0.004487	0.864206

TYPE 72 PI1 = 7.0 PI3 = 2.0
RUN 3   POSITION 6

1	0.7123	0.000219	0.000025	1.250000
1	1.4246	0.000889	0.000163	0.781136
1	2.1371	0.002062	0.000350	0.841837
1	2.8495	0.003482	0.000687	0.723593
1	3.5620	0.005387	0.001050	0.732993
1	4.2743	0.007421	0.001450	0.731117
1	5.9128	0.014714	0.002862	0.734300
1	7.4819	0.025161	0.005238	0.686300

APPENDIX B-3

DATA FROM THE PIER EXPERIMENT - WET SAND TESTS

PI7	PI2	PI4	PI6	POZN

TYPE 32 PI1 = 3.0 PI3 = 2.0
RUN 4 POSITION 4

PI7	PI2	PI4	PI6	POZN
1	0.0000	-0.000000	-0.000000	-0.583333
1	0.3494	-0.000000	-0.000013	-2.361111
1	0.6987	0.000114	0.000087	0.432540
1	1.0481	0.000628	0.000213	0.985294
1	1.3975	0.001347	0.000487	0.920940
1	1.7469	0.002294	0.000975	0.784188
1	2.0962	0.003218	0.001438	0.746135
1	2.4456	0.004252	0.001875	0.755926
1	2.7950	0.006140	0.002625	0.779630
1	3.4938	0.009049	0.004162	0.724641
1	4.1925	0.013212	0.006050	0.727961
1	4.9856	0.019341	0.009062	0.711379

TYPE 32 PI1 = 3.0 PI3 = 2.0
RUN 4 POSITION 9

PI7	PI2	PI4	PI6	POZN
1	0.6987	0.000225	0.000025	3.000000
1	1.3973	0.001425	0.000625	0.760000
1	2.0962	0.003654	0.001488	0.818861
1	2.7950	0.006683	0.002750	0.810101
1	3.4938	0.011012	0.004912	0.747243
1	4.1925	0.021050	0.009650	0.727116

TYPE 32 PI1 = 3.0 PI3 = 2.0
RUN 4 POSITION 2

PI7	PI2	PI4	PI6	POZN
1	0.6987	0.000171	0.000050	1.138889
1	1.3973	0.001019	0.000825	0.411616
1	2.0962	0.003551	0.002112	0.560322
1	2.7950	0.006624	0.003987	0.553727
1	3.4938	0.012297	0.007463	0.549274
1	4.1925	0.021117	0.012600	0.558642

TYPE 52 PI1 = 5.0 PI3 = 2.0
RUN 4 POSITION 5

PI7	PI2	PI4	PI6	POZN
1	0.8384	0.000442	0.000175	0.504762
1	1.6770	0.002292	0.000625	0.733333
1	2.5155	0.005196	0.001763	0.589598
1	3.4663	0.010721	0.003487	0.614815
1	4.4170	0.018792	0.005725	0.656477
1	5.3678	0.029187	0.008688	0.671942

APPENDIX B-3 (Continued)

PI7	PI2	PI4	PI6	POZN

TYPE 52 PI1 = 5.0 PI3 = 2.0
RUN 4 POSITION 2

1	0.8384	0.000536	0.000137	0.780303
1	1.6770	0.002711	0.000638	0.850654
1	2.5155	0.005640	0.001475	0.764689
1	3.4663	0.010124	0.002788	0.726383
1	4.4170	0.016768	0.004712	0.711627
1	5.3678	0.025376	0.007212	0.703668

TYPE 52 PI1 = 5.0 PI3 = 2.0
RUN 4 POSITION 1

1	0.8384	0.000408	0.000100	0.816667
1	1.6770	0.001703	0.000538	0.633721
1	2.5155	0.004127	0.001325	0.622956
1	3.4663	0.008265	0.002575	0.641909
1	4.4170	0.013839	0.004362	0.634432
1	5.3678	0.021905	0.006762	0.647843

TYPE 72 PI1 = 7.0 PI3 = 2.0
RUN 4 POSITION 3

1	0.5989	0.000173	0.000087	0.282313
1	1.1978	0.001073	0.000287	0.533126
1	1.7968	0.002519	0.000663	0.543127
1	2.4855	0.004706	0.001287	0.522191
1	3.1399	0.007610	0.001812	0.599836
1	3.8190	0.010898	0.002638	0.590273
1	4.4981	0.014623	0.003588	0.582296
1	5.1773	0.019592	0.004550	0.615123

TYPE 72 PI1 = 7.0 PI3 = 2.0
RUN 4 POSITION 7

1	0.5989	0.000262	0.000075	0.500000
1	1.1978	0.000850	0.000300	0.404762
1	1.7968	0.001929	0.000475	0.580201
1	2.4511	0.003198	0.000837	0.545487
1	3.1302	0.004975	0.001250	0.568571
1	3.8094	0.006902	0.001763	0.559439
1	5.1676	0.012169	0.002963	0.586799
1	5.1676	0.014306	0.003287	0.621673
1	4.4885	0.009383	0.002300	0.582816

APPENDIX B-3 (Continued)

PI7	PI2	PI4	PI6	POZN
		TYPE 72 PI1 = 7.0 PI3 = 2.0		
		RUN 4 POSITION 8		
1	0.5989	0.000269	0.000075	0.511905
1	1.1978	0.000785	0.000275	0.408009
1	1.7968	0.001858	0.000500	0.530952
1	2.4715	0.003491	0.000862	0.578157
1	3.1399	0.005216	0.001363	0.546855
1	3.8190	0.007561	0.001813	0.595977
1	4.4981	0.010312	0.002450	0.601312
1	5.1773	0.013820	0.003112	0.634299

APPENDIX C

THE COMPUTER PROGRAM FOR ANALYZING RIGID FRAMES ON

YIELDING PIER FOUNDATIONS

APPENDIX C-1

THE COMPUTER PROGRAM FOR ANALYZING FRAMES
ON YIELDING PIER FOUNDATIONS (FAPMOD)

This program is written in Fortran IV for the IBM 7040 digital
computer. It is designed to compute reactions, moments, shears, and
axial forces within an elastic single bay rigid gable frame having
vertical legs. Asymmetry of the frame and variable moment of inertia
are accommodated. The frame is considered to be rigidly attached to
foundation piers which deflect under the forces and moments applied to
them by the frame. Functions relating foundation movements to applied
force and moment are required: such functions, valid for piers embedded
in dry sand, are included in subroutine PIER.

An Outline of the Method

The program uses the unit load method of computing the deflections
of an elastic structure, with approximate integration over forty
intervals along the frame center line (ten equal intervals per member),
as shown in Figure C-1. Moments of inertia and internal moments are
averaged arithmetically over each interval. (Although the arithmetic
averaging over a comparatively large interval does introduce some
inaccuracy, it is not believed to be serious.

In the initial cycle reactions are computed for the frame with
deflection and rotation of the supports assumed to be zero. The second
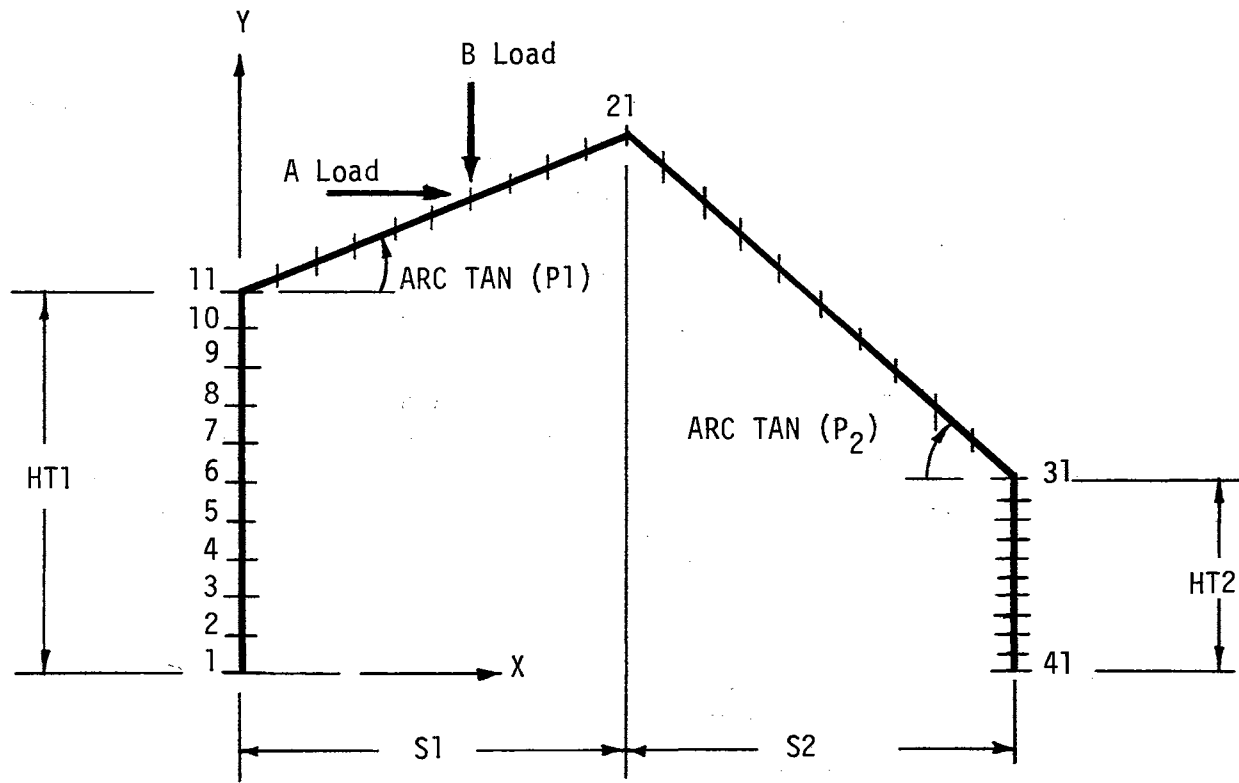
Figure C-1. Frame Notation Used in the Computer Program.

step of the program applies these computed reactions to the foundation piers and computes the horizontal displacement and rotation of the piers, using the prediction equations of Chapter VII.

In the third step the pier movements computed in step 2 are introduced into the deflection equations for the frame and new reactions are computed.

Steps 2 and 3 are repeated until either the difference between subsequent computed reactions is less than 0.01 of the first computed reaction or the process diverges.

Input

Four types of card are used in input. The first (a single card) carries geometric information on the frames, identified in Figure 13-1, in F10.5 format (7 fields) as follows: (All dimensions are in pounds and inches.)

Field 1 Left leg height   HT1

Field 2 Right leg height   HT2

Field 3 Span of left rafter   S1

Field 4 Span of right rafter   S2

Field 5 Slope of left rafter   P1

Field 6 Slope of right rafter   P2

Field 7 Elastic Modulus of the
         frame material   E

The second type of card conveys moment of inertia data. Moment of inertia (EYE) must be determined at each of the 41 points of the frame axis. These values are entered on six cards, 8 per card, in F10.5

format, starting with the base of the left leg as position 1 and going clockwise around the structure to position 41.

The third type of card presents data for the piers. For the pier displacement functions included in subroutine PIER three parameters are required; the depth of the pier, D; the diameter of the pier, B; and the specific weight of the sand, GAMMA. (Both piers use the same values.) Format is 3 F10.5. One card is required.

The fourth type of card is a load card. Forty-one cards are required; one for each grid point. Loads must be computed at the grid points and resolved into horizontal and vertical components. They are entered in the first two (F10.2) fields of the card with the horizontal component first. Horizontal forces are considered positive to the right, and vertical forces are positive downward.

APPENDIX C-2

THE COMPUTER PROGRAM LISTING


```
$IBFTC FAPMOD  NODECK
C     FAPMOD, T. R. C. ROKEBY, JUNE - SEPT 1967
C     FRAME ANALYSIS PROGRAM, 40 DIVISIONS, 4 MEMBER SINGLE BAY FRAME
C     HT1 IS HEIGHT OF LEFT LEG, HT2  OF RIGHT LEG. S1 IS SPAN OF LEFT
C     BEAM, S2 OF RIGHT BEAM. P1 IS SLOPE ,TAN. OF LEFT, P2 OF RIGHT.
C     EYE IS MOMENT OOF INERTIA, E ELASTIC MODULUS, HLOAD IS HORIZONTAL
C     LOAD, VLOAD IS VERTICAL LOAD, AM IS APPLIED MOMENT  EXTERNAL TO
C     STRUCTURE.
C     SIGN CONVENTION, ORIGIN AT BASE OF LEFT LEG, X + TO RIGHT, Y +
C     UPWARD,  FORCES + DOWNWARD AND RIGHT, MOMENTS + CLOCKWISE.
C     CONVERGENCE CHECK ADDED JUNE14, 1967
      DOUBLE PRECISION AM, V, H, AMOM, DIFF, DELTA, TEMP, CONDEL
     1,HLOAD, VLOAD, VT, AM1, V41
      DIMENSIONY(41),X(41),H(41),HLOAD(41),VLOAD(41),V(41),AM(41)
      DIMENSION EYE(42),AMOM(41,4),DIFF(41),DELTA(4,4),ALOAD(41),BLOAD(4
     11),CONDEL(4,4)
      DIMENSIONT(4,2),TT(4),TEST(4),DEL(3),EM(41)
      DIMENSION SHEAR(41),AXIAL(41)
    1 READ(5,5)HT1,HT2,S1,S2,P1,P2,E
      IF(HT1.LE.0.1) GO TO 99
    5 FORMAT(7F10.5)
      ALPH1=ATAN(P1)
      ALPH2=ATAN(P2)
      DO 400 J=1,4
      DO 400 K=1,4
      CONDEL(J,K)=0.
  400 DELTA(J,K) = 0.
      NSTOP=0
      NN=0
      READ(5,14)(EYE(I),I=1,41)
   14 FORMAT(8F10.5)
      READ(5,4) D,B,GAMMA
    4 FORMAT(3F10.5)
      DO 402 I=1,41
      EM(I)=0.
      ALOAD(I)=0.
  402 BLOAD(I)=0.
      INDEX = 0
      Y(1)=0.
      X(1)=0.
      DO 21 I=2,11
      Y(I)=HT1/10.+Y(I-1)
   21 X(I)=0.
      DO 31 I=12,21
      X(I)=X(I-1)+S1/10.
   31 Y(I)=Y(I-1)+(S1/10.)*P1
      DO 41 I=22,31
      X(I)=X(I-1)+S2/10.
      Y(I)=Y(I-1)-(S2/10.)*P2
   41 CONTINUE
      DO51 I=32,41
      X(I)=S1+S2
   51 Y(I)=Y(I-1)-HT2/10.
  206 AM(1)=0.
```

APPENDIX C-2 (Continued)

```
      NDEX=0
    6 H(1)=0.
      VT=0.
      AM1=0.
C     REQUIRES LOAD AT EACH GRID POINT TO BE PREDETERMINED. INSERT
C     BLANK CARD FOR ZERO LOAD
      DO 61 I=1,41
      IF(INDEX.GT.0) GO TO 52
      READ(5,15)ALOAD(I),BLOAD(I)
      WRITE(6,335)I,X(I),Y(I),ALOAD(I),BLOAD(I)
  335 FORMAT(5X,I2,4(5X,F10.2))
      VLOAD(I)=BLOAD(I)
      HLOAD(I)=ALOAD(I)
   15 FORMAT(2F10.2)
   52 H(1)=(H(1)+HLOAD(I))*(-1.)
      VT=(VT+VLOAD(I))
   61 AM1=AM1+HLOAD(I)*Y(I)+VLOAD(I)*X(I)+EM(I)
      V41=(AM1/(S1+S2))*(-1.)
      V(1)=(VT+V41)*(-1.)
      AM(1)=EM(1)
      WRITE(6,25)H(1),V(1),V41,VT
C     H(1), V(1), AND V(41) ARE INITIAL REACTIONS ON DETERMINATE STRUCT.
   25 FORMAT(1H1,4(5X,F12.4))
      WRITE(6,135)
  135 FORMAT( // 10X,27HFORCES AND MOMENTS IN FRAME//6X,1HI,13X,1HX,16X,
     11HY,11X,6HMOMENT,15X,2HFV,15X,2HFH,12X,5HSHEAR,6X,11HAXIAL FORCE/)
      WRITE(6,35) INDEX,X(1),Y(1),AM(1),V(1),H(1)
      DO 71 I=2,41
      V(I)=V(I-1)+VLOAD(I-1)
      H(I)=H(I-1)+HLOAD(I-1)
   71 AM(I)=AM(I-1)-(V(I-1)+VLOAD(I-1))*(X(I)-X(I-1))-(H(I-1)+HLOAD(I-1)
     1)*(Y(I)-Y(I-1))
      DO 501 I=1,11
      SHEAR(I)=H(I)*(-1.)
  501 AXIAL(I)=V(I)
      DO 502 I=12,21
      SHEAR(I)=(H(I)*SIN(ALPH1)+V(I)*COS(ALPH1))*(-1.)
  502 AXIAL(I)=V(I)*SIN(ALPH1)-H(I)*COS(ALPH1)
      DO 503 I=22,31
      SHEAR(I)=H(I)*SIN(ALPH2)-V(I)*COS(ALPH2)
  503 AXIAL(I)=(V(I)*SIN(ALPH2)+H(I)*COS(ALPH2))*(-1.)
      DO 504 I=32,41
      SHEAR(I)=H(I)
  504 AXIAL(I)=V(I)*(-1.)
      DO 571 I=2,41
  571 WRITE(6,35)I,X(I),Y(I),AM(I),V(I),H(I),SHEAR(I),AXIAL(I)
   35 FORMAT(5X,I2,7(5X,F12.2))
      IF(NSTOP.EQ.1) GO TO 311
      IF(NN.EQ.20) GO TO 11
      INDEX = INDEX+1
      DO 81 I=1,41
      AMOM(I,INDEX)=AM(I)
      AM(I)=0.
      HLOAD(I)=0.
```

```
   81 VLOAD(I)=0.
      IF(NDEX.GT.0) GO TO 66
      DO 401 I=1,41
  401 EM(I)=0.
      GO TO (7,8,9,10,11),INDEX
    7 HLOAD(41)=1.
      GO TO 6
    8 EM(41)=1.
      GO TO 6
    9 EM(1)=1.
      GO TO 6
   10 CONTINUE
      DO 93 K=1,4
      DO 92 J=K,4
      DO 91 I=2,41
      DIFF(I)=((AMOM(I,K)+AMOM(I-1,K))/2.)*((AMOM(I,J)+AMOM(I-1,J))/2.)*
     1SQRT((X(I)-X(I-1))**2+(Y(I)-Y(I-1))**2)/(E*(EYE(I)+EYE(I-1))/2.)
   91 DELTA(K,J)=DELTA(K,J)+DIFF(I)
   92 CONTINUE
   93 CONTINUE
      DELTA(3,2)=DELTA(2,3)
      DELTA(4,2)=DELTA(2,4)
      DELTA(4,3)=DELTA(3,4)
      WRITE(6,54)
      WRITE(6,55)DELTA
   54 FORMAT(//5X,7HDELTA P,14X,3H*HR,14X,3H*MR,14X,3H*ML/)
   55 FORMAT(4(5X,F15.8))
      DO 101 J=2,4
      TEMP=DELTA(1,J)*(-1.)
      DO 100 K=2,4
      KM1=K-1
      JM1=J-1
  100 DELTA(KM1,JM1)=DELTA(K,J)
  101 DELTA(4,JM1)=TEMP
      IF(IND.GE.4) GO TO 66
      DO 103 J=1,4
      DO 102 K=1,4
  102 CONDEL(K,J)=DELTA(K,J)
  103 CONTINUE
   66 DO 104 J=1,4
      DO 105 K=1,4
  105 DELTA(K,J)=CONDEL(K,J)
  104 CONTINUE
      IND=INDEX
   56 CALL SOLM(DELTA,AM,V,H,DEL)
  125 FORMAT(//3(10X,F12.2))
      WRITE(6,125)AM(1),AM(41),H(41)
      DO 12 I=1,41
      HLOAD(I)=ALOAD(I)
   12 VLOAD(I)=BLOAD(I)
      EM(1)=AM(1)
      EM(41)=AM(41)
      HLOAD(41)=H(41)+ ALOAD(41)
      H(1)=0.
```

```
      DO 58 I=1,41
  58 H(1)=(H(1)+HLOAD(I))*(-1.)
      WRITE(6,715)(DEL(I),I=1,3)
 715 FORMAT(1H1,8H DEFL = ,E12.5,5X,9HTHETAR = ,E12.5,5X,9HTHETAL = ,E1
     12.5)
      WRITE(6,145)H(1),H(41),V(1),V(41),AM(1),AM(41)
 145 FORMAT (//5X,19H REACTIONS TO PIER ,6H HL = ,F12.2,5X,6H HR = ,F12
     1.2,5X,6H VL = ,F12.2,5X,6H VR = ,F12.2/ 5X,6H ML = ,F12.2,5X,6H MR
     2 = ,F12.2//)
      IF (NDEX.GT.0) GO TO 126
      TEST(1)=ABS(AM(1)*.01)
      TEST(2)=ABS(AM(41)*.01)
      TEST(3)=ABS(H(1)*.01)
      TEST(4)=ABS(H(41)*.01)
 126 CALL PIER(AM,H,D,B,GAMMA,DEL,NSTOP)
      IF(NSTOP.EQ.1) GO TO 11
      DO 200 I=1,4
      T(I,1)=T(I,2)
 200 T(I,2)=TT(I)
      TT(1)=AM(1)
      TT(2)=AM(41)
      TT(3)=H(1)
      TT(4)=H(41)
      IF(NN.LT.3) GO TO 210
      DO 202 I=1,4
      IF((ABS(T(I,1)-T(I,2))).LT.(ABS(T(I,2)-TT(I)))) GO TO 211
      IF((ABS(TT(I)-T(I,2))).GT.TEST(I)) GO TO 202
      NSTOP=1
 202 CONTINUE
 210 CONTINUE
      NN=NN+1
      INDEX=INDEX-1
  57 CONTINUE
      NDEX=1
      GO TO 6
 311 WRITE(6,245)
 245 FORMAT(/10X,17HTEST(I) SATISFIED)
      GO TO 11
 211 WRITE(6,235)I,TT(I)
 235 FORMAT(//5X,29H***** FAILS TO CONVERGE *****,5X,I1,10X,F10.2)
  11 GO TO 1
  99 CALL EXIT
      END
```

APPENDIX C-2 (Continued)

```
$IBFTC SOLM    NODECK
      SUBROUTINE SOLM(DELCON,AM,V,H,DEL)
      DOUBLE PRECISION DELTA, DELCON, TEMP, AM, H
      DIMENSION DELTA(4,4),AM(41),H(41),V(41),
      DIMENSION DEL(3), DELCON(4,4)
      DO 10 I=1,4
      DO 10 J=1,4
   10 DELTA(I,J)=DELCON(I,J)
      DO 12 J=1,3
   12 DELTA(4,J)=DELTA(4,J)-DEL(J)
C     ************* TEMP PRINT FOR DIAGNOSIS *************************
      WRITE(6,95) DELTA
      DO 103 J=1,3
  104 IF(DELTA(1,J).EQ.0.) GO TO 199
      TEMP=DELTA(1,J)
      DO 102 K=1,4
      DELTA(K,J)=DELTA(K,J)/TEMP
  102 CONTINUE
  103 CONTINUE
      DO 105J=1,2
      JP1=J+1
      DO 105 K=1,4
  105 DELTA(K,J)=DELTA(K,J)-DELTA(K,JP1)
  111 DO 112 J=1,2
  114 IF(DELTA(2,J).EQ.0.) GO TO 199
      TEMP=DELTA(2,J)
      DO 112 K=2,4
      DELTA(K,J)=DELTA(K,J)/TEMP
  112 CONTINUE
      DO 113 K=2,4
  113 DELTA(K,1)=DELTA(K,1)-DELTA(K,2)
   95 FORMAT(//4(5X,F15.8))
      AM(1)=DELTA(4,1)/DELTA(3,1)
      AM(41)=DELTA(4,2)-DELTA(3,2)*AM(1)
      H(41)=DELTA(4,3)-DELTA(3,3)*AM(1)-DELTA(2,3)*AM(41)
  199 CONTINUE
      GO TO 999
  999 RETURN
      END
```

APPENDIX C-2 (Continued)

```
$IBFTC PIER      NODECK
       SUBROUTINE PIER(AM,H,D,B,GAMMA,DEL,NSTOP)
       DOUBLE PRECISION AM, H
       DIMENSION AM(41),H(41),PI2(2),PI4(2),PI6(2),PI3(2),DEL(3),NFLAG(2)
C      SUBSCRIPT 1 IS LEFT PIER, 2 IS RIGHT PIER ( AT 41 IN MAIN PROGRAM
C      PIERS ARE IDENTICAL IN GEOMETRY
     1 PI1=D/B
       PI2(1)=H(1)/(B*B*D*GAMMA)
       PI2(2)=H(41)/(B*B*D*GAMMA)
       PI3(1)=AM(1)/(H(1)*D)
       PI3(2)=AM(41)/(H(41)*D)
       DO 11 I=1,2
       IF(PI2(I).LE.0.) GO TO 21
       NFLAG(I)=0
    12 CONTINUE
       IF(PI3(I).LE.0.) GO TO 22
    13 CONTINUE
       PI4(I)=.0001369*PI1**(-.5021)*PI2(I)**3.193*3.637**PI3(I)
       PI6(I)=.00007425*PI1**(-.8158)*PI2(I)**3.027*3.5302**PI3(I)
       IF(NFLAG(I).EQ.1) GO TO 41
    11 CONTINUE
    51 DEL(1)=(PI4(1)-PI4(2))*B*(-1.)
       DEL(2)=PI6(2)
       DEL(3)=PI6(1)
       GO TO 99
    21 PI2(I)=PI2(I)*(-1.)
       NFLAG(I)=1
       IF(PI2(I).EQ.0.) GO TO 31
       GO TO 12
    22 CONTINUE
       PI3(I)=PI3(I)*(-1.)
       IF(PI3(I).EQ.0.) GO TO 31
       GO TO 13
    31 WRITE(6,10)PI2(I),PI3(I)
    10 FORMAT(//10X,24H***** ERROR IN PIS *****,F10.5,10X,F10.5//)
       NSTOP=1
       GO TO 999
    41 PI4(I)=PI4(I)*(-1.)
       PI6(I)=PI6(I)*(-1.)
       GO TO 11
    99 CONTINUE
   999 RETURN
       END
```

APPENDIX D

DATA FROM THE FRAME EXPERIMENTS

APPENDIX D-1

OBSERVED AND PREDICTED DEFLECTIONS AND ROTATIONS OF THE

PIERS OF THE MODEL FRAME

Load lb	Ground Line Deflection, in		Rotations, radians	
	Observed	Predicted	Observed	Predicted
	Left Pier, Test 1			
3	0.00040	0.00035	0.000050	0.000068
5	0.00160	0.00171	0.000200	0.000305
7	0.00325	0.00470	0.000475	0.000792
9	0.00727	0.00966	0.001013	0.001567
	Right Pier, Test 1			
3	0.00033	0.00035	0.000087	0.000068
5	0.00095	0.00171	0.000225	0.000305
7	0.00195	0.00470	0.000425	0.000792
9	0.00438	0.00966	0.000862	0.001567
	Left Pier, Test 2			
3	0.00048	0.00035	0.000063	0.000068
5	0.00185	0.00171	0.000275	0.000305
7	0.00385	0.00470	0.000575	0.000792
9	0.00698	0.00966	0.001062	0.001567
	Left Pier, Test 3			
3	0.00035	0.00035	0.000125	0.000068
5	0.00148	0.00171	0.000312	0.000305
7	0.00438	0.00470	0.000412	0.000792
9	0.00638	0.00966	0.000963	0.001567
	Right Pier, Test 3			
3	0.00143	0.00035	0.000138	0.000068
5	0.00343	0.00171	0.000288	0.000305
7	0.00680	0.00470	0.000600	0.000792
9	0.01040	0.00966	0.00110	0.001567

APPENDIX D-2

OBSERVED HAUNCH DEFLECTIONS AND ROTATIONS AND DEFLECTIONS OF THE

BASES OF THE FULL-SIZED WOODEN FRAMES

Load No.	Frame No.	Total Load lb.	Rotation, radians		Deflection, inches		
			Left Leg	Right Leg	Left Leg	Right Leg	Haunch
First Cycle of Loading							
1	1	1750	0.00085	0.00051	0.0138	0.0119	0.079
	2	1450	0.00069	0.00061	0.0077	0.0047	0.069
	3	1400	0.00175	0.00073	0.0029	0.0072	0.078
2	1	3430	0.00168	0.00111	0.0239	0.0197	0.152
	2	3150	0.00134	0.00106	0.0159	0.0133	0.137
	3	3340	0.00341	0.00154	0.00909	0.0155	0.165
3	1	4960	0.00252	0.00170	0.0348	0.0286	0.223
	2	4720	0.00252	0.00165	0.0247	0.0222	0.219
	3	4820	0.00496	0.00250	0.0174	0.0260	0.253
4	1	6510	0.00363	0.00244	0.0514	0.0427	0.304
	2	6110	0.00352	0.00219	0.0357	0.0337	0.294
	3	6340	0.00679	0.00356	0.0305	0.0423	0.351
5	1	8020	0.00498	0.00328	0.0662	0.0576	0.388
	2	6840	0.00408	0.00280	0.0501	0.0384	0.329
	3	7980	0.00849	0.00473	0.0421	0.0593	0.461
6	1	9460	0.00678	0.00412	0.0806	0.0756	0.473
	2	8540	0.00570	0.00383	0.0876	0.00560	0.405
	3	9390	0.00990	0.00590	0.0612	0.0752	0.561
7	1	10700	0.00805	0.00516	0.0934	0.0931	0.558
	2	10400	0.00953	0.00588	0.1350	0.0905	0.573
	3	10900	0.01150	0.00740	0.0785	0.0971	0.707
Second Cycle of Loading							
1	1	2070		0.00140		0.0372	0.258
	2	1330	0.00316	0.00251	0.0531	0.0359	0.240
	3	1700	0.00283	0.00152	0.0441	0.0357	0.134
2	1	3210		0.00150		0.0450	0.293
	2	3050	0.00374	0.00295	0.0611	0.0426	0.313
	3	3620	0.00405	0.00243	0.484	0.0458	0.228
3	1	4620		0.00203		0.0527	0.356
	2	4640	0.00478	0.00347	0.0717	0.0543	0.406
	3	5090	0.00528	0.00338	0.0516	0.0584	0.323

APPENDIX D-2 (Continued)

Load No.	Frame No.	Total Load lb.	Rotation, radians		Deflection, inches		
			Left Leg	Right Leg	Left Leg	Right Leg	Haunch
4	1	6000		0.00262		0.0635	0.425
	2	6040	0.00583	0.00405	0.0850	0.0644	0.487
	3	6540	0.00684	0.00432	0.0570	0.0692	0.415
5	1	7640					0.503
	2	7580	0.00685	0.00473	0.0997	0.0742	0.571
	3	8120	0.00845	0.00539	0.0666	0.0813	0.517
6	1	9050		0.00392		0.0860	0.573
	2	9120	0.00814	0.00548	0.118	0.0862	0.656
	3	9480	0.00984	0.00633	0.0759	0.0921	0.605
7	1	10600		0.00469		0.0997	0.655
	2	10600	0.00980	0.00645	0.137	0.102	0.787
	3	11100	0.0114	0.00746	0.0903	0.106	0.716

Third Cycle of Loading

Load No.	Frame No.	Total Load lb.	Left Leg	Right Leg	Left Leg	Right Leg	Haunch
1	1	1350		0.00127		0.0358	0.227
	2	1470	0.00358	0.00284	0.0641	0.0409	0.281
	3	1660	0.00291	0.00177	0.0521	0.0437	0.150
2	1	3160		0.00179		0.0485	0.310
	2	3760	0.00475	0.00373	0.0670	0.0443	0.358
	3	3570	0.00419	0.00260	0.0577	0.0558	0.246
3	1	4690		0.00233		0.0590	0.379
	2		0.00547	0.00425	0.0764	0.0520	0.436
	3	5000	0.00823	0.00362	0.0252	0.0656	0.336
4	1	6100		0.00302		0.0698	0.453
	2	6060	0.00591	0.00418	0.0961	0.0708	0.520
	3	6530	0.00987	0.00466	0.0315	0.0780	0.440
5	1	7560		0.00373		0.0833	0.528
	2	7730	0.00737	0.00513	0.1180	0.0824	0.631
	3	8090	0.01150	0.00574	0.0405	0.0882	0.536
6	1	9050		0.00432		0.0942	0.601
	2	9330	0.00866	0.00585	0.1420	0.0947	0.702
	3	9480	0.01280	0.00670	0.0509	0.0936	0.628
7	1	10600		0.00500		0.1070	0.728
	2	10900	0.01010	0.00666	0.1540	0.1080	0.828
	3	11000	0.01430	0.00763	0.0600	0.1090	0.722

Fourth Cycle of Loading

Load No.	Frame No.	Total Load lb.	Left Leg	Right Leg	Left Leg	Right Leg	Haunch
1	1	1340		0.00129		0.0415	0.234
	2	1460	0.00337	0.00270	0.0715	0.0427	0.283
	3	1530	0.00299	0.00171	0.0591	0.0564	0.155

APPENDIX D-2 (Continued)

Load No.	Frame No.	Total Load lb.	Rotation, radians		Deflection, inches		
			Left Leg	Right Leg	Left Leg	Right Leg	Haunch
2	1	3270		0.00175		0.0529	0.310
	2	3430	0.00427	0.00331	0.0858	0.0553	0.391
	3	3460	0.00415	0.00254	0.0642	0.0686	0.249
3	1	4440		0.00260		0.0648	0.390
	2	4870	0.00542	0.00400	0.0990	0.0660	0.488
	3	5000	0.00530	0.00368	0.0664	0.0818	0.353
4	1	6250		0.00313		0.0765	0.460
	2	6380	0.00662	0.00466	0.1150	0.0791	0.586
	3	6430	0.00700	0.00462	0.0710	0.0926	0.445
5	1	8560		0.00362		0.0876	0.528
	2	7860	0.00777	0.00547	0.134	0.0893	0.669
	3						
6	1	9230		0.00434		0.0999	0.611
	2	9380	0.00894	0.00616	0.149	0.101	0.764
	3	9550	0.00996	0.00664	0.0915	0.115	0.641
7	1	10700		0.00500		0.110	0.686
	2	10800	0.0105	0.00699	0.171	0.111	0.848
	3	10900	0.0114	0.00738	0.101	0.128	0.732

VITA

Thomas Rupert Collinson Rokeby

Candidate for the Degree of

Doctor of Philosophy

Thesis: AN ANALYTICAL AND EXPERIMENTAL STUDY OF SINGLE SPAN RIGID FRAMES ON YIELDING PIER FOUNDATIONS

Major Field: Agricultural Engineering

Biographical:

Personal Data: Born in South Walsingham Township, Ontario, Canada, May 9, 1921, the son of Conrad C. and Sadie C. Rokeby.

Education: Graduated from Tillsonburg High School, Tillsonburg, Ontario, Canada, in June 1939. Attended the Ontario Agricultural College majoring in Agricultural Mechanics. Received the degree of Bachelor of Science in Agriculture with a major in Agricultural Mechanics from the University of Toronto in May, 1948. Attended the Graduate School, University of Toronto, and received the degree of Master of Science in Agriculture in November, 1950. Completed the requirements for the degree of Doctor of Philosophy from Oklahoma State University in May, 1968.

Professional Experience: Operated a general farm near Port Rowan Ontario, Canada, 1941-1942; served in the Royal Canadian Air Force, 1942-1944; taught and conducted research in the Agricultural Engineering Department, Ontario Agricultural College, 1947-51; served as Assistant Professor of Agricultural Engineering at South Dakota State College, 1951-1955; taught and conducted research at the University of Arkansas as Assistant Professor, Associate Professor and Professor of Agricultural Engineering from 1955 to the present.

Professional Organizations: Member of the American Society of Agricultural Engineers; member of the American Society for Engineering Education; Registered Professional Engineer in the State of Arkansas.